✕USCAP 2018

ABSTRACTS

LIVER
(1719-1811)

107TH ANNUAL MEETING
GEARED
to LEARN

MARCH 17-23, 2018

Vancouver Convention Centre
Vancouver, BC, Canada

EDUCATION COMMITTEE

Jason L. Hornick, Chair
Rhonda Yantiss, Chair, Abstract Review Board
and Assignment Committee
Laura W. Lamps, Chair, CME Subcommittee
Steven D. Billings, Chair, Interactive Microscopy
Shree G. Sharma, Chair, Informatics Subcommittee
Raja R. Seethala, Short Course Coordinator
Ilan Weinreb, Chair, Subcommittee for
Unique Live Course Offerings
David B. Kaminsky, Executive Vice President
(Ex-Officio)
Aleodor (Doru) Andea
Zubair Baloch
Olca Basturk
Gregory R. Bean, Pathologist-in-Training
Daniel J. Brat

Amy Chadburn
Ashley M. Cimino-Mathews
James R. Cook
Carol F. Farver
Meera R. Hameed
Michelle S. Hirsch
Anna Marie Mulligan
Rish Pai
Vinita Parkash
Anil Parwani
Deepa Patil
Lakshmi Priya Kunju
John D. Reith
Raja R. Seethala
Kwun Wah Wen, Pathologist-in-Training

ABSTRACT REVIEW BOARD

Narasimhan Agaram
Christina Arnold
Dan Berney
Ritu Bhalla
Parul Bhargava
Justin Bishop
Jennifer Black
Thomas Brenn
Fadi Brimo
Natalia Buza
Yingbei Chen
Benjamin Chen
Rebecca Chernock
Andres Chiesa-Vottero
James Conner
Claudiu Cotta
Tim D'Alfonso
Leona Doyle
Daniel Dye
Andrew Evans
Alton Farris
Dennis Firchau
Ann Folkins
Karen Fritchie
Karuna Garg
James Gill
Anthony Gill
Ryan Gill
Tamara Giorgadze
Raul Gonzalez
Anuradha Gopalan
Jennifer Gordetsky
Ilyssa Gordon
Alejandro Gru

Mamta Gupta
Omar Habeeb
Marc Halushka
Krisztina Hanley
Douglas Hartman
Yael Heher
Walter Henricks
John Higgins
Jason Hornick
Mojgan Hosseini
David Hwang
Michael Idowu
Peter Illei
Kristin Jensen
Vickie Jo
Kirk Jones
Chia-Sui Kao
Ashraf Khan
Michael Kluk
Kristine Konopka
Gregor Krings
Asangi Kumarapeli
Frank Kuo
Alvaro Laga
Robin LeGallo
Melinda Lerwill
Rebecca Levy
Zaibo Li
Yen-Chun Liu
Tamara Lotan
Joe Maleszewski
Adrian Marino-Enriquez
Jonathan Marotti
Jerri McLemore

David Meredith
Dylan Miller
Roberto Miranda
Elizabeth Morgan
Juan-Miguel Mosquera
Atis Muehlenbachs
Raouf Nakhleh
Ericka Olgaard
Horatiu Olteanu
Kay Park
Rajiv Patel
Yan Peng
David Pisapia
Jenny Pogoriler
Alexi Polydorides
Sonam Prakash
Manju Prasad
Bobbi Pritt
Peter Pytel
Charles Quick
Joseph Rabban
Raga Ramachandran
Preetha Ramalingam
Priya Rao
Vijaya Reddy
Robyn Reed
Michelle Reid
Natasha Rekhtman
Michael Rivera
Mike Roh
Marianna Ruzinova
Peter Sadow
Safia Salaria
Steven Salvatore

Souzan Sanati
Sandro Santagata
Anjali Saqi
Frank Schneider
Michael Seidman
Shree Sharma
Jeanne Shen
Steven Shen
Jiaqi Shi
Wun-Ju Shieh
Konstantin Shilo
Steven Smith
Lauren Smith
Aliyah Sohani
Heather Stevenson-Lerner
Khin Thway
Evi Vakiani
Sonal Varma
Marina Vivero
Yihong Wang
Christopher Weber
Olga Weinberg
Astrid Weins
Maria Westerhoff
Sean Williamson
Laura Wood
Wei Xin
Mina Xu
Rhonda Yantiss
Akihiko Yoshida
**Xuefeng Zhang**
Debra Zynger

LIVER

1719 Extent of Lesional Cell Spread in Hepatic Epithelioid Hemangioendothelioma: Implications for the Diagnosis in Minimal Samples

Diana Agostini-Vulaj[1], Burcin Pehlivanoglu[2], Sharon Weiss[3], Alyssa Krasinskas[2], Michael Feely[4], Jason L Hornick[5], Justin Cates[6], N. Volkan Adsay[7], Raul S Gonzalez[1]. [1]University of Rochester Medical Center, Rochester, NY, [2]Emory University, Atlanta, GA, [3]Emory University Hospital, Atlanta, GA, [4]University of Florida, Gainesville, FL, [5]Brigham and Women's Hospital, Boston, MA, [6]Vanderbilt University Medical Center, Nashville, TN, [7]Medical College of Wisconsin, Milwaukee, WI

Background: Epithelioid hemangioendothelioma (EHE) can arise in the liver and typically has a WWTR1-CAMTA1 fusion. Lesional cells are known to involve the sinusoids of adjacent parenchyma, but this phenomenon has received little scrutiny. Following an index case in which an attempt to biopsy a mass lesion (ultimately diagnosed as EHE) yielded only adjacent parenchyma with lesional cells in sinusoids, we undertook this study to further characterize these cells.

Design: We identified 18 cases of hepatic EHE (including the index case), and a comparison group of 6 EHEs from other sites. All had classic EHE cytomorphology, lacking high-grade cytologic atypia. For all cases, we recorded EHE multifocality and largest lesion size. We identified lesional cells away from the main tumor mass (when present) and noted their location, maximum distance from the main tumor, density per high-power field (hpf), and cytomorphology. Immunohistochemical staining for CAMTA1, ERG, and CAM 5.2 was performed on all cases.

Results: Lesional cells were present away from the main mass in 17 of 18 (94%) liver cases, always within sinusoids and occasionally (4/17, 24%) in central veins. They were intensely hyperchromatic with vaguely cerebriform nuclei; they appeared multinucleated in 6 (35%) cases, somewhat mimicking megakaryocytes (Figure 1). They were positive for CAMTA1 (Figure 2) and ERG in all 17 cases, though ERG also stained sinusoidal endothelium. Two cases (12%) were focally positive for CAM 5.2. The number of cells per hpf ranged from 12 to 80 (mean 32). The main EHE lesion was available for comparison for 16 of the 17 cases with lesional cells in sinusoids. Sinusoidal EHE cells ranged from 0.1 to 0.8 cm away from the main tumor (mean 0.35 cm). Fifteen main EHEs contained morphologically similar cells, though they were less dense (range 1-9 cells/hpf, mean 4). There were no statistically significant associations between cell density and EHE size or multifocality. In the 6 non-hepatic cases, tumor cells did not extend beyond the main EHE.

CAMTA1
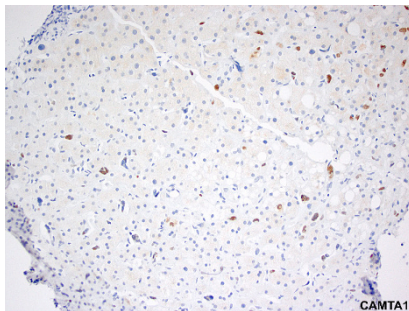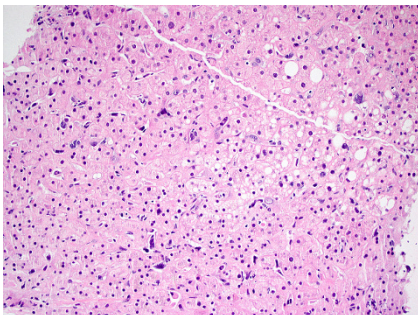
Conclusions: Lesional cells in hepatic EHEs often extend beyond the main lesion into sinusoids, where they demonstrate an unusual and somewhat distinctive morphology. They may be of utility in confirming the diagnosis of EHE, particularly in situations where the main lesion is not present in the sampled tissue or shows unusual morphology. CAMTA1 staining best assists in identifying these cells.

1720 Hepatic Secondary Iron Overload as a Radiographic Mimic of Cirrhosis

Lindsay Alpert[1], Stephen Thomas[1], Helen S Te[1], John Hart[1]. [1]University of Chicago, Chicago, IL

Background: Patients who are clinically suspected to have cirrhosis based on imaging findings alone often undergo a liver biopsy; occasionally, the only histologic abnormality present is iron deposition. Yet iron deposition as a radiographic mimic of cirrhosis is not well documented in the literature. In this study, we investigated the clinicopathologic and imaging features of cases with hepatic iron deposition radiographically mimicking cirrhosis.

Design: Liver biopsies obtained from 2010-2015 showing moderate to severe iron deposition without evidence of cirrhosis were identified from the surgical pathology archives. Clinical data, including imaging results, were collected for all cases, and those with radiographic findings suggestive of cirrhosis were included in the study.

Results: Five liver biopsies were identified, all of which were obtained to evaluate for cirrhosis based on concerning imaging findings. The patients were all males and ranged in age from 27-71 years (mean 54 years, S.D. 18 years). One patient was status post liver transplant for cirrhosis due to hepatitis C virus hepatitis complicated by hepatocellular carcinoma, and two other patients had a history of heavy alcohol use. All of the patients had end-stage renal disease requiring hemodialysis or peritoneal dialysis. Computed tomography (CT) and/or ultrasound studies showed "possible cirrhotic morphology", "early changes of cirrhosis", "nodularity concerning for cirrhosis" or "findings of chronic liver disease with… capsular nodularity". The primary histologic finding in all cases was hemosiderosis, with iron deposition present mainly in Kupffer cells (Figure 1). Three cases also exhibited mild hepatocellular iron deposition, and in one case iron was seen in endothelial cells as well. One case demonstrated moderate centrilobular fibrosis and another showed mild portal fibrosis, but there was no evidence of cirrhosis or even bridging fibrosis in either of these cases, and the other three cases were free of fibrosis. No additional pathologic abnormalities were identified. No patient underwent HFE mutational analysis.
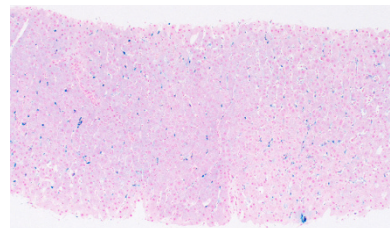
Conclusions: Kupffer cell iron deposition can appear as nodularity and/or fibrosis on CT and ultrasound studies, which may raise clinical concern for cirrhosis. This situation seems to arise primarily in male patients who are undergoing dialysis for chronic renal failure. Awareness of this phenomenon may aid pathologists in explaining the apparent discrepancy between clinical and histologic findings.

1721 Immunohistochemical and Molecular Findings in Cholangiolocellular Carcinoma are Similar to Well-Differentiated Intrahepatic Cholangiocarcinoma

Dana Balitzer[1], Nancy Joseph[1], Linda Ferrell[1], Dhanpat Jain[2], Xuchen Zhang[2], Nafis Shafizadeh[3], Sanjay Kakar[1]. [1]University of California San Francisco, San Francisco, CA, [2]Yale University School of Medicine, New Haven, CT, [3]Kaiser Permanente, Oak Park, CA

Background: Cholangiolocellular carcinoma (CCC) is characterized by low grade cytologic atypia, and anastomosing cords and glands resembling cholangioles or canals of Hering. CCC was regarded as a subtype of intrahepatic cholangiocarcinoma (ICC), but was then classified as combined hepatocellular-cholangiocarcinoma of stem cell subtype in WHO 2010, which has led to confusion about this entity.

Design: Resected ICC cases 1995-2017 were reviewed, and 3 cases with pure CCC, 4 cases with both CCC and well-differentiated (WD)-ICC components (mixed tumors) and 3 cases with WD-ICC were identified. Immunohistochemistry (IHC) for putative stem cell markers (CK19, CD56) was performed. Capture-based next generation sequencing (NGS) targeting the coding regions of 479 cancer genes and select introns was performed. For 4 cases with mixed components of CCC and WD-ICC, the individual areas were micro-dissected prior to sequencing. Single nucleotide variants, insertions/ deletions, copy number alterations (CNAs), and selected rearrangements were evaluated.

Results: IHC and molecular data were examined in 7 CCC areas (3 from pure CCC, 4 from mixed tumors) and 7 WD-ICC areas (3 from pure WD-ICC, 4 from mixed tumors). IHC for CK19 showed diffuse strong positive in 86% (6/7) of CCC areas and 43% (3/7) of WD-ICC areas, while CD56 was positive in 43% (3/7) of CCC areas and 86% (6/7) of WD-ICC areas (table 1). *IDH1/2* mutations, chromatin-remodeling

gene mutations (*ARID1A* or *PBRM1*) and *MDM2* amplification were similar in pure CCC, mixed CCC/WD-ICC, and WD-ICC cases (figure 1) Similar CNAs were seen in cases of pure CCC, mixed CCC/WD-ICC, and WD-ICC, many of which are characteristic of ICC, including losses in 1p, 3p, 6q, 12q, 14q and gains in 1q and 19.

	Diffuse CK19	CD56+	IDH 1/2 mutation	FGFR2 fusion	ARID1A mutation	PBRM1 mutation	TERT promoter mutation
CCC areas, n=7	86% (6/7)	43% (3/7)	43% (3/7)	14.3% (1/7)	14.3% (1/7)	57.1% (4/7)	14.3% (1/7)
WD-ICC areas, n=7	43% (3/7)	86% (6/7)	43% (3/7)	0% (0/7)	14.3% (1/7)	57.1% (4/7)	14.3% (1/7)
ICC*	44-94%	1 2.5-86.7%	5-23.6%	13.6%-45%	6.9-20%	10.9-17%	5.2-14.3%
Hepato-cellular (HCC)*	6-10%	2%	< 1%	< 1%	2.3 -16%	< 1%	50.4-60%

*Data cited from literature
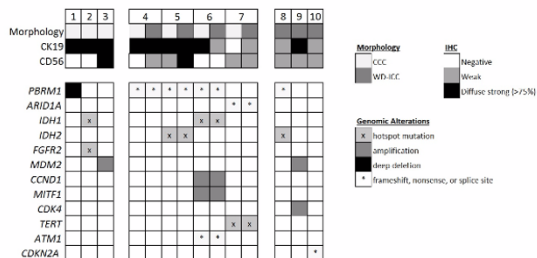
Conclusions: IHC results, mutational spectrum and CNAs in CCC are similar to WD-ICC as well as to the reported data for ICC in literature. The morphologic and molecular features typically seen in HCC are not seen in CCC. CCC should be considered as a histologic subtype of WD-ICC, and should not be classified as combined HCC-CC unless a distinct HCC component is also present. Presence of an ICC component can lead to important treatment decisions like choice of chemotherapy and denial of transplantation, making it imperative to use of stringent criteria for diagnosis.

1722 Comparison of Clinicopathologic Features of Plasma Cell Hepatitis and Recurrent Autoimmune Hepatitis

Dana Balitzer, Linda Ferrell, Marion Peters, Sanjay Kakar. University of California San Francisco, San Francisco, CA

Background: Plasma cell hepatitis (PCH) is thought to represent a variant of rejection, and is associated with elevated IgG, autoantibodies and prominent plasma cells. The clinical and histologic features can be indistinguishable from recurrent autoimmune hepatitis (AIH).

Design: Clinical data and liver biopsies from recurrent AIH and PCH cases (n=12 each) were reviewed. C4d immunohistochemistry was performed on 12 recurrent AIH and 6 PCH. Statistical analysis was performed using Student's t-test and Fisher exact test.

Results: Autoantibodies were seen in both recurrent AIH (ANA 75%, SMA 57%) and PCH (ANA 45%, SMA 67%). PCH occurred significantly closer to transplant than recurrent AIH (average 3.1 vs 8.4 years, p = 0.01). Immunosuppression noncompliance (58% vs 25%, p=0.10) and development of chronic ductopenic rejection (50% vs 17%, p= 0.09) were more common in PCH with borderline statistical significance. PCH was associated more often with bile duct injury, acute cellular rejection (ACR) and >25% plasma cells. On follow-up, there was a trend towards chronic ductopenic rejection in PCH and cirrhosis in AIH. There were no significant differences in portal inflammation, interface activity, centrizonal necrosis and C4d positivity [table].

Clinical and Pathologic Features			
	PCH (n=12)	Recurrent AIH (n=12)	p value
Autoantibodies present	64% (7/11)	67% (6/9)	1.00
Elevated serum IgG	75% (6/8)	88% (7/8)	1.00
Mixed portal Inflammation	33% (4/12)	8% (1/12)	0.16
Concomitant acute cellular rejection	83% (10/12)	3/12 (25%)	0.01
Acute cellular rejection in past 12 months	33% (4/12)	0% (0/12)	0.05
Interface activity, >grade 2	50% (6/12)	50% (6/12)	1.00
Bile duct injury, more than focal	83% (10/12)	16% (2/12)	<0.01
Lobular activity, >2 foci/10x field	83% (10/12)	100% (12/12)	0.48
Centrizonal necrosis	67% (8/12)	42% (5/12)	0.41
Plasma cells >25%	83% (10/12)	42% (5/12)	0.05
C4d	33% (4/12)	17% (1/6)	0.61
Outcome			
- Cirrhosis:	0% (0/12)	33% (4/12)	0.05
- Chronic ductopenic rejection:	50% (6/12)	17% (2/12)	0.09

Conclusions: Serum IgG and autoantibodies are similar in PCH and recurrent AIH. Earlier onset, bile duct injury and concomitant features of acute cellular rejection are associated with PCH. Non-compliance with immunosuppression and more numerous plasma cells tend to be seen in PCH. Follow-up data showed a trend towards association of ductopenic rejection with PCH and cirrhosis with rAIH. Despite overlapping characteristics, PCH and recurrent AIH are likely distinct clinicopathologic entities and differ in their clinical course.

1723 Comparison of Clinicopathologic Features Between Recurrent and De Novo Post-Transplant Non-Alcoholic Steatohepatitis

Dana Balitzer[1], *Jia Huei Tsai*[2], *Ryan Gill*[2]. [1]University of California San Francisco, San Francisco, CA, [2]National Taiwan University Hospital, Taipei, Taiwan

Background: NAFLD/NASH has become an increasingly recognized problem in patients after orthotopic liver transplant. NAFLD recurrence is common in the first 5 years after transplantation, but NASH recurs in only approximately 25% of patients. Fewer studies have evaluated *de novo* NAFLD/NASH. The aims of this study were to evaluate the clinicopathologic features and compare the differences between recurrent and *de novo* NASH.

Design: From 1995 to 2016, we performed a retrospective review of patients with a histological diagnosis of steatohepatitis made more than 6 months after liver transplant at our institution. The cases were categorized into de novo (n = 19) or recurrent steatohepatitis (n = 37)

Results: De novo NASH presented on average 4.8 years after transplant, which was significantly longer than recurrent NASH (2.8 years, p=0.02). There were no differences with respect to BMI, or hyperlipidemia. Percent of patients with new onset diabetes mellitus was significantly higher in *de novo* NASH (p=0.0003). Histologically, there was no difference in presence of diffuse or focal glycogenosis, grade 3 steatosis, or presence of any ballooned hepatocytes, although significantly more recurrent NASH biopsies had small non-classic ballooned hepatocytes (62.5% of cases) compared to *de novo* NASH (26.7%) (p=0.03), in which the diagnosis was based on more well-developed ballooned hepatocytes. Recurrent NASH biopsies were also less likely to show "more than mild" portal inflammation (5% vs 40.5%, p = 0.0049). *De novo* NASH biopsies with recurrent HCV had higher stage fibrosis than recurrent NASH (P = 0.05) and hepatitis C virus (HCV) infection-related cirrhosis was the most common etiology of transplantation in *de novo* NASH patients (78%).

Conclusions: Recurrent NASH demonstrates distinct clinicopathologic features compared to *de novo* NASH arising in the post-transplant setting. *De novo* NASH is more likely associated with new onset diabetes mellitus, occurs later, and shows more well-developed ballooned hepatocytes. In patients with *de novo* NASH, recurrent HCV may worsen fibrosis.

1724 Asialoglycoprotein Receptor: Novel Highly Sensitive Hepatocellular Differentiation Marker

Andrew Bellizzi, Daniel Pelletier. University of Iowa Hospitals and Clinics, Iowa City, IA

Background: We read with great interest a recent *N Engl J Med* study in which a small interfering RNA directed against a molecule involved in LDL metabolism was specifically targeted to the liver by conjugation to *N*-acetylgalactosamine, through that carbohydrate's interaction with asialoglycoprotein receptor (ASGPR). We subsequently learned that ASGPR (alternatively termed hepatic lectin) is a major autoantigen in autoimmune hepatitis and that it is being studied as a means of delivering oligonucleotides (or chemotherapy) to the liver in diverse

metabolic diseases, viral hepatitis, and hepatocellular carcinoma (HCC). We hypothesized that immunohistochemistry (IHC) for ASGPR would be sensitive and specific for hepatocellular differentiation.

Design: IHC for ASGPR, HepPar1, and glypican-3 (GPC3) was performed on tissue microarrays (triplicate 1 mm cores) of 99 non-neoplastic livers (NNL; 69 with cirrhosis), 8 dysplastic nodules (DN), 162 HCCs, 135 cholangiocarcinomas (CC), and 93 small intestinal adenocarcinomas (SIA). Tumor grade was assessed by re-review of original glass slides (well [WD], moderately [MD], poorly differentiated [PD]). IHC was evaluated for intensity (0-3+) and extent (0-100%) of expression with an H-score calculated (intensity*extent). McNemar's test was used with p<0.05 considered significant.

Results: ASGPR was moderately to strongly expressed (H-scores in the 200 range) by nearly all liver tissues and tumors, weakly to moderately expressed by 30% of CCs (mean H-score 83), and only very weakly expressed by 4% of SIAs (see Table).

Table: Detailed Expression Data: % Positive (Mean H-score if Positive)

			HCC				
	NNL	DN	WD (n=34)	MD (n=104)	PD (n=24)	CC	SIA
ASGPR	100% (278)	100% (245)	97% (238)	93% (211)	100% (137)	30% (83)	4% (6)
HepPar1	99% (298)	100% (291)	97% (270)	92% (235)	79% (204)	20% (94)	42% (127)
GPC3	1% (13)	13% (3)	50% (67)	60% (122)	71% (177)	8% (49)	2% (9)

Conclusions: ASGPR is comparable to HepPar1 in terms of overall sensitivity (p=0.18) and appears to compare favorably in PD HCC (p=0.063) and especially SIA (in which HepPar1 is often positive; p<0.000001). ASGPR compares favorably to GPC3 in terms of overall sensitivity (p<0.000001), though it is more frequently expressed by CCs (p<0.000001). Based on these results we plan on adding ASGPR to our clinical IHC test menu.

1725 Steatohepatitic Hepatocellular Carcinoma: background liver disease and histology

Mark Benedict, Benjamin L Mazer, Anisha Jain, Romulo Celli, Tamar Taddei, Charles Cha, Dhanpat Jain, Xuchen Zhang. Yale University School of Medicine, New Haven, CT

Background: Steatohepatitic hepatocellular carcinoma (SH-HCC) is a recently described HCC subtype that has been reported to occur in association with metabolic syndrome. Recently it has been suggested that SH-HCC can occur in the absence of metabolic syndrome or background liver steatosis. Case control studies looking at degree of background steatosis and cirrhosis in SH-HCC are lacking. The aim of this study was to examine the association of steatosis in the background liver and cirrhosis with SH-HCC.

Design: All HCC cases at our institution from 2010-2014 were reviewed and clinical history and laboratory data were recorded for all cases. Detailed pathologic evaluation for histologic findings in the tumor and background liver, specifically steatosis and extent of fibrosis in the background liver was performed for each case. The steatosis was recorded as percentage area involved at 10% intervals. Diagnosis of SH-HCC was made based on previously published criteria. Findings of the background liver in SH-HCC were compared with conventional HCC/ HCC-NOS (not otherwise specified). Statistical analysis was performed using Chi-square or Fisher exact tests for categorical variables and t-test or Wilcoxon rank sum tests for continuous variables.

Results: A total of 231 (146 biopsies, 85 resections) HCC cases (60 non-cirrhotic and 171 cirrhotic) were identified of which 51 (22%) cases met the criteria for SH-HCC. Most patients (84%) with HCC-NOS had no significant background steatosis (<5%), while 47% of SH-HCC cases had significant steatosis (>33%) and the findings were statistically significant. In the SH-HCC cases of 23 patients with available data on metabolic syndrome, 17 had metabolic syndrome, but 6 did not and 3 of these did not show any steatosis in the background liver. SH-HCCs developed in a range of background liver diseases with hepatitis C being most common however, there was no statistically significant background cirrhosis or liver disease between SH-HCC and contols (Table 1). Comparision of various features between SH-HCC and HCC-NOS is shown in table.

	SH-HCC N=51 (%)	HCC-NOS N= 120 (%)	P Value
Age range (mean)	62	63	
Male: Female	7:3	4.5:1	
Cirrhosis	44 (86%)	95 (79%)	p=0.391
Background liver steatosis			
No significant steatosis (<5%)	27 (53%)	101 (84%)	p=0.0001
Mild steatosis (5-33%)	17 (33%)	14 (12%)	p=0.003
Moderate (34-66%)	3 (6%)	4 (3%)	p=0.427
Severe (>66%)	4 (8%)	1 (1%)	p=0.282
Tumor size (cm)	3.0 ± 0.35	3.1 ± 0.23	p=0.923
High grade (>=3)	0	14	p=0.011
AJCC Pathologic stage >2	1	1	p=0.509
Background liver disease			
Hepatitis C	29	70	p=0.867
Hepatitis B	1	6	p=0.676
NASH	6	6	p=0.186
ASH	5	4	p=0.128
Others	1	1	p=0.509
Unknown	8	28	p=0.310
Siderosis	1	3	p=1.00
Hep B and C	0	2	p=1.00

Conclusions: Our findings suggest that the majority (74%) of SH-HCC occur in patients with metabolic syndrome, but these can also occur in patients without metabolic syndrome or background steatosis. The pathophysiology of SH-HCC arising without metabolic syndrome or background steatosis remains unclear and needs further evaluation.

1726 Early Liver Transplantation for Severe Alcoholic Hepatitis: Clinico-Pathologic Features in a Controversial Therapeutic Setting

Feriyl Bhaijee[1], Atoosa Rabiee[2], Sepideh Besharati[2], Ahmet Gurakar[2], Andrew Cameron[2], Kiyoko Oshima[2], Robert Anders[2], Qingfeng Zhu[2]. [1]AmeriPath Indiana, Indianapolis, IN, [2]Johns Hopkins University, Baltimore, MD
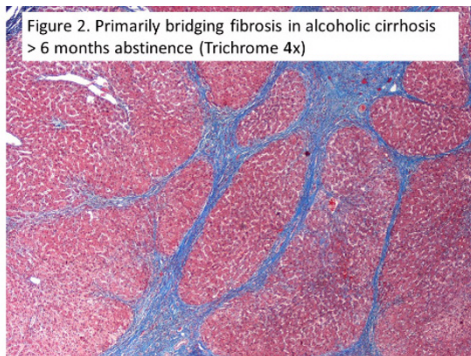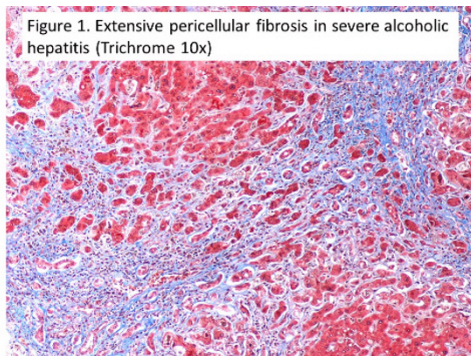
Background: Severe alcoholic hepatitis (AH), a disease with an exceptionally high mortality rate, rarely leads to early ("rescue") liver transplantation (LT), as many centers usually require 6 months of alcohol abstinence prior to LT. In 2011, however, a small Franco-Belgian study showed that early LT could improve survival with low incidence of alcohol relapse. A subsequent 3-year pilot program at Johns Hopkins Hospital including 43 carefully-selected patients (17 with severe AH and 26 with alcoholic cirrhosis and >6 months of alcohol abstinence) showed that early LT provides excellent short-term survival with similar rates of alcohol relapse between the two groups. Herein, we evaluate the pathologic features in the explanted livers from 21 patients with severe AH and compare these to the explanted livers from 10 patients with alcoholic cirrhosis and >6 months abstinence prior to LT.

Design: Using our institutional electronic medical record, we identified 21 patients who met the stringent criteria for the pilot program at Johns Hopkins Hospital, as well as 10 patients with alcoholic cirrhosis and >6 months abstinence. H&E, trichrome, and iron slides were reviewed independently by 2 blinded pathologists, who scored various criteria as follows: 0 (none), 1 (mild/rare), 2 (moderate), and 3 (severe). Iron staining and fibrosis were scored on 0-4 scales and steatosis was quantified.

Results: Table 1 delineates clinico-pathologic parameters in cases of severe AH and those with alcoholic cirrhosis and >6 months abstinence. Clinically, while the two groups differed significantly in terms of days of abstinence prior to LT and MELD score at the time of listing, the following parameters were not significantly different: age, BMI, grams of alcohol ingested per day (remotely for the latter group), years of alcohol consumption overall, and one-year survival rate (95% vs. 100%). Histologically, the severe AH cases showed significantly more steatosis, portal and lobular inflammation, Mallory-Denk hyaline, ductular reaction, cholate stasis, canalicular cholestasis, and pericellular fibrosis (Figures 1 and 2).

Table 1. Clinico-Pathologic Features in Cases of LT for Severe AH and Alcoholic Cirrhosis with >6 Months Abstinence

	Severe AH	Alcoholic Cirrhosis with >6 months abstinence	p-value
Total number (n)	21	10	
Mean age at transplant (years)	46.8	51.0	0.27
BMI	28.8	26	0.27
Alcohol consumption (mean grams/day)	227	216	0.91
Overall years of alcohol consumption	16.8	21.0	0.34
Mean days of alcohol abstinence prior to LT	113	1074	0.01
MELD score at time of listing	35.9	22.5	0.000162
Child-Pugh Class A	0	0	
Child-Pugh Class B	1 (5%)	5 (50%)	>0.05
Child-Pugh Class C	20 (95%)	5 (50%)	>0.05
Survival at 1 year (n)	20 (95%)	10 (100%)	0.50
Rejection episode at 1 year (n)	11 (52%)	3 (30%)	0.25
Recidivism at 1 year (n)	2 (10%)	0	0.32
Steatosis (%)	18.5	1	0.07
Portal inflammation (0-3)	2.2	0.9	0.00001
Lobular activity (0-3)	2.4	0.3	0.00001
Steatohepatitis (n)	11 (52%)	0	0.1
Mallory-Denk bodies (0-3)	1.6	0	0.00001
Cholate stasis (n)	1.1	0.1	0.004
Canalicular cholestasis (n)	1.5	0.3	0.01
Ductular reaction (0-3)	1.5	0.7	0.00001
Portal fibrosis (0-4)	2.9	3.7	0.07
Pericellular fibrosis (0-3)	2	0.5	0.00002
Iron deposition (0-3)	1	1.3	0.68
Established cirrhosis (n)	14 (65%)	9 (90%)	0.17
HCC (n)	1 (5%)	2 (20%)	0.19

Figure 1. Extensive pericellular fibrosis in severe alcoholic hepatitis (Trichrome 10x)

Figure 2. Primarily bridging fibrosis in alcoholic cirrhosis > 6 months abstinence (Trichrome 4x)

Conclusions: Despite nearly-identical one-year survival rates between our severe AH patients and our control group with alcoholic cirrhosis and >6 months abstinence, the histologic changes in cases of severe AH are strikingly different - and significantly worse - than those seen in the explanted livers from patients who abstained from alcohol consumption prior to LT.

1727 Use of Multispectral Imaging Microscopy to Phenotype Immune Cells in Formalin-Fixed Paraffin-Embedded Human Liver Biopsy Tissue

Adam L Booth[1], Omar Saldarriaga[2], Netanya Utay[3], MinKyung Yi[2], Monique Ferguson[2], Laura Beretta[4], Edward Stack[5], Heather Stevenson[6]. [1]University of Texas Medical Branch, Galveston, TX, [2]University of Texas Medical Branch, [3]University of Texas Health Science Center at Houston, [4]University of Texas MD Anderson Cancer Center, [5]PerkinElmer, Inc, [6]Univ. of Texas Medical Branch, Galveston, TX

Background: Analysis of fresh liver tissue by flow cytometry cannot visualize immune cells in the context of intact hepatic architecture. Routine immunohistochemical (IHC) staining of liver biopsies can identify inflammatory cells in formalin-fixed paraffin-embedded (FFPE) tissues, however, there are limitations, including the inability to stain multiple antigens on the same cell or cellular compartment. Recently, multispectral imaging has been developed, although primarily used to study tumor infiltrating lymphocytes. We adapted this cutting-edge technology to identify antigens on the same cell, in non-neoplastic, human FFPE liver biopsy tissue from patients with chronic viral hepatitis C.

Design: Multiplex immunofluorescence staining of FFPE tissue was performed using the Opal 6-color multiplex IHC kit and analyzed using the Vectra 3 Platform (PerkinElmer). We developed two panels: 1) CD3, CD4, CD8, FOXP3, CD56, and DAPI; and 2) CD68, CD14, CD16, and DAPI. Imaging data were analyzed using inForm software. We used monoplex stains and an unstained slide to generate our spectral imaging library which allowed spectral unmixing of our above multiplex panels. Our multiplex panels were optimized to ensure proper mean fluorescence intensities of each signal and absence of overlap between neighboring fluorophores.

Results: The tissue segmentation feature of the software was able to separate liver parenchyma into portal tracts and lobules. The cell segmentation feature was able to identify individual cells by the DAPI nuclear stain. The software was then trained to properly phenotype and characterize individual cells. Our multiplex panels were successfully able to identify and quantify CD3+/CD4+, CD3+/CD8+, CD3+/CD56+, and CD3+/CD4+/FOXP3+ lymphocytes, as well as CD68+/CD14+ and CD68+/CD16+ macrophages in portal tracts and lobules.

Conclusions: Spectral imaging microscopy is a cutting-edge technique that enables differentiation and quantification of hepatic immune cells in human FFPE liver tissue.

1728 Validation of a Congestive Hepatic Fibrosis Scoring System

Dustin Bosch, Paul E Swanson, Benjamin Hoch, Florencia Jalikis, Lisa Koch, Camtu Truong, Elizabeth Richards, Konstantin Koro, Matthew M Yeh. University of Washington, Seattle, WA

Background: Congestive hepatopathy is a complication of right heart failure and chronically elevated right heart pressure. Histologic findings include sinusoidal dilatation, centrilobular hepatocellular plate atrophy, and fibrosis. A scoring system for congestive hepatic fibrosis (PMID 24925051) has been recently proposed. We performed a validation study in a set of liver biopsies and correlate with clinical data.

Design: 38 liver biopsies at our institution with congestive hepatopathy were reviewed. Congestive hepatic fibrosis was scored on a 0-4 scale, using previously published histologic criteria (PMID 24925051). Average fibrosis score was correlated with clinical parameters, including right atrial and hepatic wedge pressure, right atrium and ventricle dilation, serum liver tests, portal hypertension and ascites, and all-cause mortality.

Results: Fibrosis score did not correlate significantly to all-cause mortality, although follow up data were variable. However, average congestive hepatic fibrosis score did correlate with significantly higher right atrial pressure, severity of right atrial dilation, presence of right ventricular dilation, serum alanine aminotransferase (ALT), platelet counts, and prothrombin time (PT).
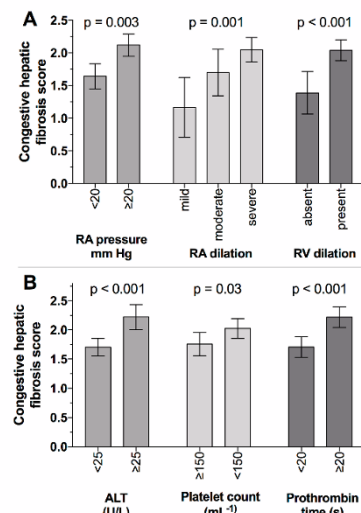
Conclusions: Our data show that congestive hepatic fibrosis scores correlated with clinical findings of right heart failure, including elevated right atrial pressure, right atrial and ventricular dilation, as well as serum ALT, platelet counts, and prothrombin time, validating this scoring system as a robust and useful scheme in assessing liver fibrosis in congestive hepatopathy.

1729 Immunological and Cancer-related Genes Differentiate Between Hepatocellular Adenoma and Well-differentiated Hepatocellular Carcinoma

Christopher J Bowman, Jarish Cohen, Sanjay Kakar, Sarah Umetsu, G. Zoltan Laszik. University of California, San Francisco, San Francisco, CA

Background: Hepatocellular adenoma (HCA) is an uncommon benign liver neoplasm, of which there are four subtypes – inflammatory HCA (I-HCA), HNF1-alpha-inactivated HCA (H-HCA), beta-catenin-activated HCA (B-HCA), and unclassified. Activating beta-catenin mutations are a leading cause of malignant transformation of benign HCA to hepatocellular carcinoma. Tumors resembling HCA but with beta-catenin activation are often labeled as atypical hepatocellular neoplasms and managed like well-differentiated hepatocellular carcinoma (WDHCC). Despite the utility of current immunohistochemical (IHC) tools, diagnostic differentiation between WDHCC and benign HCA remains a challenge. The determination of beta-catenin activation in biopsies is often based on the evaluation of glutamine synthetase staining, which can be difficult to interpret, especially in limited biopsies. Identification of molecular markers that can be applied in clinical settings to identify beta-catenin activation with greater sensitivity and specificity is needed.

Design: Gene expression profiles of nine WDHCC were gathered using Nanostring's multiplex assay, and compared with the previously determined profiles of four I-HCA and six H-HCA. Briefly, mRNA was extracted from FFPE tissue and quantitated using NanoString's nCounter system. A total of 1375 genes representing immune and cancer pathways were normalized and analyzed using nSolver Analysis Software v3.0.

Results: Unsupervised hierarchical clustering showed clear separation of I-HCA, H-HCA and WDHCC. The most deranged pathways included the JAK-STAT in I-HCA and the Wnt/beta-catenin in WDHCC. In addition, WDHCC showed significantly upregulated gene expression in numerous other pathways (e.g., Hedgehog, PI3K-AKT, RAS, and MAPK). Interestingly, LEF1, AXIN2 and NKD1 are Wnt-pathway genes that are upregulated up to 16-fold higher in WDHCC as compared to I-HCA and H-HCA.

Conclusions: Gene expression profiling of immunological and cancer-related genes demonstrates clear separation of benign HCA from WDHCC and highlights significant changes within the Wnt, Hedgehog, PI3K/AKT, RAS, and MAPK pathways. Differential expression analyses have identified numerous genes, such as LEF1, AXIN2, and NKD1, that are significantly upregulated in WDHCC relative to HCA. Candidate IHC markers based on these genes can be helpful in distinguishing WDHCC from benign HCA.

1730 Liver Histology in Septic Patients: Is It All About Ductular Cholestasis?

Caroline Bsirini, Raul S Gonzalez. University of Rochester Medical Center, Rochester, NY

Background: Sepsis often causes cholestatic jaundice, and liver biopsy may be performed to exclude other diagnoses. Cholestasis within bile ductules is generally touted as a key histologic finding in the liver of septic patients. However, it is not always present, nor is it entirely specific. Additionally, the spectrum of other histopathologic findings in septic patients has not been thoroughly studied.

Design: For 126 liver biopsies where sepsis was mentioned in the provided clinical information or in the pathologic differential diagnosis, we searched medical records for patient outcome, clinical impression (sepsis or not), blood culture results, and whether processes that might cause overlapping histologic changes (e.g., total parenteral nutrition or large duct obstruction) were present. We evaluated each case for histologic findings, including portal and lobular inflammation, ductular reaction, duct injury, lobular or ductular cholestasis, and acidophil bodies. Histologic findings between patients with and without clinical sepsis, and between patients with Gram-positive vs. Gram-negative results on blood culture, were compared using Fisher's exact test.

Results: Common histologic findings in clinically septic patients (n=79) included portal chronic inflammation (55 cases, 70%), lobular acute inflammation (46, 58%), ductular reaction (60, 76%), lobular cholestasis (69, 87%), ductular cholestasis (53, 67%), and acidophil bodies (37, 47%), though 19 patients (24%) had other diagnoses with potential histologic overlap. Findings between clinically septic and non-septic patients were similar, though the latter more often had lobular chronic inflammation (22% vs. 40%, P=0.027). Ductular cholestasis rates were similar in both groups (67% vs. 53%, P=0.13). There were no significant differences among findings in patients with

Gram-positive vs. Gram-negative sepsis, though the former tended to have acidophil bodies more often (64% vs. 32%, P=0.069). Clinically septic patients more often died soon thereafter than clinically non-septic patients (P=0.0002), lending credence to that categorization.

Conclusions: Ductular cholestasis can be present in septic and non-septic liver samples, though its presence should at least suggest the possibility of sepsis. Other common findings in sepsis include lobular cholestasis, ductular reaction, portal chronic inflammation, lobular acute inflammation, and acidophil bodies. Clinical history should always be reviewed for potentially confounding cholestatic conditions.

1731 Clinicopathologic Findings in Hepatic Epithelioid Hemangioendothelioma

Kathleen Byrnes[1], John S Chrisinger[2], Bella Goyal[3], Armen Khararjian[4], Rifat Mannan[5], Elizabeth Montgomery[6], Robert Anders[7], Kiyoko Oshima[5]. [1]Johns Hopkins Hospital, Baltimore, MD, [2]Washington University School of Medicine, St. Louis, MO, [3]Washington University School of Medicine, Saint Louis, MO, [4]Baltimore, MD, [5]The Johns Hopkins Hospital, [6]Johns Hopkins Medical Institutions, Baltimore, MD, [7]John Hopkins, Baltimore, MD

Background: Epithelioid hemangioendothelioma (EHE) primary to the liver is a rare entity. Prognostic histologic features have not been well described. Risk stratification criteria have been suggested for soft tissue EHE. However, no such criteria have been identified for hepatic EHE. In this review, we characterize the clinicopathologic features of a larger series of hepatic EHE.

Design: All pathology reports of hepatic EHE from 1984 to August of 2017 were reviewed from two institutions. Slides of EHE were reviewed to record pathologic features [size, mitoses, necrosis, tumor morphology, stroma, nuclear features, and architecture]. Patient follow-up and clinical information was obtained by chart review.

Results: Of 19 cases of EHE available for review, 74% were in women with a mean age of 52 years. The size of the tumors ranged from 0.9 to 13 cm (mean 4.5 cm) with no predilection to right or left lobes. Morphologically, the tumors were predominantly epithelioid (53%, n=10) with hyalinized stroma (73%, n=14). The growth pattern was infiltrative into the adjacent hepatic parenchyma in 63% of the cases (n=12). Prominent nucleoli (37%) were noted predominantly in tumors with hyalinized stroma and epithelioid morphology. Necrosis was identified in 31% (n=6) of cases. The mitotic count ranged from 0 to 5 per 50 HPF (mean 1). In the cases where imaging was available, the tumors ranged from single (41%) to multifocal (59%). Of the cases where treatment information was available, 86% (n=12) were treated with resection; two of which were liver transplants. At the time of last follow-up, 3 patients were alive with disease and 3 died of disease. Four patients had recurrences. In two patients, the recurrence was limited to the liver and occurred within 28 months. The other patients developed distant metastasis (spleen and peritoneum). Two of these patients did not receive surgical treatment. In the patient that received surgical treatment, the metastatic disease occurred 13 years and 2 months after transplant. In these cases, there was necrosis (n=2), low nuclear grade (n=2), and mitotic count ranged from 0 to 2.

Conclusions: Hepatic EHE is indolent but recurrence and metastasis is possible. In our study, the metastatic rate is 10% (n=2) and mortality rate is 16% (n=3), in keeping with those rates of soft tissue EHE. Complete resection of the tumor appears to be curative. While tumor size and high mitotic count were proposed for risk stratification criteria in soft tissue, there was no correlation in the liver.

1732 Immunohistochemical Co-overexpression of CPEB1 and GPC3 Indicates Poor Prognosis in Hepatocellular Carcinoma

Wenqing Cao[1], Rami Imam[2], Jiangzhou Yu[3]. [1]New York University Langone Medical Center, New York, NY, [2]New York University, New York, NY, [3]University of Illinois at Chicago

Background: There remains controversy in whether immunohistochemical marker glypican 3 (GPC3) could assist in HCC prognostication. Novel markers that can accurately predict prognosis of HCC is needed to optimize therapeutic strategy and improve patient outcome. Our previous study suggested that cytoplasmic polyadenylation element-binding protein 1 (CPEB-1) might contribute to tumor progression and associated with poor prognosis of HCC. In this study, we evaluated the prognostic value of CPEB1 or/and GPC3 in HCC via correlating their expression with patient survival.

Design: 43 HCC resection specimens from 37 patients were selected for evaluation. Sections were immunostained with CPEB1 and GPC3 antibodies. Expression of CPEB1 and GPC3 was estimated with the H-Score method and correlated with tumor grade, stage, small/large vessel invasion, lymph node metastasis and patient survival. Student t-test, ANOVA, and Kaplan–Meier methods were adopted for data analysis.

Results: Compared to the adjacent nontumoral areas, HCCs showed significantly higher expression of CPEB1 (H-Score 101.7±19.1 vs.

141.7±52.2, P<0.001), and GPC3 (H-Score 3.0±1.7 vs. 121.9±15.1, P<0.01). Neither CPEB1 nor GPC3 expression was associated with tumor grade, stage, vessel invasion or lymph node metastasis. The patients with high expression of CPEB1 (H-Score ≥120) or GPC3 (H-Score≥140) in HCC had a poor prognosis with median survival times of 72 and 56 months, respectively. Co-overexpression of CPEB1 (H-Score ≥120) and GPC3 (H-Score≥140) in HCC was associated with poorer outcomes with a median survival of 52 months (figure 1).
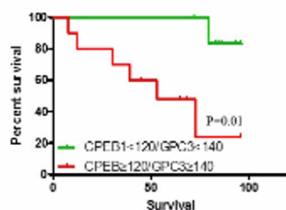
Conclusions: CPEB1 and GPC3 are overexpressed in HCC. High expression of either CPEB1 or GPC3 may relate to poor prognosis of HCC. Moreover, co-overexpression of CPEB1 and GPC3 associates with worse patient outcomes. The data suggests co-overexpression of CPEB1 and GPC3 may be a potential predictor of HCC prognosis.

1733 Network Analysis Identifies Phenotypic Subgroups of Autoimmune Hepatitis

Romulo Celli[1], *Ananta Gurung*[2], *David N Assis*[3], *Dhanpat Jain*[4]. [1]Yale University School of Medicine, Branford, CT, [2]Royal Columbian Hospital, New Westminster, BC, [3]Yale Pathology School of Medicine, Hamden, CT, [4]Yale Univ./Medicine, New Haven, CT

Background: Autoimmune hepatitis (AIH) demonstrates remarkable diversity in clinical and pathologic presentation, and response to primary treatment. Clinical diagnosis relies upon clinicopathologic correlation and is aided by scoring systems. Conventional analysis of associations of various features with AIH simply tells us how strongly they are associated with AIH. Unlike conventional data analysis which is hypothesis driven, network analysis is able to generate hypotheses and has to date has not been used on surgical pathology datasets. The goal of this study was to apply network analysis to identify potential associations among various pathologic features of AIH.

Design: A search of the Yale-New Haven Hospital database yielded 69 biopsies of AIH from 44 women and 8 men. Slides were reviewed by two liver specialist pathologists and the presence or absence of 23 pathologic characteristics (e.g. grade of plasma cell or lymphocyte inflammation, fibrosis, cholestasis, presence of rosettes) were recorded for each case. Non-parametric correlation among variables was assessed using the Spearman rho test and all correlations with a p value <0.01 were used. A network graph was created based on the qualifying correlations.

Results: The network model comprised 27 clinico-pathologic characteristics and 60 correlations. A property of networks, modularity, was used to divide the network into component groups of characteristics which tend to co-occur. Four specific modules were identified in the network. Broadly, these were divided into cholestatic, lymphocyte-rich, plasma cell rich, and lobular-predominant groups. Kupffer cell hyaline globules were associated with cholestasis and ductopenia. Men with AIH often tended to have endotheliitis (5 of 8) and cholangitis (8 of 8).
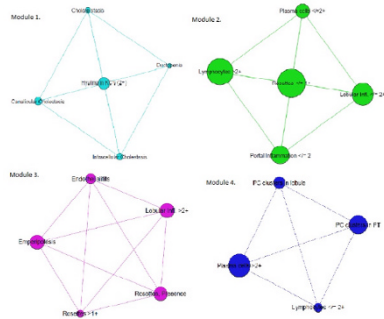
Conclusions: Using a novel network analysis technique, we identified four groups of pathologic characteristics which tend to occur together in the setting of AIH and may point to different pathobiology of AIH. These represent subgroups of pathologic disease phenotypes which may be associated with different clinical parameters, including treatment response and are not evident on conventional statistical analysis. Our hypothesis-generating approach raises the possibility that endotheliitis and cholangitis are more frequent in men with AIH, and Kupffer cell globules may be markers of cholestatic AIH. Further

studies using such subgroup analysis and evaluating clinicopathologic features and treatment response are needed.

1734 Post-Sustained Viral Response Histologic changes and Occult Hepatitis C

Romulo Celli[1], *Saad Saffo*[2], *Saleem Kamili*[3], *Nicholas Wiese*[3], *Tonya Hayden*[3], *Tamar Taddei*[2], *Dhanpat Jain*[2]. [1]Yale University School of Medicine, Branford, CT, [2]Yale University School of Medicine, New Haven, CT, [3]US Centers for Disease Control and Prevention, Atlanta, GA

Background: Direct-acting antiviral agents (DAAs) treatment in patients with chronic hepatitis C virus (HCV) infection is thought to be curative; however, despite sustained virologic response (SVR) in >90% of patients, many show persistent inflammation and fibrosis on liver histology, and develop hepatocellular carcinoma (HCC). "Occult" HCV infection has been speculated to be one of the possible mechanisms. Detailed histologic analysis in post SVR liver following treatment with DAAs and its correlation with occult HCV infection has not been performed to date.

Design: Patients with chronic HCV infection at our institution during a 2-year period were screened and those with liver tissue available for histology (biopsy or resection) were identified. Patients who achieved SVR following DAA treatment were divided into those with and without HCC post-therapy. Untreated HCV patients were included as controls. RT-PCR for a conserved HCV region was performed on a subset of patients from both groups and controls. Examination of liver histology was performed, and fibrosis was assessed using the novel PIR classification (*predominantly progressive, indeterminate, and predominantly regressive*).

Results: Of a total of 148 individuals with HCV infection, 123 were treated with DAAs, 42 of whom achieved SVR and of these 21 had HCC. There was no significant age, gender or ethnic differences between SVR patients with or without HCC. Between these cohorts, there was no difference in the proportion of cases with stage 3 or 4 fibrosis-Batts and Ludwig-(83% and 67%, p= 0.7) or in inflammatory grade (58 % and 59% grade 1, p= 0.5). Post-SVR the PIR scores were 3-6-3 among cases without HCC, and 7-3-2 in cases with HCC (p=0.2). HCV RNA was undetectable in all 46 biopsies (19 SVR without HCC, 21 SVR with HCC), while all 6 controls were positive. There was a trend for SVR patients with advanced fibrosis to have higher rate of HCC (53% to 29%), but this was not significant (p=0.4).

Conclusions: Occult HCV infection is unlikely to be the primary mechanism for persistence of inflammation, progressive fibrosis and risk of HCC in patients who have achieved SVR. While numbers are small, there was a trend for patients with advanced fibrosis (regardless of SVR status) and patients with predominantly progressive fibrosis (in the setting of SVR) to develop HCC. Long term follow-up studies to fully understand the impact of HCV cure are needed to understand the impact of SVR on fibrosis reversal and risk of HCC.

1735 Comparison of Immune Microenvironment in CD8-Rich and CD8-Poor Hepatocellular Carcinoma

Anthony Chan, *Chit Chow*, *Stephen L Chan*, *Joanna H Tong*, *Ka-Fai To*. The Chinese University of Hong Kong, Shatin

Background: Dense CD8-positive cytotoxic T-cell infiltration in hepatocellular carcinoma (HCC) is an uncommon phenomenon but it is an independent prognostic factor for overall and progression-free survival among HCC patients undergoing surgical resection. However, differences of tumor immune microenvironment between CD8-rich and CD8-poor HCCs have not been fully explored yet.

A retrospective cohort of patients with solitary primary HCC underwent surgical resection was recruited. Tumor immune microenvironment was analyzed by NanoString nCounter PanCancer Immune Profiling Panel.

Results: Totally 61 patients were included in the study with median follow-up of 67.1 months. Eleven cases (18.0%) were classified as CD8-rich HCCs (Fig.1) and associated with better overall (logrank P=0.025) and disease-free suvival (logrank P=0.033) (Fig.2). CD8 expression in HCC was significantly positively correlated with surface markers of other immune cells (CD4 for T-helper cells, FOXP3 for T-reg cells, CD79A for B-cells, NCAM1 for natural killer cells and CD68 for tumor-associated macrophages), immune checkpoints (PDL1, PD1, CTLA4, LAG3 and TIM3) as well as cytokines associated with recruitment of cytotoxic T cells (CXCL9 and CXCL10) (Table). Influx of CD8-positive cytotoxic T-cells in HCC could be hence explained by elevation of CXCL9 and CXCL10, but not associated with neo-antigen loads. Antitumor effects of CD8-positive cytotoxic T-cells may be partially neutralized by co-presence of T-reg cells and tumor-associated macrophages, and increased expression of immune checkpoints.

	Spearman rho (with CD8)	Adjusted P-value	CD8-poor Median (IQR)	CD8-rich Median (IQR)	Adjusted P-value
IMMUNE CELLS					
CD4	0.526	<0.001	278 (142-332)	414 (350-755)	0.003
FOXP3	0.296	0.044	23 (13-42)	63 (42-96)	0.046
CD79A	0.778	<0.001	55 (19-103)	644 (350-829)	<0.001
NCAM1	0.575	<0.001	36 (26-57)	121 (74-180)	<0.001
CD68	0.368	0.010	573 (418-804)	913 (580-1602)	0.039
IMMUNE CHECK-POINT					
PD1	0.605	<0.001	25 (16-35)	80 (49-112)	0.001
PDL1	0.653	<0.001	21 (14-29)	86 (72-98)	<0.001
CTLA4	0.837	<0.001	44 (20-72)	253 (194-298)	<0.001
LAG3	0.639	<0.001	57 (33-79)	147 (97-205)	<0.001
TIM3	0.620	<0.001	62 (34-95)	204 (129-349)	<0.001
CYTOKINES					
CXCL9	0.756	<0.001	261 (150-501)	4095 (1423-6672)	<0.001
CXCL10	0.450	0.001	143 (56-223)	410 (171-683)	0.017
SUMMATION OF 30 CANCER-TES-TIS ANTIGENS (CTA)			8798 (7643-12530)	10696 (8738-13090)	0.285

CD8 expression
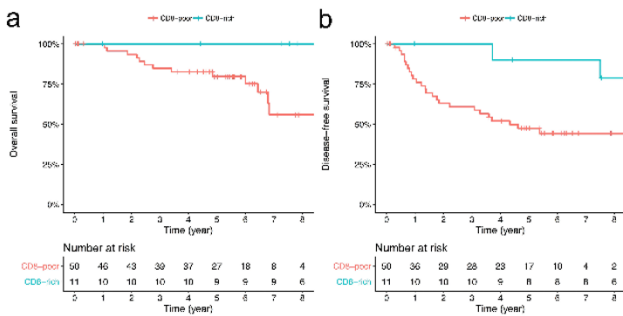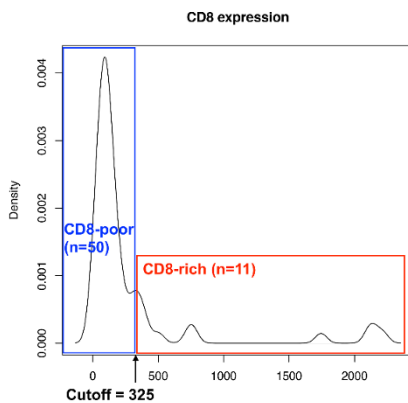
Conclusions: CD8-rich HCC is associated with better clinical outcome. Comparing tumor immune microenvironment between CD8-rich and CD8-poor HCCs allows us to have a better insight on how cytotoxic T-cells being recruited into the tumor and how their antitumor effects being counteracted by immune microenvironment.

1736 Hepatic Angiomyolipoma: Clinicopathologic Analysis of 39 Cases Including Malignant Variants

Deyali Chatterjee[1], Bella Goyal[2], Bhuvaneswari Krishnan[3], Monica Garcia-Buitrago[4], Meredith Pittman[5], Andrea L Barbieri[6], Karen Matsukuma[7], Asif Rashid[8], Dhanpat Jain[9], Deepti Dhall[10], John S Chrisinger[1]. [1]Washington University School of Medicine, St. Louis, MO, [2]Washington University School of Medicine, Saint Louis, MO, [3]Baylor College of Medicine, Houston, TX, [4]University of Miami Miller School of Medicine, Miami, FL, [5]Weill Cornell Medical College, New York, NY, [6]Yale University, New Haven, CT, [7]UC Davis Medical Center, Sacramento, CA, [8]UT-MD Anderson Cancer Center, Houston, TX, [9]Yale Univ./Medicine, New Haven, CT, [10]Cedars-Sinai Medical Center, Los Angeles, CA

Background: Hepatic angiomyolipoma (AML) is a very rare neoplasm with generally benign biologic behavior. However, malignant cases are also reported. The literature is mostly limited to case reports and case series with inconsistent reporting of histologic features.

We aimed to determine if histologic features can be associated with aggressive potential in these tumors.

Design: Due to rarity of the neoplasm, we designed a multi-institutional study approved by our IRB. All collaborators at their respective institutions performed a retrospective review of pathology material and relevant clinical information from the medical chart. In order to minimize interobserver bias, de-identified patient information and diagnostic material (glass slides or representative digital microphotographs) were reviewed by a single pathologist (DC). Only cases with histologic and immunohistochemical confirmation of AML were included in the study.

Results: A total of 39 cases were identified (17 needle core biopsies, 22 resections). There was a striking female predominance (F:M, 12:1). The mean age at diagnosis was 54.8 years (range 34-77 years). At initial presentation, multiple tumors were seen in 3 cases, while the rest presented as solitary circumscribed but unencapsulated hepatic tumors with a mean diameter of 7.4 cm (overall range 0.2-27 cm). Only 1 patient had tuberous sclerosis. The mean follow-up period was 44.4 months (range 0.2-370 months). Only 2 cases demonstrated aggressive behavior with local recurrence and distant metastasis. Both cases had mitotic activity and tumor necrosis. The other 37 cases had no evidence of disease after resection; or were alive with disease after biopsy diagnosis, with stable or slightly increasing mass size on radiologic follow-up. None of these cases showed mitosis or tumor necrosis. Histologic findings of epithelioid component of tumor cells (mean 57.5%, range 5-95%); presence of mature fat (78.5%), thick walled blood vessels (85.7%), hemorrhage (60%), ischemic necrosis (7.7%), focal cellular atypia (27%), inflammatory infiltrate (66.7%) or extramedullary hematopoiesis (36.8%) did not appear to influence biologic behavior.

Conclusions: Our study shows that the presence of mitotic activity and tumor necrosis likely portends an aggressive course in hepatic AML. Tumor size, number of tumors, or other examined histologic features, including epithelioid morphology, do not appear to correlate with adverse outcome.

1737 Argininosuccinate Synthase 1 (ASS1) is a Prognostic Marker for Tumor Hemorrhage in Inflammatory and β-Catenin-Mutated Hepatocellular Adenoma (IHCA, BIHCA)

Zhikai Chi, Brent K Larson, Maha Guindi. Cedars-Sinai Medical Center, Beverly Hills, CA

Background: Hemorrhage can be a life-threatening complication of hepatocellular adenoma (HCA). Inflammatory HCA (IHCA) is the most likely subtype to hemorrhage. Argininosuccinate synthase 1 (ASS1) was recently identified as upregulated in a subset of IHCA with hemorrhage. No studies investigating the performance of ASS1 in cohorts of IHCA are yet available beyond the initial report by Henriet et al. We evaluated ASS1 as a marker for tumor hemorrhage in a cohort of IHCA and BIHCA.

Design: 19 IHCA from 13 patients were identified using a combination of morphology and diffuse serum amyloid A (SAA) positivity, rare or patchy glutamine synthetase (GS) positivity, and intact liver fatty acid-binding protein (LFABP) expression. In addition, nuclear β-catenin stain or diffuse GS positivity was recorded to identify 4 BIHCA from 4 patients. Clinical and imaging records were reviewed as available (n=12). Microscopic hemorrhage was graded semiquantitatively as either not present (≤1% of tumor area) or present (>1% of tumor area). ASS1 immunoreactivity in each tumor was compared to that of non-tumor tissue when available, and graded as either increased/unchanged or decreased.

Results: Clinical hemorrhage was found in 2 of 12 (17%) tumors with records available for review, and both had increased/unchanged ASS1 positivity. By comparison, among the remaining 10 patients with no clinical hemorrhage, 3 (30%) had increased/unchanged ASS1 positivity. Increased/unchanged ASS1 positivity was overall 100% sensitive and 70% specific for clinical hemorrhage (Table 1).

Among all 23 IHCA and BIHCA cases, microscopic hemorrhage was found in 13 cases, of which 10 (77%) had increased/unchanged ASS1 positivity. In comparison, among 10 cases with no microscopic hemorrhage, only 2 (20%) had increased/unchanged ASS1 positivity (p<0.01, Chi-squared test) (Table 1). When positive, ASS1 was always homogenous throughout the lesion.

Table 1.

ASS1 positivity	Sensitivity	Specificity	PPV	NPV
Clinical hemorrhage (n=12)	100%	70%	40%	100%
Microscopic hemorrhage (n=23)	77%	80%	83%	73%

ASS1: argininosuccinate synthase 1; PPV: positive predictive value; NPV: Negative predictive value;

Conclusions: ASS1 positivity is highly sensitive and specific for microscopic hemorrhage in IHCA/BIHCA with high positive and negative predictive value. While the sample of cases with clinical hemorrhage is small, ASS1 showed high sensitivity and negative predictive value for clinical hemorrhage, as well, suggesting it could identify tumors at risk of hemorrhage and enable personalized management of IHCA/BIHCA. Importantly, ASS1 positivity was always homogenous and not limited to hemorrhagic areas, indicating small biopsies could be used for risk stratification without concern for tumor heterogeneity.

1738 Argininosuccinate Synthase 1 (ASS1) Identifies a Novel Subtype of Hepatocellular Adenoma (HCA) Prone to Hemorrhage with High Sensitivity and Specificity

Zhikai Chi, Brent K Larson, Maha Guindi. Cedars-Sinai Medical Center, Beverly Hills, CA

Background: Current immunohistochemistry (IHC) correlates well with molecular classification of inflammatory HCA (IHCA), β-catenin mutated HCA (BHCA), β-catenin mutated inflammatory HCA (BIHCA) and HNF-1a mutated HCA (HHCA). However, 10% HCAs remain unclassified (UHCA), which have a tendency to hemorrhage. Recently, argininosuccinate synthase 1 (ASS1) was reported as a marker for a new subtype of HCA that would otherwise be UHCA. No studies are yet available beyond the initial report by Henriet et al evaluating the performance of this new marker in cohorts of various HCA subtypes. We evaluated ASS1 expression in a cohort of HCA that included UHCA.

Design: 53 HCA from 41 patients with previously-performed serum amyloid A (SAA), β-catenin, and glutamine synthetase (GS) IHC were assessed by morphology and IHC. Additional liver fatty acid-binding protein (LFABP) and ASS1 IHC were evaluated. Subtyping was performed using a combination of the typical morphologic features and diffuse positivity for SAA (IHCA); nuclear β-catenin stain or diffuse GS reactivity (BHCA); diffuse SAA positivity with either nuclear β-catenin staining or diffuse GS positivity (BIHCA); or loss of LFABP (HHCA). ASS1 positivity in each tumor was then compared to that of non-tumor tissue when available, and graded as either increased/unchanged or decreased.

Results: Examination of morphology and IHC produced a working diagnosis of 20 (38%) IHCA, 2 (4%) BHCA, 4 (8%) BIHCA, and 20 (38%) HHCA. The remaining 7 (13%) cases would have comprised UHCA subtype. Increased/unchanged ASS1 positivity was found in 6 of 7 UHCA (86%); 10 of 20 IHCA (50%); 0 of 2 BHCA (0%); 2 of 4 BIHCA (50%); and 4 of 20 HHCA (20%) (Table 1). Increased/unchanged ASS1 positivity was overall 86% sensitive and 65% specific for the new subtype (Table 2). Half of IHCAs and BIHCA had increased/unchanged ASS1 positivity, though they are easily identified by their well-described morphological and IHC findings. Therefore, after excluding IHCA and BIHCA cases, ASS1 sensitivity remained 86%, but specificity increased to 82% (Table 2).

Table 1.

HCA subtype	ASS1 increased/unchanged, n (%)	ASS1 decreased, n (%)
HHCA	4/20 (20%)	16/20 (80%)
BHCA	0/2 (0%)	2/2 (100%)
BIHCA	2/4 (50%)	2/4 (50%)
IHCA	10/20 (50%)	10/20 (50%)
UHCA	6/7 (86%)	1/7 (14%)

HCA: hepatocellular adenoma; ASS1: argininosuccinate synthase 1; HHCA: HNF-1a mutated HCA; BHCA: β-catenin mutated HCA; BIHCA: β-catenin mutated inflammatory HCA; IHCA: inflammatory HCA; UHCA: unclassified HCA

Table 2.

ASS1 positivity	Sensitivity	Specificity	PPV	NPV
All HCA (n=53)	86%	65%	27%	97%
HCA excluding IHCA and BIHCA (n=29)	86%	82%	60%	95%

ASS1: argininosuccinate synthase 1; HCA: hepatocellular adenoma; IHCA: Inflammatory hepatocellular adenoma; BIHCA: β-catenin mutated inflammatory HCA; PPV: positive predictive value; NPV: Negative predictive value

Conclusions: ASS1 is useful for diagnosing the new ASS1-positive HCA subtype with high sensitivity, high specificity, high negative predictive value, and moderate positive predictive value in combination with an IHC panel and thorough morphological evaluation. This novel immunostain will further decrease the proportion of UHCA, and it will identify the ASS1-positive HCA subtype, which is more prone to hemorrhage, potentially impacting management.

1739 Clinical Significance of Trk Receptor Expression as a New Therapeutic Target in Hepatocellular Carcinoma

Sangjoon Choi, Sang Yun Ha. Samsung Medical Center, Seoul

Background: Hepatocellular carcinoma (HCC) does not have a target treatment other than sorafenib despite poor prognosis. Recently, the oncogenic fusion of the tropomysin receptor kinase (Trk) receptor family encoded by the NTRK gene has been found in several carcinomas, and about 10 target therapies targeted therewith have been developed and clinical trials are in progress. However, the results of studies on the expression of Trk receptor in hepatocellular carcinoma have not yet been published.

Design: Immunohistochemical staining was performed using anti-TrkA+B +C antibody (ab181560, Abcam) in the 288 curatively resected primary HCC samples at Samsung Medical Center, Seoul, from July 2000 to May 2006.

Results: Expression of Trk protein was increased in 21 (7.3%) of 288 cases. In a survival analysis with a mean follow-up of 106 months, Trk overexpression group showed a shorter trend in recurrence-free survival (RFS) (p = 0.092) and overall survival (OS) (p = 0.079) than in the low expression group. Difference in RFS and OS was statistically significant in specific sub-populations such as HCCs with AJCC T1 stage, size less than 5 cm, no cirrhosis, no vascular invasion, or Edmondson grades I and II. Multicentric occurrence was more frequently found in Trk-overexpressing group than in the low-expression group (31.6% vs. 5.6%, p = 0.001). In multivariate analysis, Trk expression was also an independent prognostic factor in both RFS (p = 0.010, hazard ratio 1.998) and OS (p = 0.008, hazard ratio 2.299).

Conclusions: Overexpression of Trk protein was confirmed in about 7% of hepatocellular carcinoma tissues, and it was related to multicentric occurrence and short survival of patients. Thus, it is indirectly demonstrated that Trk expression plays an important role in the development and progression of hepatocellular carcinoma, and emerging target therapy against Trk protein could be applicable in patients with Trk-overexpressed HCC.

1740 The Prognostic Role of Preoperative Neutrophil-Lymphocyte Ratio in Patients with Hepatocellular Carcinoma After Curative Hepatectomy: Possible Association with Tumor Necrosis and Tumor Infiltrating Lymphocytes

Sangjoon Choi, Sang Yun Ha. Samsung Medical Center, Seoul

Background: Blood neutrophil-to-lymphocyte ratio (NLR) is one of the index representing systemic inflammation, and preoperative high NLR have been suggested as an independent prognostic factor in HCCs after curative hepatectomy in previous studies. However, the cutoff value of NLR with highest prognostic significance was not consistent, and the mechanism of this phenomenon remains unclear.

Design: We calculated preoperative NLR from complete blood count obtaining before 14 days from operation day, in 234 patients with curative resection for primary HCCs at Samsung Medical Center, from July 2000 to May 2006. To find the optimal cutoff value with level of the highest statistical significance related to patient survival, X-Tile statistics package (Yale University, New Haven, CT, USA) was used. Histologically, presence of tumor necrosis and the degree of tumor infiltrating lymphocytes were determined.

Results: High preoperative NLR (≥2.5) was observed in 28 (12.0%) out of 234 HCCs, and was significantly associated with younger age, larger tumor size, high Edmonson grade, microvascular invasion, major portal invasion, advanced AJCC T or BCLC stage and low albumin level. Patients with high preoperative NLR showed shorter disease specific survival (DSS) (p=0.002) and a tendency of shorter recurrence-free survival (RFS) (p=0.096). Tumor necrosis was more frequently identified in high NLR group than in low group (25.8% vs. 7.0%, p<0.001), while tumor infiltrating lymphocytes were less frequently found in a high NLR group (p=0.012). Patients with tumor necrosis showed shorter DSS (p<0.001) and RFS (p<0.001), and patients with no tumor infiltrating lymphocytes showed shorter DSS (p<0.001) and a tendency of shorter RFS (p=0.100). On multivariable analysis including covariables (age, tumor size, Edmonson grade, microvascular invasion, major portal vein invasion, intrahepatic metastasis, serum albumin level and serum AFP level) with statistical significance in univariate analysis, preoperative NLR was an independent prognostic factor for DSS (Hazard ratio : 2.05 (95% Confidence interval 1.139-3.691), p=0.017), not for RFS. However, the independent prognostic effect of NLR for DSS was disappeared as adding tumor necrosis and tumor infiltrating lymphocytes as covariables.

Conclusions: Prognostic effect of high NLR might be originated from prognostic effect of tumor necrosis or tumor infiltrating lymphocytes.

1741 Prognostic Explant Histopathological Features in Patients Undergoing Orthotopic Liver Transplantation for Nonalcoholic Fatty Liver Disease

Ying-Hsia Chu[1], Rao Watson[1]. [1]University of Wisconsin Madison, Madison, WI

Background: Nonalcoholic fatty liver disease (NAFLD) is one of the leading indications for orthotopic liver transplantation. Post-transplantation recurrence of NAFLD has been frequent and adversely affects recipient outcome. Although prior research has shed light on the demographic and clinical predictors of NAFLD recurrence, the prognostic value of native liver histopathology remains unexplored. This study aims to investigate the prevalence of steatohepatitis in explanted liver and to correlate with recurrent disease in patients undergoing transplantation for NAFLD-related cirrhosis.

Design: Institutional surgical pathology database was queried for patients undergoing transplantation for NAFLD-related cirrhosis between 2002 and 2016. Cases with concurrent alcoholic, viral or metabolic causes of cirrhosis and/or intrahepatic neoplasms were excluded. NAFLD activity was scored and fibrosis staged in each specimen using the NASH clinical research network scoring and staging criteria. Electronic medical records were reviewed for clinical characteristics and post-transplant clinical outcome.

Results: A total of 73 patients underwent orthotopic liver transplantation for NAFLD-related cirrhosis at a mean (range) age of 58 (42-72) years. In the explants, significant steatosis was seen in 23 (32%), lobular inflammation in 17 (23%) and hepatocyte ballooning in 23 (32%) cases. During a median (range) follow-up of 51 (1-184) months, 15 (21%) patients had biopsy-proven NAFLD recurrence including steatosis (n=4), steatohepatitis (n=10) and fibrosis (n=10). Two deaths and one re-transplantation resulted from NAFLD-related allograft cirrhosis. There were no differences in baseline characteristics (including gender, race, BMI, metabolic risk factors) between patients with and without steatohepatitis at time of transplant. By chi-square test, recurrence was associated with the presence of explant steatosis (P<0.05) and hepatocyte ballooning (P<0.05), but not lobular inflammation. A trend toward significance (P=0.09 by Student's t test) was also seen with NAFLD recurrence correlated with higher pre-transplant body mass index.

Conclusions: Explant steatosis and hepatocyte ballooning are predictive of NAFLD recurrence in the current cohort, supporting the potential clinical utility of explant histopathology as an indicator of patients at risk for disease recurrence at time of transplantation.

1742 Clinicopathological Characteristics of Intrahepatic Cholangiocarcinoma According to Gross Morphologic Type: Cholangiolocellular Differentiation, Inflammatory and Proliferative Features

Taek Chung, Hyungjin Rhee, Ha Young Woo, Ji Hae Nahm, Gi Hong Choi, Young Nyun Park. Yonsei University College of Medicine, Seoul, Korea

Background: Intrahepatic cholangiocarcinoma (iCCA, ICD-O code 8160/3) is a heterogenous neoplasm, and the clinical significance of gross type remains controversial. Recently, our integrative analysis combining genomic data with histopathologic features revealed that iCCAs with cholangiolocellular differentiation (CD) (> 10 % of tumor) was related to inflammation-related features and better clinical outcome, in contrast those without CD revealed proliferation-related signature and more similarity to pancreatic ductal adenocarcinoma (PDAC). In this study, the clinicopathological features of iCCA including CD, inflammatory and proliferative features and similarity to PDAC were evaluated according to the gross types.

Design: Total 108 cases of iCCAs and 58 cases of PDAC were enrolled. Immunohistochemical staining for the markers of inflammatory (CRP, FGB and CDH2), proliferative (pERK1/2, Ki-67) and PDAC (CLDN18 and CTSE) signature, and clinicopathological analysis were performed.

Results: The gross types of iCCAs were mass forming (MF) in 87 cases, periductal infiltrative (PI) in 8 cases, and mixed type in 13 cases. CD was found in 20 (23%) cases of MF type, but not in PI or mixed type (P=0.046). CRP and FGB expression was relatively higher in MF than in PI or mixed type (P<0.1 for all). CDH2 expression showed no significant difference according to the gross type. When MF type was further subgrouped into MF with and MF without CD, CRP, FGB and CDH2 expression was significantly higher in MF with CD compared to the other types (P<0.05 for all). Proliferation-related immunophenotype revealed no significant difference according to the gross type. PDAC-like immunophenotype gradually increased in the order of MF, mixed, and PI (P=0.035). Among the cases of MF type, MF without CD showed more similarity to PDAC compared to MF with CD (P < 0.029). The overall survival showed no significant difference according to the gross types of iCCAs. When MF was further divided according to CD, MF with CD revealed a better overall survival than the other gross types (P=0.013).

Conclusions: MF type of iCCA is a heterogenous group. MF type with CD is considered to have higher inflammation-related immunophenotype, less similarity to PDAC and better outcome compared to the other gross types of iCCAs including MF type without CD.

1743 Utility of Immunohistochemical Stain for IMP3 and Ki67 Index in Differentiating Intrahepatic Cholangiocarcinoma from Benign Bile Duct Lesions on Core Biopsy

Katrina Collins, Christy Perez-Valles, Saverio Ligato. Hartford Hospital, Hartford, CT

Background: Distinction of benign from malignant biliary lesions can be diagnostically challenging, particularly on small core biopsies due to significant morphologic overlap between benign intrahepatic bile duct proliferations (e.g., bile duct adenoma) and well differentiated intrahepatic cholangiocarcinoma (ICC). The aim of our study was to evaluate if the use of insulin like growth factor II mRNA binding protein-3 (IMP3) and Ki-67 index may help in distinguishing benign from malignant intrahepatic bile duct proliferations on core biopsies.

Design: IMP3 and Ki67 index were evaluated in core biopsies of 14 benign bile duct proliferations (7 bile duct adenomas, and 7 bile duct hamartomas) and 14 peripheral ICCs [9 bile duct type (BD-ICC) and 5 cholangiolar type (CC-ICC)]. BD-ICC consisted of ductal adenocarcinoma with a minor tubular component, if present, restricted to the tumor-liver interphase, whereas CC-ICC was characterized by only a tubular component. Intermediate to strong (2+/3+) cytoplasmic stain for IMP3 involving >50% of the lesion was interpreted as positive. For Ki67 index, hot spots were identified and manual counting of positive tumor cells in five photomicrographs (x20 magnification) was performed. We considered a Ki67 value of < 5% to be negative and a value of ≥ 5% positive.

Results: IMP3 was positive in 9/14 ICCs (60%) and negative in all 14 benign lesions. Interestingly, IMP3 staining was expressed in all 9 BD-ICCs, but was negative in all 5 CC-ICCs. Ki67 index was high in all ICCs and low in all benign lesions (12.1% in ICCs and <1% in benign biliary lesions, n= 14 vs. n = 14, P <.0001). No significant difference in average proliferative index was observed between BD-ICCs and CC-ICCs (9.5% vs. 14.7%, n= 9 vs. n= 5, respectively, P=0.175).

	Total	IMP3		Ki67 Index	
		+	−	<5%	≥5%
BDA	7	0/7 (0%)	7/7 (100%)	7/7 (100%)	0/7 (0%)
BDH	7	0/7 (0%)	7/7 (100%)	7/7 (100%)	0/7 (0%)
ICC	14	9/14 (64%)	5/14 (36%)	0/14 (0%)	14/14 (100%)
ICC-BD	9	9/9 (100%)	0/9 (0%)	0/9 (0%)	9/9 (100%)
ICC-CC	5	0/5 (0%)	5/5 (100%)	0/5 (0%)	5/5 (100%)

BDA: bile duct adenoma; BDH: bile duct hamartoma; ICC: Intrahepatic cholangiocarcinoma, BD: bile duct type, CC: cholangiolar type

Conclusions: Our data suggests that in small core biopsies, IMP3 is useful in differentiating BD-ICCs (IMP3 +) from benign intrahepatic bile duct proliferations (IMP3 –), but not CC-ICCs from benign lesions (both of which are IMP3 –). Instead the use of Ki-67 index, is more specific and highly sensitive (100%) in differentiating both types of peripheral ICCs (>5%) from benign intrahepatic biliary lesions (<1%).

1744 Citrullinemia type 1 (CTLN1): clinicopathological characterization in a series of cases

Laia Coromina-Hernandez[1], Bijan Eghtesad[1], Rondell Graham[2], Daniela Allende[1]. [1]Cleveland Clinic, Cleveland, OH [2]Mayo Clinic, Rochester, MN

Background: CTLN1 is an autosomic recessive urea cycle disorder characterized by deficiency or absence of the enzyme argininosuccinate synthetase. Patients can present early in life with recurrent hyperammonemia leading to progressive neurological damage, coma and death. Liver transplant is the only curative therapy. The spectrum of histologic findings and progression of the disease over time is poorly characterized in the literature.

Design: After IRB approval, cases were identified in a clinical database (2010-2017), all patients were siblings. Clinical information was obtained from chart review. Explanted livers were examined. H&E stain slides as well as histochemical stains (Prussian Blue, PAS, PAS-D, trichrome, rhodanine stains) were assessed.

Results: We included 4 siblings (2 females), 11 to 27 years old with diagnosis of CTLN1. Three cases were diagnosed at birth, one at age 7 after seizures. Liver function tests and CT of the liver were normal in all cases. The patients underwent liver transplant at age 11, 20, 22 and 26. The explanted livers were grossly unremarkable, weighing 669 to 1774 grams. Macrovesicular steatosis was seen in 2 cases (5% of hepatocytes). Approximately 30% of hepatocytes were enlarged, pale with distinct cell membranes and seen in periportal and centrilobular perivascular regions in 3 cases. Those cells were focally positive for PAS, while negative on PAS-D. Rare eosinophilic inclusions were focally noted in swollen hepatocytes. Rare acidophil bodies were seen in 3 cases. No cholestasis was seen. Rhodanine and

Prussian Blue stains were negative. The youngest sibling demonstrated only minimal glycogenosis (<5% of the hepatocytes) and no evidence of steatosis or cholestasis. There was no evidence of portal or lobular inflammation in any of the cases. The interlobular bile ducts and hepatic vasculature were intact in all cases. There was no significant fibrosis in any of the cases on trichrome stain. Electron microscopy results are pending.

Conclusions: This is one of the largest series of CTLN1 and the first that includes members of the same family at different ages. Even though histologic findings in CTLN1 have been described as non-specific, the constellation of findings seen in our cases was very characteristic. Mild steatosis, patches of pale swollen hepatocytes and focal glycogenosis, without significant fibrosis, were the most common findings. Among this cohort, there seem to be increasing accumulation of injury and histologic changes in hepatocytes over time.

1745 Transcriptome and Exome Analysis of Mucinous Cystic Neoplasm of the Liver Reveals Novel Insights

Thomas Czeczok[1], Daniela Allende[2], Bita V Naini[3], Michelle Reid[4], Maria Westerhoff[5], N. Volkan Adsay[6], Rondell Graham[7]. [1]Mayo Clinic, Rochester, MN, [2]Cleveland Clinic, Cleveland, OH, [3]UCLA Medical Center, Santa Monica, CA, [4]Emory University Hospital, Atlanta, GA, [5]University of Michigan, Ann Arbor, MI, [6]Medical College of Wisconsin, Milwaukee, WI, [7]Mayo Clinic, Rochester, MN

Background: Mucinous cystic neoplasms (MCN) of the liver are distinctive neoplastic biliary cysts with an ovarian stroma. MCNs have various degrees of dysplasia and may progress to invasive carcinoma. Molecular characterization of MCNs of the liver has not been performed and the key genomic drivers of MCNs are unknown.

Design: MCNs of the liver were retrieved, and histologic sections reviewed to confirm the diagnoses and select appropriate blocks for ancillary studies. Immunohistochemistry for ER, keratins 7 and 19, and CDX2 were performed. RNASeq was performed on formalin-fixed paraffin-embedded (FFPE) sections of 8 tumor-normal pairs. Pathway analysis and differential expression analyses were carried out. Exome sequencing was performed on FFPE sections of 10 tumor–normal pairs.

Results: 61 MCNs (all women) affecting patients aged 22-70 years (median 41) were retrieved. The median tumor size was 10 cm (range 1.7 - 28 cm). All cases were characterized by multilocular cystic masses lined by epithelium with low grade dysplasia only and underlying spindle stroma. None of the analyzed tissue had carcinomatous transformation. ER was positive in the stromal cells in all cases tested while keratin 7 and 19 highlighted the epithelium in all cases. RNASeq revealed upregulation of the Sonic Hedgehog pathway (p-value of 3.46E-05) in the tumor compared to normal in all cases. Markers of ovarian stroma, ER, PR, inhibin α and WT-1 were also upregulated. In contrast, T helper 1 and 2 pathways (p-value of 1.74E-16) and markers of immune response, TNF-α and IFN-γ were downregulated in all cases. Recurrent somatic mutations in *PI3KCA/AKT* pathway genes were identified in 4 of 5 cases with sequencing data. Ongoing sequencing analysis of the remaining cases is pending.

Conclusions: MCN of the liver is a distinctive biliary neoplasm characterized by the presence of ovarian type stroma, consistent upregulation of the Sonic Hedgehog pathway and downregulation of the immune response pathways. Ongoing molecular analysis will attempt to validate recurrent somatic mutations in the *PI3KCA/AKT* pathway as potential oncogenic drivers of MCN and its pathway abnormalities. These data may provide insights into the neoplastic pathogenesis of these tumors.

1746 IgA anti-tTG Co-localization Technique is Useful to Identify Celiac Associated Liver Diseases

Prasenjit Das, Rimlee Dutta, Govind K Makharia, Asif Iqbal. All India Institute of Medical Sciences, New Delhi, India

Background: The aim of this study was to see the spectrum and prevalence of liver dysfunction (LD) in Indian adult patients with celiac disease (CeD) and to see if IgA anti-tissue transglutaminase (tTG) co-localization can help in diagnosis.

Design: A total of 146 patients (pt) with treatment naive CeD were investigated for presence of LD, defined as: increased serum transaminase and alkaline phosphatase levels >1.5 times of normal, coarse liver architecture, liver stiffness score >6 kPa or vascular abnormality on doppler study. Serum anti- tTG titer, along with virological, biochemical, and histological examination of duodenal biopsies were performed. IgA anti-tTG co-localization was done by dual-color immunohistochemistry and confocal microscopic examination on both intestinal and liver biopsies, along with in controls. GFD was instituted and pts were followed up till 9 months.

Results: LD was noted in 27 (18.5%) celiacs, characterized by transaminitis, hyperbilirubinemia and elevated LSM values in

85.2%, 14.8% and 7% pts respectively. Serum anti-tTG fold rise in the former was 10.6, in comparison to 6.5 in celiacs without LD. Following modified Marsh grades were seen in duodenal biopsies: 3a- 5(18.5%), 3b- 13(48.1%), 3c-9(33.3%). Histology (liver biopsy in 25 pts) along with other work-up suggested following diagnoses: chronic hepatitis (12%), autoimmune hepatitis (12%), steatohepatitis (12%), obliterative portal venopathy (8%), granuloma (4%), cirrhosis (8%) and sinusoidal dilatation (44%). IgA anti-tTG co-localization was noted in the intestinal epithelial cells, as well as in subepithelial region. Liver biopsies showed colocalization of IgA anti-tTG in sinusoidal lining cells, as well as focally in hepatocyte cytoplasm (Fig arrows). Similar colocalization was not identified in controls. Based on these findings diagnosis of celiac associated LD was established. Post-GFD serum transaminitis, fatigue and ascites improved in 17(73.9%), 14(87.5%) and 3(60%) pts respectively, while diarrhoea resolved in 7(70%) and hemoglobin normalized in 3(14.2 %) pts.
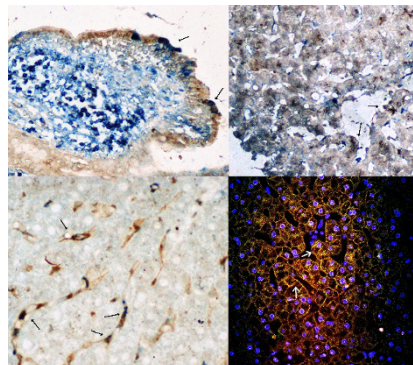
Conclusions: Co-localization of IgA anti-tTG in tissue sections helped us to establish diagnosis of celiac associated LD in our cohort. Improvement of serum transaminase level post-GFD further supports their association to CeD. Hence, IgA anti-tTG co-localization can be a useful method to establish diagnosis of extra-intestinal celiac disease.

1747 Unraveling The Genetic Mystery Of Progressive Familial Intrahepatic Cholestasis (PFIC) By Targeted Next Generation Sequencing For Deciphering The Clinical And Pathological Complexity Of This Disease

Ashim Das, Suvradeep Mitra, Babu R Thapa, Rakesh Vasishta, PGIMER, Chandigarh

Background: Progressive familial intrahepatic cholestasis (PFIC) is a rare cause of paediatric cholestasis syndrome and its exact characterization is important for the accurate management of patients. The aim is to understand the clinical and pathological complexity and heterogeneity of this disease by unraveling the genetic changes.

Design: All prospective and retrospective cases of PFIC during the period 2013-2016 were included. The detailed clinical, and histological features were carried out in all cases but ultrastructural parameters were studied in a small group of patients. Targeted next generation sequencing for PFIC1/PFIC2/PFIC3 genes covering all the exons was done for identification of PFIC variants in a small cohort of patients.

Results: A total of 48 patients of PFIC were studied. The mean age of presentation was 18 months with a male: female ratio 6:4. Positive family history (10%) and consanguineous marriage (8%) was also present. The mean biochemical parameters were total/ conjugated bilirubin (7.5/5 mg/dL), SGOT (210.7 U/L), SGPT (105.4U/L), ALP (534.8 U/L), total protein/ albumin (6.34/3.25 g/dL) and INR (1.4). The liver biopsies showed portal, periportal or portoportal bridging fibrosis. Mild to moderate portal inflammation and ductal paucity were noted along with ductular metaplasia, intracanalicular and intrahepatocytic cholestasis, giant cell transformation and cholestatic rosettes. The ultrastructural features studied in 15 cases, were non-specific and showed changes of prolonged cholestasis with or without mitochondrial changes. The DNA of 10 PFIC patients and the mother of two patients were subjected to targeted sequencing. Ninety percent of these cases showed homozygous or compound heterozygous ABCB11 missense mutation of p.Val444Ala (c.1331T>C) along with p.Asn591Ser (c.1772A>G) missense mutation in ABCB11 in 30% cases. Heterozygous ABCB4 missense p.Thr175Ala (c.523A>G) and Homozygous ABCB4 missense p.Arg652Gly (c.1954A>G) were also seen in one case each. A couple of patients showed novel deleterious missense variant of ABCB11 gene mutations involving the ABCB11 gene. Two of our patients showed a much complex genotype by lodging coexisting ABCB4 variants (Table).

Sample	GGT	Clinical suspicion	Significant known non-synonymous variant	Deleterious novel non-synonymous variant	Clinico-histopathological impression
P1	Normal	PFIC2	Heterozygous ABCB11 missense p.Val444Ala (c.1331T>C) + Homozygous ABCB4 missense p.Arg-652Gly (c.1954A>G)	Compound heterozygous ABCB11 missense p.Arg1128Gly (c.3382C>G) + p.Arg571Gly (c.1711A>G)	Morphologically PFIC2
P2	Normal	PFIC2	Homozygous ABCB11 missense p.Val444Ala (c.1331T>C)	Homozygous ABCB11 missense p.Ser809Phe (c.2426C>T)	Morphologically PFIC2
P3	High	PFIC, unclassified	Compound Heterozygous ABCB11 missense p.Val444Ala (c.1331T>C) + p.Asn591Ser (c.1772A>G)	-	Morphologically PFIC2
P4	Normal	PFIC2	Homozygous ABCB11 missense p.Val444Ala (c.1331T>C)	-	Morphologically PFIC2
P5	Not available	PFIC, unclassified	Compound Heterozygous ABCB11 missense p.Val444Ala (c.1331T>C) + p.Asn591Ser (c.1772A>G)	-	Morphologically PFIC2
P6	Normal	PFIC2	Homozygous ABCB11 missense p.Asn591Ser (c.1772A>G)	-	Morphologically PFIC2
P8	Normal	PFIC2	Heterozygous ABCB11 missense p.Val444Ala (c.1331T>C)	-	Morphologically PFIC2
P9	Normal	PFIC2	Homozygous ABCB11 missense p.Val444Ala (c.1331T>C)	-	Morphologically PFIC2
P11	Normal	Variant PFIC	Homozygous ABCB11 missense p.Val444Ala (c.1331T>C)	-	Morphologically PFIC3
1	Not done	ICP	-	Heterozygous ABCB4 missense p.Ala344Gly (c.1031C>G)	Biopsy not done
P7	Normal	PFIC2	Homozygous ABCB11 missense p.Val444Ala (c.1331T>C) + Heterozygous ABCB4 missense p.Thr175Ala (c.523A>G)	Compound heterozygous ABCB4 missense p.Arg788Trp (c.2362C>T) + p.Ala344Gly (c.1031C>G)	Morphologically PFIC2
2	Not done	H/O cholestatic jaundice during pregnancy	Homozygous ABCB11 missense p.Val444Ala (c.1331T>C)	-	Biopsy not done

Conclusions: In our population p.Valine444A and p.N591S were found to be common variants associated with PFIC 2. A. larger population case based studies are required to validate these findings. The genetic diversity of this condition can explain the clinical and pathological heterogeneity of PFIC.

1748 GRP78 Immunohistochemistry Outperforms HSP70 for the Diagnosis of Cirrhotic- and Noncirrhotic-HCC

Gustaaf de Ridder[1], *Ayako Suzuki*[1], *Liyan Xu*[1], *Diana Cardona*[2], *Jeff Groth*[1], *Rupa Ray*[1], *Manal F Abdelmalek*[1], *Salvatore V Pizzo*[1], *Cynthia Guy*[3]
[1]Duke University, Durham, NC, [2]Durham, NC, [3]Chapel Hill, NC

Background: Despite the growing number of immunohistochemical (IHC) markers, the diagnosis of hepatocellular carcinoma (HCC) can be challenging. HSP70, an endoplasmic reticulum (ER) chaperone protein, is an established IHC tool for HCC diagnosis. Other ER chaperone proteins, including GRP78 and calreticulin (CLRT), are also dysregulated in carcinogenesis. Our aim was to compare the diagnostic utility of HSP70 to GRP78 and CLRT in HCC arising from cirrhotic and non-cirrhotic backgrounds.

Design: IHC was performed on FFPE cirrhotic HCC (HCC-C, n=32), non-cirrhotic HCC (HCC-NC, n=29), cirrhotic liver (n=21), hepatocellular adenoma (HCA) (n=25), focal nodular hyperplasia (FNH, n=20), and normal liver (n=9). Staining patterns were recorded. Additionally, staining intensity was graded from 0-3+, with each grade multiplied by the percentage for a continuous score from 0 – 300. Statistical analysis included ANOVA and non-parametric pairwise post-tests performed in SAS 9.4.

Results: GRP78 expression was higher (all p<0.05) in HCC-C and HCC-NC compared to normal liver, cirrhosis, FNH, and HCA. GRP78 expression peaked in zone 3 in non-neoplastic liver. It clearly delineated tumor from background in 88% of HCC-C and 93% of HCC-NC (Fig.1 A-B). Large GRP78 aggregates were seen in background liver (cirrhotic and non-cirrhotic), but were absent in 56 of 61 HCC cases (92%). CLRT marked zone 1 in non-neoplastic liver (Fig.1 E). CLRT levels distinguished only HCC-NC from FNH and HCA. It distinguished tumor from background in 72% of HCC-NC (Fig.1 C-D), but only 22% of HCC-C. Most HCC-NC cases had large CLRT-positive aggregates, distinct from background liver. CLRT showed distinct periseptal positivity in 85% of FNHs (Fig.1 F). HSP70 levels, however, differed only between HCC-C and FNH. HSP70 distinguished tumor from background in 72% of HCC-C, but only 45% of HCC-NC.

Bar = 500µm
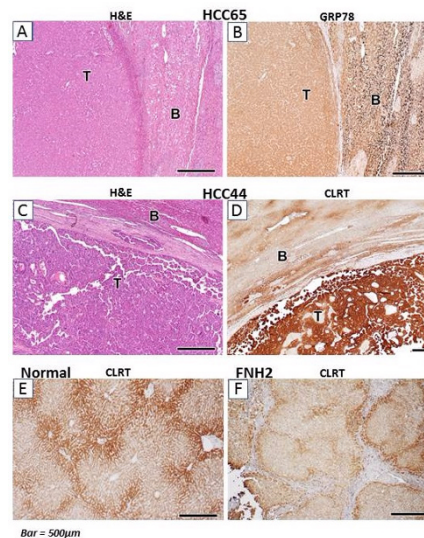
Conclusions: GRP78 IHC distinguishes ~90% of HCC-C and HCC-NC from background liver. GRP78 is most strongly expressed in zone 3 and forms large cytoplasmic aggregates in non-neoplastic liver. CLRT distinguishes >70% HCC-NC from background liver. CLRT is a novel marker of hepatic zone 1/periseptal hepatocytes. CLRT shows a distinct periseptal pattern in most FNHs. HSP70 distinguishes <50% of HCC-NC and is not an ideal marker for HCC-NC. These unique and complimentary IHC patterns suggest biologically relevant differences in the hepatic ER stress response and carcinogenesis.

1749 Impact of Specialist Review of Liver Biopsies on Clinical Care: A Five Year Review

Kyle Devins[1], *Rashmi Tondon*[2], *Emma Furth*[2], *Stuti G Shroff*[2], *Kristen Stashek*[3]. [1]Plattsburgh, NY, [2]Hospital of the University of Pennsylvania, Philadelphia, PA, [3]University of Pennsylvania, Philadelphia, PA

Background: Medical liver biopsy evaluation is critical for patient care but often complex and challenging for pathologists, especially those without liver fellowship training. The purpose of this study is to determine the frequency, types, and severity of diagnostic disagreements rendered in our subspecialty model of medical liver biopsies submitted for patients referred to our institution from community, non-specialized practices.

Design: A total of 395 cases were available for review during January 2012 and August 2017 after excluding cases with a neoplasm and/or cases referred by a community pathologist for second opinion. Diagnosis and microscopic descriptions were compared. Disagreements were categorized into major (change in pathologic diagnosis with potential for significant change in treatment or prognosis), minor, and no diagnostic disagreement based in part on additional clinical correlation.

Results: We agreed with the majority of cases (62%). However, of 38% cases with a disagreement (n=152), 74 cases involved fibrosis staging (score 0-4[cirrhosis]). Of cases with staging disagreement, 70% (n=52) were under staged by non-specialized pathologists; over all, the median difference in staging was 1.

Importantly, of the set of cases with disagreement, 24% (n= 94) were changes in disease etiology; 7% (n=29) were major with PBC/PSC (34%, n=10), autoimmune hepatitis (31%, n=9), and steatosis (21%, n=6) accounting for most major discrepancies. Other etiologies made up the remaining 14% (n=4). Interestingly, biliary diseases and autoimmune hepatitis were significantly lower in the total agreement cohort (6% and 7% of cases respectively) while steatosis was essentially the same (19%) compared to the disagreement set.

Conclusions: We suggest that targeted and novel educational modalities, including building online open-source materials, are

needed in areas of staging fibrosis and discerning biliary and autoimmune etiologies of liver disease, as these types of cases were enriched in the disagreement cohort.

1750 Cholangiocarcinoma: Era of Immune Check-Point Inhibitors

Mohamed I. El Hag[1], *Michelle Wood-Trageser*[2], *Krishna Patel*[2], *Susan Specht*[2], *Eizaburo Sasatomi*[3], *Weijing Sun*[4], *Anthony Demetris*[5]. [1]University of Pittsburgh Medical Center Presbyterian Shadyside, Pittsburgh, PA, [2]University of Pittsburgh Medical Center, [3]Department of Pathology and Laboratory Medicine, Chapel Hill, NC, [4]Kansas University Medical Center, [5]UPMC-Montefiore, Pittsburgh, PA

Background: Cholangiocarcinomas are a heterogenous group of primary liver adenocarcinomas with dismal prognosis. Arising from biliary epithelial cells (BECs), they are classified by anatomic site and histologic characteristics. BECs maintain hepatic immune homeostasis and tolerance. Malignant BECs have the ability to escape immune surveillance by influencing their microenvironment. The aim of this study is to query the immune microenvironment of these tumors for clinically actionable targets previously shown to influence hepatic-based immune reactivity: Galectin9 (Gal9; ligand) and TIM3 (receptor) which are implicated in apoptosis of lymphocytes. Markers of T cell exhaustion and/or inhibition include the co-expression of PD1 (PDL1 receptor) and TIM-3 or binding of MHCII to LAG3.

Design: 124 patients with resection specimens were selected (characteristics: 107 Caucasian, median age 68, 2 patients with viral hepatitis, 8 patients with PSC). TMA blocks were constructed from archival FFPE specimens and immunohistochemistry was performed for: mismatch repair (MMR), Gal9, PDL1, PD1, LAG3, MHCII, TIM3 and CD8. DNA extracted from the FFPE samples was sequenced using the Ion AmpliSeq Comprehensive Cancer Panel.

Results: Seven of 104 evaluable cases lacked staining for one or more MMR proteins, indicative of microsatellite instability (MSI). Of evaluable cases, 19/102 were PDL1(+), with 7/19 having>25% positivity in tumor cells. Of evaluable cases 93/103 were Gal9(+); 57/93 showed >50% positivity in tumor cells. Gal9 expression correlates with overall and recurrence free survival on Cox regression (p<0.01). No correlation was found between MSI and Gal9 expression. The tumor microenvironment is rich in PD1+/TIM3+ exhausted lymphocytes and LAG3+ and MHCII+ expressing lymphocytes. Preliminary analysis of most commonly mutated genes (>10% of specimens) include *SETD2*, *TCF7L1*, *and ARID1A*. *IDH1* and *APC* mutations were seen in only 5% of tumors while *PDGFRB* was seen in only 1 case.
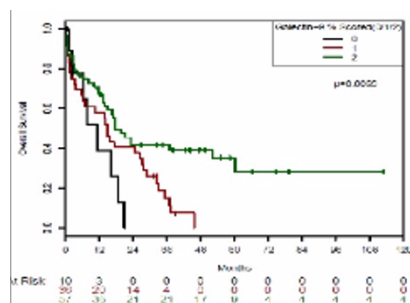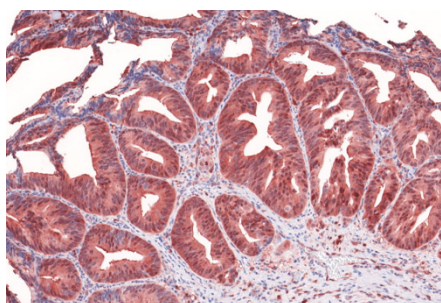
Conclusions: This preliminary analysis reveals a tumor immune microenvironment that is rich in exhausted T-cells (PD1+/TIM3+) and with abundant expression of MHCII+ and LAG3+ cells. 19% of cases were PDL1(+). 7% of cases have MSI. Results of the genomic screen are uninformative but ongoing. This analysis shows multiple targetable immune checkpoints (TIM3, LAG3 and PD1). Improved survival on cases with high Gal9 represents its tumor apoptotic properties; this dual function of Gal9 is subject of further study.

1751 Approach to The Diagnosis of Liver Allograft Antibody Mediated Rejection and The Role of C3d

Mohamed I. El Hag[1], *Nour Yadak*[2], *Anthony Demetris*[3], [1]University of Pittsburgh Medical Center Presbyterian Shadyside, Pittsburgh, PA, [2]University of Pittsburgh Medical Center, Homestead, PA, [3]UPMC-Montefiore, Pittsburgh, PA

Background: The liver is perceived as resistant to antibody mediated injury, partially due to its ability to secrete soluble class I molecules and phagocytic properties of Kupffer and liver sinusoidal endothelial cells (LSEC) which are able to clear different immune complexes, Donor Specific Antibody (DSA)-activated complement and platelet aggregates. While rare, liver allografts are not immune to acute antibody mediated rejection; usually presenting with relentless transaminitis and increased biliary complications. DSA is also associated with late graft dysfunction in pediatric liver transplants. Criteria for acute and chronic AMR have been proposed. In this blinded controlled study we aim to identify a practical approach to the diagnosis of antibody mediated injury utilizing paraffin tissue through histologic and immunophenotypic characterization of DSA positive allografts.

Design: Allograft liver biopsies with concurrent donor specific antibody measurements from 2014 to August 2017 were identified (n=89). All DSA positive cases with tissue were selected (n=20) and 29 DSA negative cases were randomly chosen. Hematoxylin and eosin stained sections were obtained and scored for: Histologic features associated with AMR h-score according to (Demetris AJ et al AM J Transplt 2016), and other morphologic features. Immunohistochemistry for C4d, C3d and CD163 was performed. C4d and C3d were given a i-score according to (Demetris AJ et al 2016) and CD163 scored based on quantity of macrophage aggregates (see tables 1,2).

Results: 9/20 DSA positive cases were C1q fixing. DSA positive allografts showed more severe biliary changes (ductular reaction and neutrophilic cholangiolitis), cholestasis, central hemorrhage and higher h-scores when compared to controls. 65% of DSA positive biopsies showed focal to diffuse C4d uptake compared to 22% of controls. CD163 showed more aggregates of macrophages in DSA positive cases. All cases showing many CD163+ aggregates or focal C3d uptake by sinusoids, central veins or portal vessels are C1q+DSA. In general, C1q+DSA allografts show higher h-score, diffuse portal and central and sinusoidal C4d uptake and severe cholestasis.

Histologic changes		DSA positive n=20	DSA negative n=29
Cellular Rejection		10 (50%)	12 (40%)
Biliary Changes	None	7	13
	Mild ductular reaction	6	13
	Mild PMN cholangiolitis	3	2
	Moderate to severe PMN chol-angiolitis	4	1
Cholestasis	None	14	21
	Mild	1	6
	Moderate	1	2
	Severe	4	0
Central Hemorrhage/necrosis		9 (45%)	6 (20%)
H-score	H-score=0	3 (15%)	16 (55%)
	H-score=1	6 (30%)	10 (34%)
	H-score=2	8 (40%)	3 (10%)
	H-score=3	3 (15%)	0

Immunophenotype		DSA positive n=20	DSA negative n=28
C4d i-score	C4d i-score=0	0	5 (18%)
	C4d i-score=1	7 (35%)	17 (60%)
	C4d i-score=2	7 (35%)	5 (18%)
	C4d i-score=3	6 (30%)	1 (4%)
		DSA positive n=17	DSA negative n=22
C3d i-score	C3d i-score=0	5 (29.5%)	12 (54.5%)
	C3d i-score=1	11 (65%)	10 (45.5%)
	C3d i-score=2	1	0
	C3d i-score=3	0	0
CD163	0= negative for macrophages	0	0
	1= positive staining/rare aggre-gates	5	19
	2= few aggregates	7	3
	3= Many aggregates	5	0
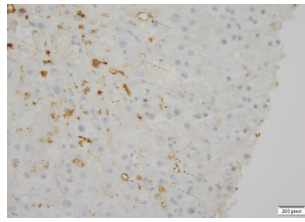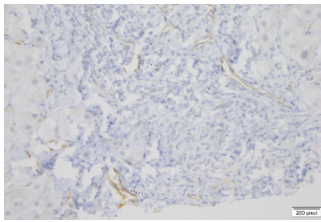
Conclusions: We illustrate that the presence of certain morphologic features with focal or diffuse C4d staining should raise suspicion for presence of donor specific antibody(ies). C3d uptake and aggregates of CD163+ macrophages appear to be associated with C1q+DSA suggesting the possibility of worse pathology for this group.

1752 Histologic Changes of Noncirrhotic Portal Hypertension (NCPH) in Post-Phlebotomy Biopsies from Hemochromatosis Patients: Evidence for Regressed Fibrosis

Tony El Jabbour[1], Kelsey McHugh[2], Deepa T Patil[3], Chunlai Zuo[1], Sungeun Kim[4], Hwajeong Lee[5]. [1]Albany Medical Center, Albany, NY, [2]Lakewood, OH, [3]Cleveland Clinic, Cleveland, OH, [4]Albany Medical College, Albany, NY, [5]Albany Medical College, Guilderland, NY

Background: Regressed cirrhosis is within the spectrum of histologic changes seen in biopsies of patients with noncirrhotic portal hypertension (NCPH). As phlebotomy is believed to induce regression of liver fibrosis in hemochromatosis patients, we decided to assess histologic changes in pre- and post- phlebotomy liver biopsies from hemochromatosis patients as a surrogate model to study regression of fibrosis.

Design: Liver biopsies from 39 hereditary hemochromatosis patients were retrieved (2002-2016). A total of 49 biopsies (21 pre- and 28 post-phlebotomy) were reviewed (8 patients had multiple biopsies), and three variables were studied. I/F index= iron quantity (multiplicative index of granularity and zonation score;0-18) in the biopsy adjusted for the fibrosis stage. Score 1 was assigned for each of the following features that were previously described in NCPH: shunt vessels, increased number of portal vessels, phlebosclerosis, rudimentary portal tract, clustered central veins, sinusoidal dilatation, incomplete septa formation, perisinusoidal fibrosis and anisocytosis (indicative of nodular regeneration). A combined score (CS) was generated by summing the score of the histologic features. SV=Shunt vessel grade (number of portal tracts with shunt vessels divided by the total number of portal tracts) was categorized as low grade (<0.5) or high grade (≥0.5). Clinical parameters were recorded.

Results: There were 27 males and 12 females, with a mean age of 54 years (range 17-83 years). Twenty-eight were C282 homozygotes, 9 H63D homozygotes, 2 were C282Y carriers. There was a trend towards higher I/F index in pre- compared to post-phlebotomy group (13 vs. 3.7; p=0.059). Compared to pre-phlebotomy group, CS was higher in the post-phlebotomy group when the cases of advanced fibrosis were excluded (3.5 vs. 4.7; p=0.022) or when patients with risk factors for NCPH were further excluded (3.0 vs. 4.7; p=0.008). High grade SV was significantly more common in post-phlebotomy group (7% (pre-) vs. 35% (post-); p=0.035) when advanced fibrosis was excluded. Serial biopsies from 3 patients showed regression of fibrosis and increased CS in later biopsies.

Conclusions: Phlebotomy induces reduction in hepatic iron load, histologic changes of NCPH including frequent shunt vessels, and regression of the fibrosis. Our data provides direct evidence that a subset of NCPH represents regressed fibrosis/cirrhosis. Hemochromatosis cohort may be used as a model to study histologic changes in regressed fibrosis/cirrhosis.

1753 PREVIOUSLY PUBLISHED

1754 Parenchymal Rejection in Liver Transplant Biopsies: A Form of Rejection Distinct from Severe Acute Cellular Rejection

Daffolyn Rachael Fels Elliott, Linda Ferrell, Bilal Hameed, Sanjay Kakar, Ryan Gill. University of California San Francisco, San Francisco, CA

Background: Acute cellular rejection (ACR) is considered as severe when accompanied by perivenular/lobular inflammation and necrosis ('Banff' criteria). The latter features can occur in the absence of ACR and have been variably designated parenchymal rejection (PR) and central perivenulitis. This study examines the clinicopathologic features and outcome in PR.

Design: Parenchymal rejection cases were identified by a database search of transplant liver biopsies (1990-2017). Exclusion criteria were age <18 years and overlapping pathology that obscured the diagnosis

of PR. PR was histologically defined by centrizonal lymphocyte predominant inflammation and hepatocellular necrosis with or without portal features of mild to moderate ACR. Drug and infectious etiologies were excluded in all cases.

Results: Fifty-one cases of isolated PR (iPR) and 26 cases of PR with ACR (PR/ACR) were reviewed. A subset of cases showed zone 2 inflammation (4 iPR, 10 PR/ACR), prominent sinusoidal lymphocytes (3 iPR, 1 PR/ACR) and periportal interface activity (3 PR/ACR). Additionally, 3 cases of plasma cell hepatitis (atypical rejection) were identified. The median time after transplant was 44 months (range 0.8-260 months) for iPR and 18.5 months (range 0.3-159 months) for PR/ACR. iPR was associated with a rise in ALT and AST that was similar to PR/mild ACR and less than PR/moderate ACR (p=0.025 (ALT), p=0.024 (AST)). Furthermore, iPR cases responded to immunotherapy intervention with decrease in ALT and AST that was similar to PR/ mild ACR, but not as pronounced as PR/moderate ACR (p=0.024 (ALT), p=0.009 (AST)). Rates of recurrent acute rejection, re-transplant or death from graft failure, and histologic evidence of chronic ductopenic rejection were similar between iPR and PR/ACR patients.

Conclusions: Parenchymal rejection represents a form of lobular injury that, in isolation, shares clinical features with cases of combined PR and mild ACR; such cases should be considered distinct from severe ACR. Standardization of terminology and classification may increase recognition of PR and help guide appropriate management.

1755 Recurrent Autoimmune Hepatitis and De-Novo Autoimmune Hepatitis in post-Orthotopic Liver Transplant, Clinical and Histologic Characterization

Iván González[1], Christopher Hartley[2], ILKe Nalbantoglu[3]. [1]Washington University School of Medicine, St. Louis, MO, [2]Milwaukee, WI, [3]Washington University in St. Louis, Saint Louis, MO

Background: Orthotopic liver transplant (OLT) is the last treatment option for end-stage liver disease, which is most commonly secondary to hepatitis C virus infection and alcoholic liver disease. Autoimmune hepatitis (AIH) is a form of severe chronic hepatitis, due to autoantibodies against hepatocyte surface antigen. AIH can recur after OLT. The clinical and histologic presentation of AIH in OLT patients without prior clinical history of AIH is termed De-novo autoimmune hepatitis (DNAIH), or Plasma cell hepatitis. It is suggested that Recurrent AIH (RAIH) has an impact on patient (pt) and graft survival. However, little is known regarding the pt and graft survival between RAIH and DNAIH.

Design: Post-OLT biopsies from 11 pts with RAIH and 22 pts with DNAIH in our institution between 2000-2017 were retrospectively identified. Attempt was made to choose the biopsy at initial presentation. All the cases were re-reviewed. The respective diagnoses were confirmed, and histologic features were noted. The clinical data were obtained from the electronic medical records.

Results: Select clinical and histologic features of RAIH and DNAIH are summarized in Table 1. Top 3 indications for OLT were HCV/HCC (41%), alcoholic cirrhosis (13.6%), and PSC/PBC (9% each) for DNAIH pts. The majority of the pts were female in both groups. RAIH pts were younger compared to DNAIH (37.8 vs 52.7 yrs, p=0.06). More cases with RAIH showed moderate portal inflammation (inf) compared to DNAIH (64 vs 27%), but severe inf was more common in DNAIH (36 vs 9%). All cases with RAIH had lobular lymphocytic inf compared to 41% of cases with DNAIH (p=0.001). Central vein endophlebitis was more common in DNAIH (64 vs 37%) and acute cholestasis in RAIH (37 vs 9%). Bile duct injury, parenchymal necrosis, and fibrosis were similar. ALT and AST levels were also similarly elevated. ANA and SMA were positive in 88 and 75% in RAIH (available in 13 pts), and 38 and 50% in DNAIH (available in 8 pts). The mean clinical follow up of pts with RAIH and DNAIH was 13 and 7.8 yrs, respectively. Graft survival was worse in pts with RAIH compared to DNAIH (55 vs 91%, p=0.016, Figure 1). Overall survival (liver related) was also worse in RAIH compared to DNAIH (64 vs 82%, p=0.25).

Table-1. Clinical and Histologic Features

	RAIH	DNAIH	p-value
Male, n (%)	4 (36%)	8 (36%)	0.3876
Age at bx, mean (range)	37.8 yrs (21.5-53.4)	52.7 yrs (23.4-78.6)	0.0686
Portal inflammation, n (%)			
Minimal	2 (18%)	1 (5%)	
Mild	1 (9%)	7 (32%)	0.42
Moderate	7 (64%)	6 (27%)	
Severe	1 (9%)	8 (36%)	
Lobular inflammation, lymphocytic, n (%)	11 (100%)	9 (41%)	0.0011
Central vein endophlebitis	4 (37%)	14 (64%)	0.522
Acute cholestasis	4 (37%)	2 (9%)	0.182
ALT IU/L, mean (range)	228 (38-526)	249 (18-1297)	0.3598
AST IU/L, mean (range)	202 (42-470)	177 (29-756)	0.2175
Follow-up, days (years)	4748 dys (13 yrs)	2853 dys (7.8 yrs)	0.1315
Graft survival (%)	55%	91%	0.0160*
Overall survival (%)	64%	82%	0.2506

Figure 1. Graft Survival from Time of Biopsy
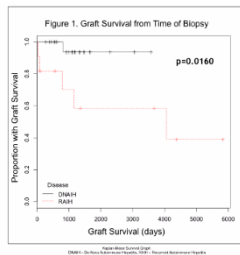
Conclusions: In our cohort, graft survival was worse in RAIH compared to DNAIH (p=0.016), as well as overall survival. Although our sample size is limited, RAIH seems to be a more aggressive form of post-OLT hepatitis associated with poor graft survival.

1756 Does Antibody-Mediated Rejection Play a Role in De-novo Autoimmune Hepatitis in Post-Transplant Liver? : An immunohistochemical characterization with C4d antibody

Iván González, John S Chrisinger, ILKe Nalbantoglu. Washington University School of Medicine, St. Louis, MO

Background: T-cell mediated rejection (ACR) and antibody-mediated rejection (AMR) are the two types of rejection in orthotopic liver transplantation (OLT). AMR it is a rare form of rejection and the histologic diagnosis is challenging, but C4d immunostaining (IHC) may be of diagnostic value. De-novo autoimmune hepatitis (DNAIH) is considered a form of rejection by some investigators. We questioned the role of AMR in DNAIH, and evaluated the utility of C4d IHC in DNAIH and ACR.

Design: A total of 54 patients (pt) from 2000 to 2017 were retrospectively identified in our institution. 22 pts with DNAIH, 15 pts with ACR and 17 control cases (post-OLT re-perfusion biopsy, all HCV negative). Biopsies (bx) with findings of typical ACR and no overlapping features with chronic rejection (CR), recurrent hepatitis C, or other pathology, were selected. All bx were re-reviewed to confirm diagnoses and assess histologic features. Clinical data was obtained from the electronic medical records. C4d IHC (Ventana®, clone SP91) was performed on all bx and slides were reviewed in a blinded fashion. Staining patterns were noted.

Results: The C4d IHC patterns are summarized in Table 1. 41% of DNAIH, 33% of ACR, and 24% of controls (total of 18 bx, 33% overall) showed C4d staining. DNAIH showed sinusoidal staining (SiS) in 4 (18%) pt and portal vein endothelium (PVEnd) positivity in 3 (13%) pt. Although graft survival was slightly worse in the these pt (89 vs 100%, p=0.1), no difference was found between C4d positive and negative (neg) DNAIH pts in terms of number of ACR episodes or CR. ACR cases showed the highest percentage of SiS (27%, p=0.08) but PVend staining was noted in one pt. Some "non-diagnostic" staining such as portal artery wall (23% of DNAIH, and 13% of ACR) and immunoreactivity within portal stroma including vein walls (13% of ACR bx) were noted. 4 control bx showed focal and weak staining with C4d: PVend and portal stroma, portal artery endothelium and wall (1 each, not mutually exclusive), and central vein positivity (2 bx). No statistical significance was found between the number of ACR episodes, CR, graft survival or liver related deaths compared to C4d neg pts.

Table-1. C4d Immunostaining patterns

		DNAIH	ACR	Control	P-value
Number of cases		22	15	17	
Total number of positive cases		9 (41%)	5 (33%)	4 (24%)	0.5211
Sinusoids		4 (18%)	4 (27%)	0 (0%)	0.0896
Central Vein	Endothelium	0 (0%)	0 (0%)	2 (12%)	0.1043
	Wall	2 (9%)	0 (0%)	0 (0%)	0.2208
Portal Vein	Endothelium	3 (13%)	1 (7%)	1 (6%)	0.6530
	Wall	0 (0%)	2 (13%)	1 (6%)	0.2201
Portal Artery	Endothelium	0 (0%)	1 (7%)	1 (6%)	0.4864
	Wall	5 (23%)	2 (13%)	1 (6%)	0.3342

Conclusions: DNAIH pts with SiS and PVEnd C4d staining showed a slightly worse graft survival (89 vs 100%) compared to neg pt. ACR pts had the highest SiS positivity. Although these results may suggest a component of AMR, C4d staining was not associated with number of ACR episodes, CR, graft survival or liver related deaths in both groups.

1757 A Comprehensive Survey of Primary Hepatic Neoplasms for the Altered Lengthening of Telomeres Phenotype

Rondell Graham[1], Dhanpat Jain[2], Michael Torbenson[1]. [1]Mayo Clinic, Rochester, MN, [2]Yale Univ./Medicine, New Haven, CT

Background: The altered lengthening of telomeres (ALT) phenotype is characterized by ultra-bright telomeres on fluorescence in situ hybridization (FISH) and is a marker of a unique mechanism of telomere maintenance in tumors. ALT does not occur in normal tissues and so it represents a unique target specific to neoplasms. Also, tumors characterized by ALT do not show activation of telomerase and are likely dependent on ALT for cell survival, making it a potential target for therapy. ALT has been described in sarcomas, pancreatic neuroendocrine tumors and rare variants of hepatocellular carcinoma (~5% of all HCC are ALT positive). However, a comprehensive review of adult primary hepatic neoplasms has not been performed.

Design: A comprehensive range of adult primary hepatic neoplasms (n=158) were retrieved. The tumors included: cholangiocarcinoma (n=40), hepatocellular adenoma (n=40), hepatocellular carcinoma (n=30), fibrolamellar carcinoma (n=15), combined cholangiocarcinoma-hepatocellular carcinoma (n=9), carcinosarcoma (10), hemangioma (n=5), angiosarcoma (n=4), calcified nested stromal epithelial tumor (n=2), embryonal sarcoma (n=1), rhabdoid tumor (n=1) and angiomyolipoma (n=1). Histologic slides were reviewed for diagnostic confirmation and unstained formalin fixed paraffin embedded tissue sections from representative tissue blocks selected for ALT FISH using a commercially available kit.

Results: ALT FISH was successful in 152 cases (96%). FISH was positive for ALT in carcinosarcoma (n=1; 10% of total, positive in both components), cholangiocarcinoma (n=1; 0.6% of total successful cases), and combined cholangiocarcinoma-hepatocellular carcinoma (n=1; 0.6%). In both cases, the cholangiocarcinoma component showed occasional cells with marked nuclear pleomorphism akin to that described ALT-positive hepatocellular carcinoma. The remaining tumors (99%) were negative.

Conclusions: ALT is positive in rare carcinosarcomas, cholangiocarcinomas, and combined cholangiocarcinoma-hepatocellular carcinoma. These ALT-positive cases show morphologic features noted in ALT-positive tumors from other organ systems suggestive of a genetic-morphologic phenotype correlation. Also, these data indicate that ALT is not a significant mechanism of telomere maintenance in hepatocellular adenoma or fibrolamellar carcinoma.

1758 Steatotic and Nonsteatotic Scirrhous Hepatocellular Carcinoma Reveals Distinct Clinicopathological Features

Mami Hatano, Hidenori Ojima, Yohei Masugi, Hanako Tsujikawa, Minoru Kitago, Michiie Sakamoto. Keio University School of Medicine, Shinjuku-ku, Tokyo

Background: Scirrhous hepatocellular carcinoma (sHCC) has not been defined as an independent entity. The aim of this study was to investigate the clinicopathological and molecular characteristics of sHCC and elucidate its specificity.

Design: Tumor area ratio with fibrous stroma, the amount of steatosis within the tumor (≥5% or not) and immunohistochemical analysis were examined by using 118 resected HCC cases. According to our previous report about HCC subgroups, our samples were immunohistochemically subclassified into biliary/stem cell markers-positive (B/S) group (cytokeratin 19 and/or sal-like protein 4 and/or epithelial cell adhesion molecule positive), Wnt/beta-catenin signaling-related markers-positive (W/B) group (β-catenin and/or

glutamine synthetase positive), and all negative as -/- group.

Results: Thirty-seven cases (31%) contained fibrous stroma in more than 50% of the largest tumor area (51-100%) and were defined as sHCC, while the remaining 81 cases (69%) as common HCC (cHCC), respectively. Clinicopathologically, sHCC had better tumor grade (p=0.039) and higher ratio of cases with tumor cell steatosis (p=0.023) than cHCC. sHCC cases were divided into two groups: sHCC with ≥5% steatosis (steatotic sHCC) and sHCC with <5% steatosis (nonsteatotic sHCC). HBV infection (p=0.029) was frequently seen in nonsteatotic sHCC and Non-B, Non-C were significantly observed in steatotic sHCC (p=0.006). Nonsteatotic sHCC had higher cumulative recurrence rate. Most of nonsteatotic sHCC were classified as B/S group, and majority of steatotic sHCC were classified as -/- group. Cases categorized as W/B group were minor in sHCC altogether, either steatotic and nonsteatotic sHCC.

Conclusions: Our results suggest that sHCC showed distinct features between steatotic and nonsteatotic sHCC. They also showed different clinicopathological and molecular features from cHCC.

1759 Microsatellite Instability Determination and Molecular Profiling of Hepatobiliary Neoplasms Using Next-generation Sequencing: A Retrospective Review of 35 Patients

Cigdem Himmetoglu Ussakli, Colin Pritchard, Paul E Swanson, Matthew M Yeh, Stephen Salipante, Sheena M Todhunter, Eric Konnick. University of Washington, Seattle, WA

Background: Liver cancer is the second most common cause of death from cancer worldwide and its incidence is increasing in developed and developing countries. Molecular profiling with sequencing has revealed variety of genomic alterations in hepatobiliary neoplasms as well as associations with risk factors and clinical outcomes. The recent FDA approval of Pembrolizumab for any cancer that is demonstrated to be microsatellite instability high (MSI-H) has prompted intense clinical interest, however data evaluating MSI status in many neoplasms is lacking. Here we evaluate the molecular mutational profile and MSI status of a clinical series of primary liver tumors using the clinically-validated UW-OncoPlex next-generation-sequencing (NGS) platform.

Design: A total of 35 neoplasms, including 19 cholangiocarcinomas (ICC, 10 intrahepatic, 9 extrahepatic), 14 hepatocellular carcinomas (HCC, 7 fibrolamellar subtype - FLC), 1 mixed ICC+HCC, and 1 hepatocellular adenoma (HA, inflammatory subtype) were evaluated. UW-OncoPlex interrogates the relevant regions of at 192+ genes using target-capture technology to enrich for sequences of interest and is capable of detecting all classes of mutations, including single-nucleotide variants, small insertions and deletions, copy number variants, and complex structural variations. Additionally, MSI status is evaluated using the clinically-validated MSINGS bioinformatics approach, which evaluates up to 65 mononucleotide loci to determine MSI status.

Results: Recurrent mutations, MSI status, and tumor characteristics are summarized in Table 1. We identified inactivating mutations in the tumor suppressor genes *TP53*, and *PTEN*, and activating mutations in the *IDH1*, *KRAS*, *BRAF*, *PIK3CA*, and *ERBB2*. *IDH*1 mutations were solely identified in intrahepatic ICC; whereas *KRAS* mutations were predominantly positive in extrahepatic ICC. The characteristic *DNAJB1-PRKACA* fusion was identified in FLC cases. Mutations of *CTNNB1* and copy gains of 1q were common among non-fibrolamellar type HCC and not identified in the HA. A single ICC case was identified as MSI-H, with a corresponding *MLH1* stopgain mutation. All other samples were microsatellite stable.

| | Median age at diagnosis (n) | Histo-logic grade G1/G2/ G3 | Stage at diagnosis T1/T2/ T3/T4 | Identified Mutations | | | | |
				MSI-H/ MSS/ not tested	ERBB2 (n)	KRAS (n)	IDH1 (n)	BRAF (n)
ICC-intrahepatic	61 (10)	1/6/3	1/0/0/9	1/7/3	1	1	3	2
ICC-extrahepatic	54 (9)	0/8/1	0/1/0/8	0/6/3	2	3	0	0
Mixed ICC+HCC	56 (1)	0/0/1	0/0/0/1	0/1/0	0	0	0	0
HCC Non-fibrola-mellar	59 (7)	0/4/3	4/1/0/2	0/0/7	0	0	0	0
HCC-fibrolamellar (FLC)	23 (7)	1/5/1	1/4/0/2	0/3/4	0	0	0	0
Hepatocellular adenoma	30 (1)	N/A	N/A	0/1/0	0	0	0	0

Conclusions: Broad genomic profiling is useful in identifying relevant genetic mutations and MSI status in a wide variety of primary liver neoplasms. Such information can serve as a rationale for therapy selection or inclusion of patients with advanced disease in ongoing clinical trials and allow for better risk stratification.


1760 The Immunological Milieu of Hepatocellular Carcinoma

Nupur Jadhav, Carolyn McDonagh, Vikram Deshpande. Massachusetts General Hospital, Boston, MA

Background: Immunotherapy, a major breakthrough in oncology has shown impressive antitumor effects in several solid malignancies, and more recently, with the introduction of nivolumab, an anti PD-1 monoclonal antibody, in hepatocellular carcinoma (HCC). Understanding the immune environment in HCC is critical to predicting response to therapy, mechanisms of resistance and developing combination immunotherapy. In this study, we determine the expression level, associations, and biological role of immune cells, the HLA apparatus and checkpoint proteins in HCC.

Design: We evaluated 75 consecutive HCCs with mean age of 62 years and M:F ratio 3.7:1 for : 1) Immune checkpoints PD-L1, PD-1, TIM-3, LAG3 and Indolamine 2,3-dioxygenase (IDO), 2) HLA apparatus (HC10), β2 microglobulin (B2M), and, 3) CD8+T cells, on an immunohistochemical platform. Whole slide scans were quantitatively scored for the percentage of tumor cells positive for IDO, PD-L1, HLA, and B2M. A quantitative analysis of CD8, PD-1, TIM-3, and LAG3, was performed and the results expressed per mm^2. One way ANOVA was used to assess continuous variables and Kaplan-Meier survival analysis was assessed for overall survival. A commercial software was used to generate heat maps.

Results: PD-L1 expression was noted in only 1% of HCCs, whereas IDO was not identified in tumour cells. IDO expression was noted in endothelial cells in 40% of HCCs and was not expressed by sinusoidal cells in non-neoplastic liver. The lymphoid, myeloid-derived, HLA proteins and checkpoint proteins did not correlate with survival. A strong correlation was noted between the presence of CD8, IDO+ myeloid-derived cells, PD-1, TIM-3 and LAG3 (p=0.001). Hierarchical clustering identified 2 distinct cohorts: 1) Inflammatory HCC (arrow) with upregulation of lymphoid elements with enrichment of checkpoint proteins and preservation of HLA complex, 2) Immunologically silent group, constituting the majority of HCCs.
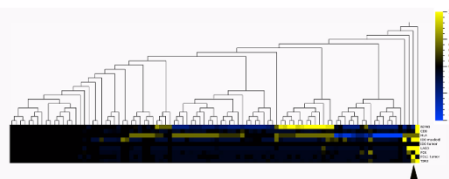
Conclusions: PD-L1 and IDO expression are uncommon in HCC. Hierarchical clustering identified Inflammatory and Immunologically silent classes of HCC. These results could support design of optimal clinical trials and paradigms for resistance to immunotherapy.

1761 What Paves the Way for Fibrosis in NAFLD: Eosinophils?

Ilija Jeftic[1], Mary Smith[2], Richa Jain[3]. [1]University of Arizona College of Medicine, [2]University of Arizona College of Medicine, Tucson, AZ, [3]Banner-University Med Ctr, Tucson, AZ

Background: The growing epidemic of non-alcoholic fatty liver disease (NAFLD) affects 30% of general population in the United States, of which 10% have advanced fibrosis. Only a subset of patients develop fibrosis and the mechanisms of progression of fibrosis remain poorly understood. Presence of eosinophils (Eos) in NAFLD liver has long been known. Recent demonstration of upregulated eosinophil chemoattractant genes, and elevated type 2 cytokines correlating with worsening fibrosis implores systematic histologic evaluation of Eos in NAFLD livers.

Design: Review of electronic medical record (EMR) was carried out to identify patients with a diagnosis of NAFLD. Those with other co-existent liver diseases e.g. Hepatitis C virus infection or significant alcohol consumption as previously defined were excluded. H&E and trichrome stained slides from liver biopsies were available from 37 patients who were included and slides reviewed by one pathologist. NAS and SAF scores were determined. Eos counted per high power field (field diameter 0.55mm) for 10 fields and number averaged (LEC). Distribution of Eos within tissue noted. Absolute peripheral blood Eos count (BEC) and other clinical parameters were obtained from EMR. Statistical analysis (p-value<0.05; Pearson coefficient r and r^2) was performed using SPSS software.

Results: There were 14 males; 17 Hispanics, 11 Whites, 5 Native American and 4 unknown ethnicity; age range from 8 to 77 years; BMI of 4 patients <25; rest >25. BEC was within normal range for all patients ($0-0.6\times10^3$), while LEC ranged from 0 (2 patients) to 2.1 (r^2 = 0.1226). LEC showed positive correlation with worsening fibrosis (r = 0.46, p-value 0.002) and lobular localization more significant than sinusoidal or portal (p-value 0.04). Increasing age strongly correlated with worsening fibrosis (r = 0.6331, p<0.0001). There was no correlation between fibrosis and NAS or activity (r = -0.1).

Conclusions: Our data indicate that eosinophil count and distribution in the NAFLD liver, and age of the patient show positive correlation with increasing fibrosis. As the absolute blood eosinophil count was normal in all patients, our data support active recruitment of eosinophils as previously demonstrated by upregulated eosinophil-chemoattractant genes. Hence, eosinophils may play an important role in progression of fibrosis in NAFLD.

1762 Molecular Studies of Hepatic Carcinosarcoma: Evidence for Common Origin of the tumor

Yuan Ji, Xin Zhang, Lingli Chen, Min Du, Qianming Bai, Akesu Sujie, Hongguang Zhu, Jing Han, Yifan Xu, Huichuan Sun. Zhongshan Hospital Fudan University, Shanghai

Background: Hepatic carcinosarcoma is a rare malignancy composed of carcinomatous and sarcomatous elements with poor prognosis. The carcinogenesis and molecular genetic mechanisms of hepatic carcinosarcoma (hCS) remain unclear.

Design: We performed targeted next-generation sequencing of 262 cancer genes together with immunohistochemical staining of selected antibodies(p53, NF1, pS6K, p4EBP1, TSC2) in two components separately in 10 liver carcinosarcomas.

Results: We identified non-synonymous somatic mutations in 90% of the cases, with 6 of 8 cases (75%) harboring TP53 alterations. The PI3K pathway was the most commonly mutated signalling pathway with mutations identified in NF1, NF2, PIK3CA, PTEN, TSC1 and/or TSC2 in two-thirds of the cases and confirmed with Sanger sequencing in NF1, NF2(Figure2) . Mutations in AXIN, ARID1A and KRAS were demonstrated in a minority of cases. In cases where the carcinomatous and sarcomata's components were separately analyzed, most of the mutations identified were present in both components, indicating a common origin for the two components. Furthermore, the amplification of FGF4, FGF19 also identified in 3cases, VEGFA in 2 cases in both carcinoma and sarcoma component in 3 cases. the same TP53 alterations and/or mTOR/PI3K pathway mutations seen in the carcinomatous tumors were also identified in the sarcoma sites. Overall, carcinosarcomas exhibited heterogeneous molecular features that resemble the heterogeneity seen in mixed hepato-cholangiocarcinomas, with some showing cholangiocarcinoma-like and others showing hepatocellular carcinoma-like mutation profiles. While patients with sarcoma-like tumors presented more frequently with advanced-stage disease compared to patients with cholangiocarcinoma-like tumors, there was no statistical difference in outcome between the two groups.
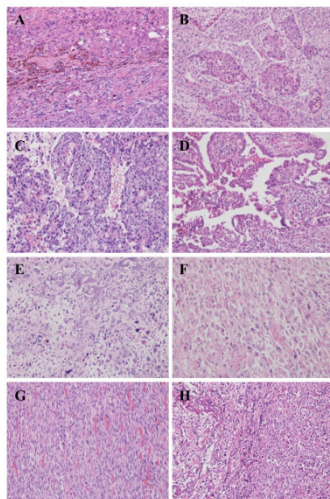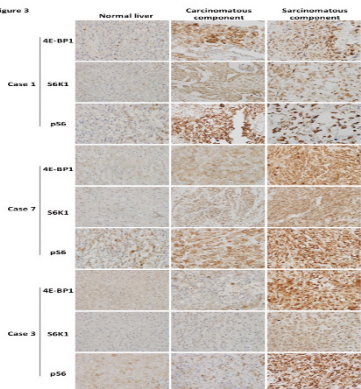

Figure 1

Figure 3

Conclusions: Our results provide insights into the oncogenesis of hepatic carcinosarcoma and identify targetable mutations that represent early oncogenic events. The findings of the different molecular types of hepatic carcinosarcoma that parallel the different molecular types in liver carcinoma may have future treatment implications with targeted therapies.

1763 Recurrent GNAQ and GNA14 Mutations in Hepatic Small Vessel Neoplasms

Nancy Joseph[1], Elizabeth Brunt[2], E. Celia Marginean[3], ILKe Nalbantoglu[4], Swan Thung[5], Matthew M Yeh[6], Sarah Umetsu[7], Linda Ferrell[8], Ryan Gill[8], Dale C Snover[9]. [1]University of California San Francisco, San Francisco, CA, [2]Washington University, Saint Louis, MO, [3]Ottawa Hospital, Ottawa, ON, [4]Washington University in St. Louis, Saint Louis, MO, [5]Mount Sinai Medical Center, New York, NY, [6]Univ of Washington Med Ctr, Seattle, WA, [7]UCSF, San Francisco, CA, [8]Univ. of California, San Francisco, San Francisco, CA, [9]Fairview Southdale Hospital, Edina, MN

Background: Hepatic small vessel neoplasm (HSVN) is a recently described infiltrative hepatic vascular neoplasm composed of small vessels. Because of its infiltrative nature, HSVN can mimic angiosarcoma, but does not show cytologic atypia or increased proliferation as seen in angiosarcoma. We described *GNAQ* hotspot mutations in 2 of 3 cases in our original report. *GNAQ* mutations have since been identified in some visceral anastomosing hemangiomas and *GNAQ, GNA11,* and *GNA14* mutations are now well-documented to occur in congenital hemangiomas. We expanded our genetic evaluation of HSVN last year which did not identify additional *GNAQ* or other pathogenic mutations. We now performed exome sequencing to more fully characterize the spectrum of mutations in a series of hepatic vascular lesions including HSVN, cavernous hemangioma (CH), and variant hepatic vascular lesions (VL) that had overlapping features between HSVN and CH.

Design: DNA was extracted from 8 HSVN, 6 CH, 4 VL, and matched normal tissue. Capture-based next generation sequencing (NGS) targeting the coding regions of 479 cancer genes and select introns was performed on all 18 cases. In this abstract, we add the results of exome sequencing, which was performed on 6 HSVN and 3 VL that had no driver mutations detected by the targeted panel. Single nucleotide variants, insertions/deletions, copy number alterations (CNAs), and selected rearrangements were evaluated, as previously described in our 2017 USCAP abstract.

Results: All 18 cases had diploid genomes without CNAs. No pathogenic mutations were detected in any of 6 CH. As summarized in Figure1, 75% (6/8) of HSVN demonstrated known activating hotspot mutations in *GNAQ* (2/8, p.Q209H) or *GNA14* (4/8, p.Q205L). The remaining 2 HSVN had the same missense mutation in *GNAQ*, p.G48L, which has not been previously described. 1 of 4 VL had a hotspot *GNAQ* p.Q209H mutation and another VL had a *GNAQ* p.G48L mutation. The remaining 2 VL had no pathogenic mutations detected. The 2 VL with GNAQ mutations had a small vessel component that resembled HSVN but also had areas with large vascular spaces like CH. The 2 VL without pathogenic mutations were homogenously composed of medium sized vessels.

Case			HSVN						Variant Lesions			
	1	2	3	4	5	6	7	8	9	10	11	12
GNAQ p.Q209H		■							■			
GNA14 p.Q205L			■	■	■	■						
GNAQ p.G48L							▨	▨				
PIK3CA p.H1047R	■											

Genomic Alterations
- ☐ No pathogenic mutations
- ■ Known hotspot mutation
- ▨ Missense mutation, unknown significance

Conclusions: All HSVN in our series show recurrent mutations in *GNAQ* or *GNA14*, suggesting that these neoplasms share a similar molecular pathogenesis as anastomosing hemangioma and congenital hemangioma. Molecular testing for *GNAQ* and *GNA14* mutations could aid in the diagnosis of HSVN.

1764 Characterization of hepatocellular carcinoma patients with FGF19 amplification using FISH: A large cohort study

Hyo Jeong Kang[1], Farhan Haq[2], Chang Ohk Sung[1], Jene Choi[3], Soo-Heang Eo[4], Hui Jeong Jeong[3], Jinho Shin[3], Ju Hyun Shim[3], Han Chu Lee[5], Jihyun An[3], Seung-Mo Hong[3], Mi-Ju Kim[3], Sung-Min Ahn[7], Eunsil Yu[8]. [1]Seoul, [2]COMSATS Institute of Information and Technology, [3]Asan Medical Center, [4]Korea University, [5]Asan Medical Center, Seoul, Seoul, [6]Asan Medical Center, Seoul, [7]Gachon University Gil Medical Center, [8]University of Ulsan College of Medicine Asan Medic, Seoul

Background: *FGF19* amplifcation is a relatively novel type of genetic aberration that has been proposed to be a driver of hepatocarcinogenesis. Selective inhibitors of FGFR4, a receptor of

FGF19, have been developed as targeted therapies for hepatocellular carcinoma (HCC). Despite the importance of *FGF19* in mediating HCC progression, the clinicopathological characterization of HCCs exhibiting *FGF19* amplification remains unclear.

Design: Thus, we investigated the prognostic value of *FGF19* amplifcation via fluorescence *in situ* hybridization (FISH) in a large cohort of HCC patients. The relationship between *FGF19* amplification and clinicopathological features was analyzed in two cohorts of 227 and 764 patients diagnosed with HCC via FISH.

Results: *FGF19* amplfications were detected by FISH in 9/227 (3.52%) and 42/764 (5.50%) of the patients in cohorts 1 and 2, respectively. In addition, *FGF19* amplification was determined to be associated with a recurrent *TP53* mutation but was mutually exclusive of a *CTNNB1* mutation. *FGF19* amplificatios detected by FISH were 96% concordant (k = 0.551) with those detected using copy number variation array, with statistically significant similarity (Fisher's exact test, *P* < 0.001). *FGF19* amplifcation was also found to be independently associated with poor survival and higer risk of tumor recurrence, as well as with poor prognostic factors such as young age, high alpha-fetoprotein level, hepatitis B virus, larger tumor size, microvascular invasion, and necorsis.

Conclusions: Our current results support the hypothesis that the FGF19-FGFR4 signaling pathway plays an important role in hepatocarcinogenesis, and that HCC with *FGF19* amplification represents a unique and novel molecular subtype of the disease.

1765   SOX9, a useful Immunohistochemical Marker to Discriminate Hepatocellular Carcinomas from Intrahepatic Cholangiocarcinomas

Reema Khan, Xianzhong Ding, Yihong Ma, Hannah Chen, Stefan Pambuccian, Xiuzhen Duan. Loyola University Medical Center, Maywood, IL

Background: Hepatocellular carcinoma (HCC) and Intrahepatic cholangiocarcinoma (ICC) are two most common primary liver cancers. The differential diagnosis between these 2 entities is relatively straightforward if the tumor exhibits typical histological features. However, a differential diagnosis between ICCs and HCCs could be challenging, particularly in cases of poorly differentiated carcinoma. Immunohistochemical markers that are commonly used in current clinical practice include arginase-1, HepPar-1, glypican-3, and CK19. However, none of these are sensitive enough to distinguish high grade HCC from poorly differentiated cholangiocarcinoma. Sex-determining Region Y box 9 (SOX9) has been shown to be a tumor stem cell marker as well as be dysregulated in certain cancer. In this study, we examined the expression of SOX9 in HCCs, CCs and combined HCC and cholangiocarcinoma.

Design: We herein examined the immunohistochemical expression of SOX9 in HCCs (n=20), ICCs (n=18), combined HCC and cholangiocarcinoma (n=7) in surgical resection specimen. A nuclear staining of SOX9 was treated as positive and was scored for intensity (weak, moderate and strong staining). Cytoplasmic staining was considered nonspecific. Fisher's exact test with two tails was performed using the GraphPad statistical software.

Results: Benign hepatic bile duct epithelium exhibits diffuse moderate to strong SOX9 nuclear staining while benign hepatocytes are completely negative for SOX9 expression. 20 HCC cases tested are all negative for SOX9 expression. 7 of 18 CC cases show diffuse strong nuclear staining of SOX-9 while 11 of 18 CC cases exhibit diffuse moderate SOX-9 nuclear expression. For combined HCC and cholangiocarcinoma cases tested, the cholangiocarcinoma component is diffusely positive for SOX-9 while the HCC component is completely negative.

Conclusions: SOX-9 is a highly specific and sensitive marker to distinguish cholangiocarcinoma from hepatocellular carcinoma. Positive SOX-9 staining could be used to exclude hepatocellular carcinoma. Further study will be conducted to elucidate SOX-9 expression in different hepatic metastatic tumors from other organs.

1766   Patterns of Fibrosis Progression and Regression in Steatohepatitis

David E Kleiner[1], Arun Sanyal[2], Mark Van Natta[3], Patricia H Belt[4], Daniela Allende[5], Elizabeth Brunt[6], Danielle Carpenter[7], Melissa Contos[8], Oscar Cummings[9], Ryan Gill[10], Cynthia Guy[11], Matthew M Yeh[12], Laura Wilson[3], Cynthia A Behling[13]. [1]National Cancer Institute, Rockville, MD, [2]Virginia Commonwealth University, [3]Johns Hopkins Bloomberg School of Public Health, [4]Johns Hopkins Bloomberg School of Public Health, Baltimore, MD, [5]Cleveland Clinic, Cleveland, OH, [6]Washington University, Saint Louis, MO, [7]Saint Louis University, [8]Richmond, VA, [9]Indiana University School of Medicine, Indianapolis, IN, [10]Univ. of California, San Francisco, San Francisco, CA, [11]Chapel Hill, NC, [12]Univ of Washington Med Ctr, Seattle, WA, [13]Pacific Rim Pathology Group, San Diego, CA

Background: Fibrosis progression in nonalcoholic steatohepatitis

---

(NASH) is complex and involves both portal/periportal (PF) and centrilobular perisinusoidal fibrosis (PSF). As a step towards understanding the factors involved, we characterized the grade of PSF and the relative dominance of PSF vs PF in NAFLD cases with advanced fibrosis.

Design: Cases of NAFLD in adults from the NASH CRN database protocol as well as the PIVENS and FLINT trials with paired biopsies were blindly assessed by the Pathology Committee using the NASH CRN method. The grade of PSF was recorded as 0-none, 1-mild or 2-moderate. Relative dominance of fibrosis by location was scored as 0-PF dominant, 2-PSF dominant or 1-equivocal. If no fibrosis at last visit (n=70), PSF location and PSF grade were not graded; imputed as category = 0 for analysis. Analysis of covariance models were used to evaluate association between changes in histological features and changes in PSF grade or dominance adjusted for baseline value of fibrosis feature.

Results: 400 cases (155, 115, 118 and 13 cases at baseline fibrosis stage 1 to 4) were available for review. 23% (92/400) showed progression of fibrosis stage while 34% (137/287) showed fibrosis improvement over a median of 2.0 yrs (range 0.6 to 11.6 yrs). At baseline, PSF grade was none in 3%, mild in 28%, and moderate in 69%. Distribution was PSF dominant in 75%, PF predominant in 8%, and equivocal in 17%. Changes in fibrosis stage and PSF grade were both positively associated with changes in steatosis (p<0.001), ballooning (p<0.001), lobular inflammation (p<0.001) and portal inflammation (p<0.001 for stage and p=0.04 for grade). Shift in dominance towards more PSF was positively associated with changes in ballooning and steatosis (p<0.001) and lobular inflammation (p=0.04) but not associated with portal inflammation.

ANCOVA models of change in fibrosis features vs. change in steatosis, ballooning, lobular and portal inflammation

Change in Fibrosis feature	Change in Fibrosis feature per grade change in other histologic feature (Slope±SE)			
	Change in Steatosis – Grade	Change in Ballooning – grade	Change in Lobular inflammation – grade	Change in Portal inflammation - grade
Stage	0.28±0.05 (p<0.001)	0.34±0.05 (p<0.001)	0.37±0.06 (p<0.001)	0.40±0.07 (p<0.001)
PSF Location	0.16±0.04 (p<0.001)	0.18±0.04 (p<0.001)	0.10±0.05 (p=0.04)	0.01±0.06 (p=0.84)
PSF Grade	0.26±0.04 (p<0.001)	0.29±0.04 (p<0.001)	0.21±0.04 (p<0.001)	0.12±0.06 (p=0.04)

Conclusions: As steatosis, lobular inflammation and ballooning worsen or improve, the degree of PSF (both absolute and relative) and stage of fibrosis correspondingly worsen or improve. These results have implications for monitoring fibrosis during clinical trials.

1767   Platelet Aggregation Contributes to Reperfusion Injury, Is Histologically Detectable and is Prevented by Normothermic ex vivo Liver Perfusion

Dagmar Kollmann[1], Ivan Linares[2], Sujani Ganesh[2], Roizar Rosales[2], Matyas Hamar[3], Aryn Wiebe[2], Peter Urbanellis[4], Markus Selzner[2], Nazia Selzner[2], Oyedele Adeyi[5]. [1]Toronto Organ Preservation Laboratory, Multi Organ Transplant Program, Toronto General Hospital, Toronto, Canada, [2]Toronto Organ Preservation Laboratory, Multi Organ Transplant Program, Toronto General Hospital, Toronto, Canada, [3]UHN, Toronto, ON, [4]University of Toronto, Toronto, ON, [5]Toronto General Hospital, Toronto, ON

Background: Normothermic *ex vivo* perfusion is a rapidly evolving method of preservation as an alternative to static cold storage (SCS) of liver grafts and other solid organs. The role of platelets in hepatic sinusoidal endothelial cell injury after ischemia and reperfusion has been reported mainly in SCS settings. In this study we investigated the impact of normothermic ex vivo liver perfusion (NEVLP) vs SCS on platelet aggregation and platelet-mediated endothelial cell injury in a pig allotransplantation model (PLT), as well as demonstrate evidence of intrahepatic platelet aggregation.

Design: PLT was performed in 2 groups of pigs: SCS vs NEVLP (n=5/group). Liver biopsies (LB) were obtained 3hrs post-PLT and stained for H&E, CD31, & CD61. Platelet aggregation was scored as clumps per 5 20x HPF on a Leica® microscope (Fig. 1). CD31 was scored on a scale of 1-4 (none to minimal loss of staining=1; diffuse loss of staining=4) (Fig. 2). Liver enzymes, platelet counts, Platelet-factor-4 (PF-4) & TGF-β as well as other blood parameters (Prothrombin Time, [PT]; INR; Hemoglobin) were measured during a 3-day survival period.

Results: As expected, the NEVLP group showed less ischemic injury with lower AST on postoperative day (POD)1 (581 vs. 1675 U/L, p=0.003) & POD2 (190 vs. 1198 U/L, p=0.005). Platelet recovery was

faster in NEVLP vs. SCS group (% of baseline) at 12hrs after PLT (67% vs. 31%; p=0.019) & at 24hrs (72% vs. 21%; p=0.007). Intrahepatic platelets aggregation is demonstrated by CD61, the SCS group having significantly more sinusoidal aggregation: NEVLP mean # clumps/5 HPF=4 ±1.6 vs. SCS=70 ±46, p=0.039. Platelet aggregation correlated with sinusoidal endothelial injury: mean SCS CD31 score=3.6 ±1 vs. NEVLP 1.9 ±0.2; p=0.018. Also, PF-4 levels increased in SCS, but not in NEVLP at 24hrs (SCS vs. NEVLP: 204 ng/ml vs. 104 ng/ml, p=0.006). Both groups had increased TGF-ß but was significantly higher at POD3 in SCS (7.4 vs. 5.3 ng/µl, p=0.026).
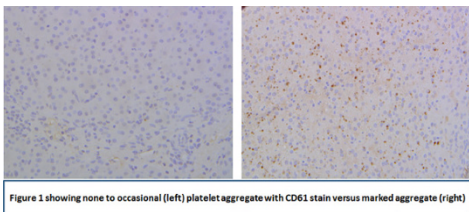

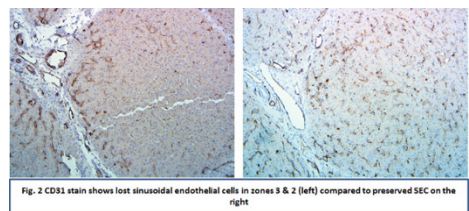Figure 1 showing none to occasional (left) platelet aggregate with CD61 stain versus marked aggregate (right)

Fig. 2 CD31 stain shows lost sinusoidal endothelial cells in zones 3 & 2 (left) compared to preserved SEC on the right

Conclusions: This study demonstrates intrahepatic platelet aggregation as a contributor to and a measure of ischemic endothelial injury in a deceased donor pig liver transplantation model. Platelets aggregation after reperfusion was prevented by normothermic perfusion of the grafts prior to transplantation.

1768   Young and Cirrhotic: Non-Pediatric Causes of Advanced Fibrosis in the Young Adult Population

Konstantin Koro[1], *Elizabeth Richards*[2], *Paul E Swanson*[2], *Maria Westerhoff*[3]. [1]University of Washington Medical Center, Seattle, WA, [2]University of Washington, [3]University of Michigan, Ann Arbor, MI

Background: Approximately 3.9 million adults in the US are affected by liver disease, with mortality mostly due to cirrhosis. The most common risk factors for cirrhosis include viral hepatitis, ethanol (ETOH), and obesity. However, cirrhosis in young adults (18-44 years) not due to pediatric conditions may have different risk factors. As most available epidemiological data is based on age adjusted statistics, etiologies for cirrhosis in this age group are not available. This can be problematic for pathologists evaluating an unexpectedly cirrhotic liver from a young patient. Our study sought to elucidate the most common non-pediatric causes of cirrhosis in this patient population.

Design: Cirrhotic liver samples obtained from 2014-2017 in patients aged 18-44 at diagnosis were identified. Medical records were reviewed for primary diagnosis, contributing causes, serologic and viral studies (ANA, AMA, ASMA, IgG levels, HBV, & HCV), and body mass index (BMI). Patients with known pediatric conditions (e.g. biliary atresia) were excluded.

Results: Of 636 liver cases meeting age criteria, 65 showed advanced fibrosis (32F, 33M; average age 37 (range 18-44)). Average BMI was 29 (range 116-43). 52 patients had one predominant etiology for cirrhosis. The most common was ETOH (25%), followed by AIH (18%), NASH (14%), cryptogenic cirrhosis (9%), and chronic viral hepatitis (13%). α-1-antitrypsin deficiency, hereditary hemochromatosis, and Wilson disease accounted for 3% each. 13 patients had a secondary cause (9 ETOH, 4 NASH) contributing to cirrhosis. As a primary or secondary cause, ETOH played a significant clinical role in 38% of the cohort. BMI >30 was observed in most cases, including all NASH, 50% of ETOH, 83% of cryptogenic cirrhosis, and 80% of HCV patients.

Conclusions: Cirrhosis is an unexpected finding in patients aged 18-45 years. Pathologists should be aware that 20% of cases are caused by a combination of diseases, with ethanol and BMI>30 the most common contributors to other primary causes of cirrhosis. As in older patients, ethanol and NASH were among the most prevalent primary causes. However, unlike older age groups, there was less chronic viral hepatitis and AIH was the 3rd most common. This study demonstrates that etiologies of cirrhosis in adults differ among age groups and emphasizes the importance of considering combined etiologies when faced with an unexpected scenario of cirrhosis in a young patient.

1769   Comparison of Clinicopathologic Features and Mutational Status Between each Subtype of Combined Hepatocellular Cholangiocarcinomas

Hironori Kusano, *Yoshiki Naito*, *Yutaro Mihara*, *Reiichiro Kondo*, *Sachiko Ogasawara*, *Jun Akiba*, *Osamu Nakashima*, *Hirohisa Yano*. Kurume University School of Medicine, Kurume, Fukuoka

Background: Combined hepatocellular cholangiocarcinomas (CHCs) are divided into classical type (CHC-classical) and subtypes with stem-cell features (CHC-SC). The latter is further classified into typical subtype (CHC-SC-typical), intermediate-cell subtype (CHC-SC-int), and cholangiolocellular subtype (CHC-SC-CLC) in the recent WHO classification. This classification of CHC-SCs is controversial and still unclear how relevant it is. In this study, we analyzed a series of CHCs to clarify the clinicopathologic features and mutational status of each subtypes. Genes that we investigated in this study are KRAS, IDH1, and IDH2 which have been reported as potential driver mutation in cholangiocarcinoma.

Design: We used 70 cases of CHC which were resected at our institution from 2000 to 2014. Histologic classification was performed according to the current WHO classification and their clinicopathologic features were analyzed. Mutation hot spots of KRAS, IDH1, and IDH2 were amplified by polymerase chain reaction (PCR). Subsequently, direct sequencing was performed on the PCR products.

Results: Seventy cases of CHC used in the present study were classified into 3 CHC-classical, 45 CHC-SC-int, 22 CHC-SC-CLC, and none of CHC-SC-typical. Patients with CHC-SC-CLC showed lower prevalence of chronic viral hepatitis (CHC-SC-CLC/others 23%/67%, P=0.0008), lower serum alpha fetoprotein level (CHC-SC-CLC/others median 3.7 ng/ml/9.9 ng/ml, P=0.00032), lower serum des-gamma carboxyprothrombin level (CHC-SC-CLC/others median 20 mAU/ml/32 mAU/ml, P=0.01108), and higher rate of IDH1/2 mutation (CHC-SC-CLC/others 24%/0%, P=0.0235), compared to those with other types of CHC. There were no significant differences in age, sex, maximum tumor diameter, the presence of vascular invasion, the presence of intrahepatic metastasis, the presence of nodal metastasis, serum CEA level, serum CA19-9 level, and the presence of KRAS mutation between CHC-SC-int and CHC-SC-CLC.

Conclusions: The patients with CHC-SC-CLC are likely to have different etiology and mutational background from those with other subtypes. Our results suggest that CHC-SC-CLC may be a distinct entity among CHCs.

1770   Evaluation of Histologic Changes in the Livers of Patients With Early and Late Hepatic Artery Thrombosis

Michael J Lee[1], *Raul S Gonzalez*[2]. [1]Columbia University, Long Island City, NY, [2]University of Rochester Medical Center, Rochester, NY

Background: Hepatic artery thrombosis (HAT) following orthotopic liver transplantation (OLT) can cause hepatic parenchymal necrosis and ischemic cholangiopathy, as the hepatic artery is the sole blood supply for the biliary tree. Histologic changes are generally secondary to these effects (parenchymal necrosis and hemorrhage, bile duct necrosis). While HAT is usually diagnosed on clinical/imaging findings, it is sometimes not evident until explanted allograft evaluation. This study investigates additional histologic features that may suggest HAT in post-OLT liver biopsy (bx).

Design: For 94 liver specimens (explanted allografts and bxs) from patients with a clinical or pathologic diagnosis of HAT, we recorded length of time between OLT and procedure, categorizing cases into early HAT ($\leq$30 days since OLT) and late HAT (>30 days since OLT). We evaluated each case for clinical sepsis and several histologic findings (including lobular necrosis or inflammation, hemorrhage, portal inflammation, arteritis, duct disarray, ductitis, duct necrosis, ductular reaction, lobular or ductular cholestasis, large duct injury, bile flecks within portal/central veins, and bile-tinged macrophages). Features were compared between bx and resection specimens, and between early and late HAT, using Fisher's exact test.

Results: Common histologic findings included lobular necrosis (60 cases, 64%), portal inflammation (68 cases, 72%), ductular reaction (73 cases, 78%), lobular cholestasis (70 cases, 74%), and bile-tinged macrophages (40 cases, 43%). Ductular cholestasis was seen in 30 cases (32%); 10 of those patients were clinically septic. Bile in veins was seen in 16 (17%) cases (Fig. 1), and arteritis in 6 (6%) cases. Findings more common in resection than bx specimens included lobular necrosis (P<0.0001), hemorrhage (P=0.0044), ductular cholestasis (P=0.0003), and bile-tinged macrophages (P<0.0001). Lobular necrosis was more common in early HAT (P=0.0002), and ductular reaction and bile in veins were more common in late HAT (P=0.0055).
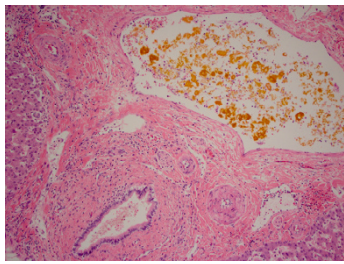
Conclusions: Histologic changes in HAT vary based on specimen type and whether HAT is early or late. In late HAT, biliary injury might occur after a prolonged period of ischemia, with subsequent bile duct necrosis, bile in veins, and remodeling (e.g., ductular reaction). Bile in veins is an unusual finding that may occur in HAT, though it can be seen in bile infarcts from other causes. While histology is rarely needed to diagnose HAT, these findings may be useful in certain circumstances.

1771 Does ASS1 Immunohistochemistry Predict an Increased Risk of Hemorrhage in Hepatocellular Adenomas?

Heidi Lehrke[1], Taofic Mounajjed[1], Raul S Gonzalez[2], Riyam T Zreik[3], Laura J Denham[4], Rory Smoot[6], Daniela Allende[6], Bita V Naini[7], Roger K Moreira[5], Rondell Graham[1]. [1]Mayo Clinic, Rochester, MN, [2]University of Rochester Medical Center, Rochester, NY, [3]Baylor Scott & White Medical Center, [4]Loma Linda University Medical Center, Loma Linda, CA, [5]Mayo Clinic, Rochester, [6]Cleveland Clinic, Cleveland, OH, [7]UCLA Medical Center, Santa Monica, CA

Background: Argininosuccinate synthase 1 (ASS1) was recently reported to be of potential use in the identification of hepatocellular adenomas (HCA) with an increased propensity to hemorrhage. Confirming the predictive value of ASS1 is imperative prior to initiating its routine use in directing patient care.

Design: We identified 72 cases of HCA across our institutional archives (1991-2016). Hematoxylin and eosin-stained tumor sections were examined, and blocks were selected for ASS1 immunohistochemistry (IHC) (BD Transduction Laboratories, San Jose, CA; dilution 1/3500) and HCA subtyping by IHC (as described previously, using LFABP, beta catenin, CRP, and SAA stains). The adenomas were classified as Type 1, Type 2, Type 3, and Type 4 per World Health Organization criteria. ASS1 IHC intensity was interpreted as negative, weak, or positive and distribution was recorded as patchy or diffuse. Patient records were reviewed for clinical evidence of tumor bleeding.

Results: The 72 HCAs (47 resections, 25 needle biopsies) included: 16 Type 1 (22.2%), 6 Type 2 (8.3%), 36 Type 3 (50%), and 14 Type 4 (19.4%). Women comprised 92% of cases (n=66); males 8% (n=6). Six (8.1%) HCAs were associated with clinical bleeding, which included HCA types 1 (n=1, 16.7%), 2 (n=1, 16.7%), and 3 (n=4, 66.6%). No type 4 HCAs were associated with clinical bleeding. In HCA with clinical hemorrhage, all cases were positive for ASS1 (diffuse cytoplasmic expression in 4 of 6 cases, patchy in 2 of 6). Adjacent normal liver was present in 2 of 6 cases; ASS1 expression was less intense than in the adjacent normal in 1 case and of similar intensity in the other. In HCAs without clinical hemorrhage (control group), ASS1 expression was positive in all cases (n=66). The background liver was available for review in 26 controls (39.4%). In 16 cases (61.5%), ASS1 expression was similar in the HCA and the background liver. In 8 (30.8%), expression was less intense in the HCA compared to the background liver and in 2 (7.7%), ASS1 expression was more intense in the HCA than in the background liver. ASS1 expression in the HCA control group was patchy in 9 (13.6%) and diffuse in 57 (86.4%). There was no difference in the intensity or distribution of ASS1 expression in cases with hemorrhage and those without.

Conclusions: Despite recent reports, our results suggest that ASS1 IHC may not reliably predict HCAs with an increased risk of hemorrhage. Evaluation of a larger cohort of HCAs with hemorrhage should be performed to validate these findings.

1772 De Novo Autoimmune-Like Hepatitis After Hematopoietic Stem Cell Transplant: Analysis of a Case Series

Xiaoyan Liao[1], Grace Lin[2], Swan Thung[3], Maria Isabel Fiel[1], Mojgan Hosseini[2]. [1]Icahn School of Medicine at Mount Sinai, New York, NY, [2]University of California San Diego, San Diego, CA, [3]Mount Sinai Medical Center, New York, NY

Background: Autoimmune-like hepatitis (AILH) following allogeneic hematopoietic stem cell transplantation (HSCT) is rare; its incidence and clinical features are not well described. We analyzed 6 such cases from two institutions to better understand its clinicopathological characteristics.

Design: A 17-year retrospective review of the databases from both pathology departments was performed. AILH diagnosis requires 2 of 3 criteria: 1. ALT level >5 x upper limit of normal (ULN). 2. Serum IgG levels >2 x ULN and/or (+) smooth muscle antibodies (SMA). 3. Liver biopsy with moderate to severe interface hepatitis and/or lobular necroinflammation. Cases fulfilling the above criteria but with concurrent duct damage/ductopenia were excluded.

Results: Six cases of AILH were identified, 4 males, 2 females, with average age of 51 years (r=32-69). The reasons for HSCT included non-Hodgkin lymphoma (n=2), B-cell acute lymphoblastic leukemia (n=1), and aplastic anemia (n=3). The average duration between HSCT and AILH development was 36 months (r=1 month~11 years). Laboratory results showed increased ALT (up to 1,132 IU/L), increased IgG (up to 2,682 mg/dL), (+) anti-SMA (all patients). Steroid treatment was initiated in 5 of 6 patients, and 3 showed improvement, while 2 died at one month and 1 year post HSCT, respectively; 1 patient did not get steroid therapy and survived. Both patients who died had higher ALT levels compared to the others who survived. Histologically, moderate to severe interface hepatitis and lymphoplasmacytic portal infiltration were found in all cases. Plasma cells >30% were seen in two patients; in one case, plasma cells were in sheets, necessitating a work-up for plasmacytic neoplasm, which was negative. The other 4 cases had variable amount of plasma cells (5-20%). Two cases had a diagnosis of classical duct damage/ductopenia graft-versus-host disease (GVHD) in prior liver biopsies; yet, when the diagnosis of AILH was rendered in the subsequent biopsies, significant bile duct damage/loss was absent.

Conclusions: We present the clinicopathologic features of 6 cases of AILH, and show that higher liver enzyme tests may be associated with higher mortality and that this entity may occur post-HSCT performed due to any type of hematologic malignancy; response to steroid therapy is variable. Additional studies are currently in progress to better characterize AILH to enable to better distinguish this from classical GVHD and non-HSCT related autoimmune hepatitis.

1773 Histopathology of Small-for-Size Syndrome after Living Donor Transplantation

Su-Yang Liu, Hillary Braun, John Roberts, Linda Ferrell, Sarah Umetsu. University of California, San Francisco, San Francisco, CA

Background: Small for size syndrome (SFSS) following liver transplantation is a common complication of living donor transplantation (LDT), which typically manifests as persistently elevated bilirubin and/or INR and often prompts a liver biopsy to distinguish it from other etiologies of dysfunction such as acute rejection or ischemia. To this date, the histopathologic findings of SFSS have only been described for a very few selected cases, most of which were associated with adverse outcome. At our center, most patients with LDT and an initial period of allograft dysfunction show improvement and have good prognosis. The spectrum of histopathologic changes for these milder SFSS cases has not been previously described. Further characterization of these changes could improve post-transplant biopsy evaluation and management.

Design: Clinical data from all (n=134) patients who underwent LDT at UCSF medical center between 2004-2015 were reviewed (65 left lobe LDT, 60 right lobe LDT). LDT patients with a clinical diagnosis of SFSS, as defined by a total bilirubin of >10 or INR>1.5 on day 7 post-transplantation (PT) who underwent initial liver biopsy within the first 30 days were reviewed (15 cases, 11 left LDT and 4 right LDT) by 3 liver pathologists (SL, SEU, and LDF). All cases except one had graft to body weight ratio of 0.8% or less.

Results: The liver biopsies from all patients who fit the clinical criteria for SFSS demonstrated cholestasis. Ischemic-type changes including hepatocyte swelling, vacuolization of macrophages, and small-droplet fat were seen in the majority of cases. In 8 cases that had a second biopsy, the changes were found to persist at least two weeks PT (Table 1). Regenerative changes were also seen in almost all cases. Portal vein and periportal sinusoidal endothelial denudation was not seen. Eleven of 15 patients showed clinical improvement without other complications. One patient developed recurrent hepatitis C after initial resolution of SFSS. Two patients developed histological evidence of ischemia on biopsy after 1.5 and 3 months.

Conclusions: The majority of patients undergoing liver biopsy for clinical diagnosis of SFSS showed clinical improvement without further complications. The most common histopathologic changes seen in these biopsies were cholestasis, hepatocyte swelling, steatosis, and regenerative changes.

1774 Classic Hepatocellular Carcinoma Arising in Absence of Chronic Liver Disease: a 35-Case Series

Steven Mann[1], Romil Saxena[2], Shefali Chopra[3]. [1]Hamilton, AL, [2]Indiana Univ/Medicine, Indianapolis, IN, [3]University of Southern California, San Marino, CA

Background: Cirrhosis in the setting of chronic liver disease (CLD) is the most common risk factor for classic (non-fibrolamellar) hepatocellular carcinoma (cHCC). However, cHCC also occurs in the absence of cirrhosis in patients with CLD (chronic hepatitis B virus, HBV; chronic hepatitis C, HCV; non-alcoholic steatohepatitis, NASH) or metabolic syndrome (MS). Additionally, cHCC may occur in patients with no evidence of CLD or MS.

Design: The pathology databases of two institutions were queried to identify cases of cHCC without cirrhosis. The medical records and pathology reports were reviewed to identify three cohorts: (1) patients without underlying CLD or MS (study group), (2) patients with underlying CLD (control group 1), and (3) patients with clinical evidence of MS (obesity, hyperlipidemia, diabetes mellitus) without CLD (control group 2). Clinicopathologic data including gender, age, and tumor multifocality, size, vascular invasion, grade, and stage was compared.

Results: Thirty-five cases were identified (15 male, 20 female). The median patient age was 64 years (range 9-92). Nine cases (26%) were multifocal and the average tumor size was 8.1 cm (range 2.5-18.5). Vascular invasion was identified in 10 cases (29%). According to AJCC 8th, 23% of cases were pT2 and 20% were pT3. Control group 1 (non-cirrhotic CLD) contained 14 cases with male:female ratio (M:F) of 4:3, a younger median age (58 years), more frequent multifocal disease, larger tumor size (average 9.1 cm), more cases with vascular invasion (50%), and fewer poorly differentiated and higher stage (pT3) tumors compared to the study group. Control group 2 (MS without CLD) contained 69 cases with more males (M:F 2:1), an older median age (68 years), fewer multifocal cases, larger tumors (average 9.3 cm), more frequent vascular invasion (45%), and fewer poorly differentiated and high stage (pT3) tumors compared to the study group.

Clinicopathologic Data of Hepatocellular Carcinoma Arising in Non-Cirrhotic Liver			
	Without Chronic Liver Disease or Metabolic Syndrome (Study Group)	With Viral Hepatitis or Non-Alcoholic Steatohepatitis (Control Group 1)	With Metabolic Syndrome (Control Group 2)
Number of Cases	35	14	69
Median Age at Presentation	64 years	58 years	68 years
Gender (M:F)	3:4	4:3	2:1
Number of Multifocal Cases	9 (26%)	5 (36%)	14 (20%)
Average Tumor Size	8.1 cm	9.1 cm	9.3 cm
Presence of Vascular Invasion	10 cases (29%)	7 cases (50%)	31 cases (45%)
Grade	24% Well differentiated 57% Moderately differentiated 19% Poorly differentiated	7% Well differentiated 86% Moderately differentiated 7% Poorly differentiated	12% Well differentiated 71% Moderately differentiated 17% Poorly differentiated
Pathologic Stage	8 pT2 (23%) 7 pT3 (20%)	6 pT2 (43%) 2 pT3 (14%)	20 pT2 (29%) 13 pT3 (19%)

Conclusions: The demographic spectrum of classic, non-fibrolamellar HCC is wide. Although the majority of cases occur in a background of cirrhosis or advanced fibrosis, HCC may occur without these risk factors, NASH, or MS. The presence of bland steatosis is variable. The patients without CLD or MS had a median age between the 2 control groups and a slightly higher female preponderance. These tumors were more often well differentiated and had a lower incidence of vascular invasion.

1775 Expanding the TMA Method to Investigate Phylogenetic Relationships Between Primary and Metastatic Hepatocellular Carcinoma

Sebastiao N Martins Filho[1], Alda Wakamatsu[2], Carlos Villacorta-Martin[3], Aline K Assato[4], Amanda Craig[5], Flair Carrilho[2], Swan Thung[6], Augusto Villanueva[5], Venancio Alves[7]. [1]Faculdade de Medicina FMUSP, Sao Paulo, SP, [2]Faculdade de Medicina FMUSP, [3]Icahn School of Medicine at Mount Sinai, New York, NY, [4]Faculdade de Medicina FMUSP, São Paulo, [5]Icahn School of Medicine at Mt. Sinai, [6]Mount Sinai Medical Center, New York, NY, [7]Faculdade de Medicina da USP, Sao Paulo

Background: TMAs allow for high throughput analyses of multiple tumors and prevent IHC-ISH pre-analytical and analytical issues. We aimed at expanding the classical applications of TMAs by investigating their ability to infer phylogenic relationships between primary and metastatic cancer. We focused on HCC due to the limited data on advanced-metastatic disease in the present literature.

Design: We included 88 patients submitted to autopsy with viable HCC (no signs of autolysis and PMI <24 hours) and histological representation of usual metastatic sites. Multinodular and metastatic disease were identified in 55 and 20 patients, respectively. Spotting for TMA aimed at specific areas in each of the 194 primary and 36 metastatic nodules. Tumors ≥2cm or depicting a nodule-in-nodule or other distinctive histological pattern had more than one representative area selected (118 nodules). The cytological and structural features assessed included degree of differentiation, cellular crowding, architectural organization, and nuclear and nucleolar grades. Results were dichotomized in low (0) and high (1) grade, and an algorithm with the sum of the morphological criteria was generated. IHC focused on markers of hepatocyte differentiation (HepPar1, Arginase, CD10 and CEAp) and stem/EMT properties (K19, EpCam, SALL4 and Vimentin). Phylogenetic relationships were investigated by integrating the morphological and IHC results in a patient-by-patient basis, thus avoiding inter-patient variations related to post-mortem changes.

Results: IHC intra and inter-tumor heterogeneity within the primary disease was observed in 41/106 (39%) nodules and 29/50 (58%) patients. Metastases showed much lower intra (2/10, 20%) and inter-tumor (2/12, 17%) heterogeneity. Also, all metastatic nodules could be histologically traced back to the primary disease – sometimes to a specific area on a primary nodule –, suggesting that only a small sub-clone within the primary tumor could direct metastatic spread. Metastases were enriched in stem/EMT markers and in multiple histological features, notably morphological algorithm ≥3.

Conclusions: TMAs constructed based on an individual area/nodule from a cancer would most likely underrepresent the full scope of the disease, particularly in advanced stages, illustrated herein by the high tumor heterogeneity in HCC. By expanding the technique to encompass multiple areas/nodules, we showed its competence to evaluate inter-tumor heterogeneity and to suggest a cancer evolutionary pattern.

1776 Morphological Analysis of IDH Mutant Intrahepatic Cholangiocarcinoma

Elena Maryamchik, Vikram Deshpande. Massachusetts General Hospital, Boston, MA

Background: Somatic mutations of the *isocitrate dehydrogenase (IDH) 1* and *2* genes are detected in up to 30% of intrahepatic cholangiocarcinomas (ICC) and only rarely in hepatocellular carcinomas (HCC). An *IDH1* inhibitor, currently in phase 3 trials, offers a new paradigm for the treatment for ICC with *IDH* mutation. However, accurate classification is essential and misdiagnosis as either a HCC or a metastatic carcinoma would potentially preclude the use of an IDH inhibitor. The aim of this study is to compare the morphologic appearance of *IDH* mutant (m*IDH*) ICC to that of IDH wild type ICC (wt*IDH*), in an attempt to identify features in an ICC that could potentially mimic HCC.

Design: We evaluated 41 in-house cases of ICC genotyped using a SNaPshot multiplex platform system. The morphologic analysis included architectural patterns and cytologic features. Mixed tumors and those classified as HCC were excluded. The distinction of ICC from HCC was based on histologic and immunohistochemical analysis. Abundant eosiophilic cytoplasm was defined as cytoplasm greater than twice the nuclear size and resemblance to hepatocytes. The histologic features in the ICC cohort of The Cancer Genome Atlas (TCGA) database were also evaluated, and the results correlated with mutational data and mRNA expression.

Results: The in-house cohort was comprised of 16 m*IDH* ICC and 25 wt*IDH* ICC. m*IDH* ICC were more likely to show abundant eosinophilic cytoplasm resembling cytoplasm of hepatocytes (76%) than wt*IDH* ICC (20%) (p=0.001). m*IDH* ICC were also more likely to show clear cytoplasm than wtICC, although the results did not reach statistical significance (67% vs. 32%, p=0.11). There were no differences in architectural patterns, intratumoral stroma, or level of histologic differentiation between the two cohorts. In the TCGA cohort, a higher proportion of m*IDH* cases also showed abundant eosinophilic cytoplasm (44% vs. 17%) (p=0.09). Expression of HCC-related genes did not correlate with eosinophilic cytoplasm. There was no difference in survival between the two groups in either cohort (in-house p=0.5, TCGA p=0.8).

Conclusions: m*IDH* tumors are histologically similar to wt*IDH* tumors with the exception that m*IDH* tumors preferentially show cytoplasmic characteristics that may overlap with HCC. Given the promise of *IDH* targeted therapy, awareness of the overlapping cytoplasmic features would potentially help to avoid misclassification as HCC, a diagnosis that could preclude patients from enrollment in an *IDH* inhibitor clinical trial.

1777 PREVIOUSLY PUBLISHED

1778 Correlation of Histologic Findings and Clinical Outcome In Liver Transplant With Pre-Transplant Non-Alcoholic Steatohepatits Diagnosis

Patrick Memari, M. S Siddiqui, C. S Bhati, Melissa Contos, Michael Idowu. Virginia Commonwealth University Health System, Richmond, VA

Background: Nonalcoholic steatohepatitis (NASH) related cirrhosis is the fastest growing indication for liver transplantation (LT), and disease recurrence is almost universal after LT. There are significant clinical and biochemical differences between patients with NASH in the general population and LT recipients with higher rates of obesity, diabetes, hypertension and dyslipidemia after LT. The current histological staging system for post-LT NASH is derived from non-transplant patients and it is unclear if this schema is applicable to post-LT patients who not only have more metabolic derangements but also chronic exposure to immunosuppression. Thus, the aim of the current study was to provide a detail histological assessment of liver biopsies performed in patients with LT for NASH and correlate these findings with clinically significant outcomes.

Design: Patients who had a LT for NASH cirrhosis and a liver biopsy after LT were included in the current analysis. Those with evidence of active acute cellular rejection or chronic rejection were excluded. The liver biopsy was graded by pathologists with expertise in liver pathology using the NASH CRN scoring criteria. The histologic features are correlated with clinical outcomes. The relationship between histological parameters and clinical outcomes was evaluated via binary logistical regression.

Results: 34 patients met the inclusion criteria for the study. The median follow-up interval from LT to analysis was 47 months (interquartile range: 23-95 months). 44% and 56% had grade 0 and grade 1 lobular inflammation (LI), respectively. 62% of the patients had no hepatocellular ballooning. 62% and 35% had "none" and "mild" portal inflammation (PI), respectively. 44%, 32%, 3%, 21%, 0% had stages 0, 1, 2, 3 and 4 fibrosis, respectively. Fibrosis and LI were not significantly associated with any clinical outcome. Presence of PI was linked to presence of coronary artery disease (P=0.04), while ballooned hepatocytes were associated with all-cause mortality (P=0.048). Finally, presence of steatosis was associated with cardiovascular disease related mortality (P=0.01).

Conclusions: The histological features of post-LT NASH are similar to non-transplant population with the exception of reduced inflammation, which may be linked to use of chronic immunosuppression. Additionally, the association between histological parameters and cardiovascular disease likely represents shared metabolic derangements resulting from exposure to immunosuppression.

1779 Surveillance Protocol Liver Transplant Biopsies Reveal Allograft Pathology in Asymptomatic Pediatric Liver Transplant Recipients

Cherise Meyerson[1], Laura Wozniak[2], Bita V Naini[3]. [1]UCLA Medical Center, Reseda, CA, [2]UCLA Medical Center, [3]UCLA Medical Center, Santa Monica, CA

Background: Liver transplantation (LTx) is a standard procedure for pediatric patients with acute liver failure or end-stage liver disease. In contrast to adults, LTx in children is usually for potentially curable, non-recurrent diseases. However, it remains unknown whether these children can expect an eventual decline in graft function or loss. Our aim was to evaluate the efficacy of scheduled protocol liver biopsies in pediatric LTx patients.

Design: We studied all pediatric patients that underwent protocol post-transplant liver biopsies at our institution since implementation of the program in Jan 2016. Comprehensive clinical data were collected in all patients including the clinical course of management. A detailed histopathologic study of each biopsy was performed and histologic findings were correlated with clinical, laboratory, and serological results. Inflammation and fibrosis were graded on a scale of 0 to 4 (see Table 1).

Results: Nineteen children (12 males, 7 females) underwent protocol liver biopsies. Median age at the time of LTx was 1.9 years (range: 0.5-9.1). The median time between LTx and time of biopsy was 14.2 years (range: 6.2-18.3). All patients were asymptomatic and liver biochemical tests (ALT, AST, bilirubin and GGT) were normal or near-normal at the time of biopsy. Eight of 15 patients tested had at least one donor-specific antibody (DSA). Two biopsies had grade 2 inflammatory activity, 8 had grade 1, and the rest had no inflammation. One had cirrhosis, 1 had bridging fibrosis, 5 had periportal fibrosis, and 1 had portal fibrosis. Patients with stage 0 or 1 fibrosis were less likely to have DSAs than those with stage 2 to 4 fibrosis [3/12 (25%) vs. 5/7 (71%), p=0.074]. Three showed chronic ductopenic rejection, and two showed mild acute T cell-mediated rejection. One had diffuse staining for C4d, while five showed focal staining. No features of bile duct obstruction, recurrent disease, or vascular abnormalities were seen.

These results led to changes in immunosuppressive medications for 4 patients.

Table 1. Grading system for inflammation and fibrosis.

Grade/ Stage	Inflammation	Fibrosis
0	No inflammation	No fibrosis
1	Minimal portal inflammation, no interface hepatitis	Portal fibrosis
2	Mild portal inflammation, interface hepatitis in some but not all portal tracts, and/or mild lobular inflammation	Periportal fibrosis
3	Moderate portal inflammation, interface hepatitis in the majority of portal tracts, and/or moderate lobular inflammation	Bridging fibrosis
4	Severe portal inflammation with bridging necrosis	Cirrhosis

Conclusions: Although patients were asymptomatic and liver biochemical tests were normal, 68% of biopsies showed inflammation and/or fibrosis, and 26% showed rejection. The results of the protocol biopsies led to changes in clinical management in 4 of 19 patients (21%). Our results indicate the importance of protocol biopsies in pediatric LTx patients, which can lead to early detection of pathologic abnormalities before there is clinical evidence of declining graft function.

1780 ATP7B Genomics in the Chinese Population---A Systematic Whole Exon Study of ATP7B Gene of 1536 Chinese Patients with Probable Wilson Disease in a CAP-Accredited Clinical Genomic Center

Guiling Mo[1], Changshun Yu[1], Dongfeng Tan[2]. [1]Clinical Genomic Center at KingMed Center, KingMed College of Laboratory Medicine, Guangzhou, China, [2]MD Anderson Cancer Center, Houston, TX

Background: Wilson disease (WD) is a treatable disease if diagnosed promptly. *ATP7B* gene mutation test is the golden standard for diagnosing WD, due to the extreme variably clinical presentations and equivocal laboratory results of many WD patients. Although *ATP7B* gene has been extensively studied in the western countries, little is known regarding its characteristics in the Chinese population.

Design: From Aug 2010 to Aug 2017, 1536 probable WD patients were identified by clinical features and laboratory tests. The age of the patients ranged from 11 months to 62 years. The blood specimens of these patients were collected from all provinces in China except the Tibet region. *ATP7B* mutation was tested in a CAP-accredited genomic center in Guangzhou, China. Briefly, after the genomic DNA extraction, PCR amplifications of *ATP7B* were performed. The PCR amplification covered the promoter region, all 21 exons of the gene, and the intervals (100bp) between exons and introns. The Sanger sequencing(ABI 3500Dx) was performed to analyze mutations of *ATP7B*.

Results: 210 types of *ATP7B* mutations were identified, including 146 missense mutations (69.5%), 28 frameshift mutations (13.3%), 28 nonsense mutations (13.3%) and 8 splicing mutations(3.8%). The most frequent mutation was Arg778Leu (35.7%), a mutation involving replacement of arginine with leucine at position 778. Other "high frequent" mutations included Pro992Leu (13.1%), Ile1148Thr (6.4%), and Met769fs (5.9%), while the most majority (n=199) of *ATP7B* gene mutations occurred less than 1%. Interestingly, His1069Gln mutation, the most frequent *ATP7B* mutation in the Europeans (up to 55%), was very infrequent (0.69%) in our cohort. Among the 1536 probable WD patients, *ATP7B* mutation was identified in 1241(80.8%) patients. Specifically, 158 patients demonstrated *ATP7B* mutation in one focus, while *ATP7B* mutations involving two and three foci were identified in 1084 and 13 patients, respectively. Moreover, among the patients with *ATP7B* mutations involving two gene foci, 138 were homozygotes, while 946 were heterozygotes which usually show vague clinical features.

Conclusions: This study represents the first population-based analyses of *ATP7B* gene in Chinese. Our results have enriched the Wilson Disease Mutation Database. The characteristics of *ATP7B* mutations in Chinese are significantly different from those of the western ethnics. Variable *ATP7B* mutations are identified among Chinese WD patients, which warrants a comprehensive sequencing of the entire *ATP7B* gene.

1781 Use of Mutational Analysis and BAP1 Immunohistochemistry for Diagnosis of Intrahepatic Cholangiocarcinoma

Brent Molden, Nancy Joseph, Aras Mattis, Daiva Mattis, Sanjay Kakar. University of California San Francisco, San Francisco, CA

Background: It is challenging to distinguish intrahepatic cholangiocarcinoma (ICC) and metastatic adenocarcinomas (AC) from other sites such as pancreas, biliary tree, gallbladder (GB), stomach and esophagus. Similarly, it can be difficult to distinguish ICC from poorly differentiated hepatocellular carcinoma (HCC) in a subset

of cases using the currently available immunohistochemistry (IHC). Recent studies have shown distinct genetic abnormalities in ICC such as mutations in *IDH1/IDH2* and *BAP1*, and fusions in *FGFR2*, while these are rare or absent in HCC and AC from other sites. This study examines the use of genetic changes and BAP1 IHC for diagnosis of ICC.

Design: ICC, HCC and AC cases from a variety of sites were retrieved, and the mutational spectrum was reviewed from the available sequencing data obtained by next generation sequencing. IHC for BAP1 was performed in 14 cases of ICC, 3 cases of HCC and 4 cases of pancreatic AC.

Results: *IDH1* mutations were observed in 27% of ICC, but not in any HCC or other AC. *FGFR2* fusions were present in 15% of ICC, and 5% of biliary AC, but not in HCC or AC from gallbladder, pancreas or stomach. *BAP1* mutations were noted in 12% of ICC and 17% of HCC, but not in AC of pancreas or stomach. *TERT* promoter mutations were identified in 33% of HCC compared to 4% of ICC and no other AC. IHC for BAP1 done in a separate set of 14 ICC cases showed loss of nuclear staining in 6 (43%) cases; there was no loss in HCC (n=3) or pancreatic AC (n=4) cases.

*Figures in parentheses reflect numbers from literature

	ICC (n=26)	Extrahepatic biliary AC (n=20)	GB AC (n=5)	Pancreas AC (n=41)	HCC (n=12)	Gas-tro-esopha-geal AC (n=26)
IDH1 mutation	27% (13-36%)*	0% (0-11%)	0%	0%	0% (2%)	0% (0%)
IDH2 mutation	0% (0-6%)	5% (0-4%)	0%	0%	0%	0%
FGFR2 fusion	15% (6-50%)	5% (0-5%)	0%	0%	0% (1%)	0%
BAP1 mutation	12% (7-38%)	0% (0-10%)	0%	0% (0%)	17% (5%)	4% (8%)
DPC4 mutation	0% (0-4%)	30% (10-25%)	0%	27% (35-60%)	0%	19% (8-24%)
ARID1A mutation	15% (15-36%)	30% (5%)	40%	10% (15%)	0% (3%)	19% (44%)
PBRM1 mutation	4% (11-21%)	0% (5%)	20%	0% (6%)	0%	8%
TERT promoter mutation	4% (0-3%)	0%	0%	0%	33% (44%)	0%
CTNNB1 mutation	4%	0%	0%	0%	8% (27%)	0%

Conclusions: *IDH1* mutation is characteristic of ICC, and along with *BAP1* mutation and *FGFR2* fusion can help to distinguish ICC and metastatic AC from other sites such as biliary tree, GB, pancreas and stomach. *IDH* mutations can rarely be seen in extrahepatic biliary AC. Loss of *BAP1,* which can be demonstrated by IHC, supports ICC over AC from pancreas. *DPC4* mutation favors extrahepatic biliary or pancreatic AC over ICC. For ICC vs HCC, *IDH1* mutation and *FGFR2* fusion point towards ICC, while *TERT* promoter and *CTNNB1* mutation favors HCC. *BAP1* mutation does not help in ICC vs HCC. These results show that evaluation of specific mutations and BAP1 IHC are valuable tools for the diagnosis of ICC.

1782 Revisiting the Histological Parameters of Donor Liver: New Insight to Predict Recipient's Outcome

Melissa A Monica, Francesco Vasuri, Mattia Riefolo, Antonietta D'Errico. S.Orsola-Malpighi Hospital, Bologna University, Bologna, Italy

Background: Frozen-section analysis of donor livers is still required for the assessment of graft suitability for Orthotopic Liver Transplantation (OLT), especially in the case of marginal donors. The present study aims to better define the role of arteriolar thickening and other well-known histopathological variables in OLT recipient outcome.

Design: We retrospectively collected liver biopsies from 132 heart-beating liver donors between January 2013 and September 2016 in the intensive care units of the region. Wedge and fine needle biopsies were taken from each donor at the time of vascular clamping, sent in gauze soaked with saline solution to the regional centralized 24-hour pathology service for frozen section evaluation. 4-μm sections were cut from each sample and stained with hematoxylin and eosin and with reticulin. Frozen and permanent histological sections were reviewed to evaluate arterial thickening (defined as the lumen/wall ratio) and other 8 histopathological variables, as well as 10 clinical donor variables. These features were correlated with the function of the graft at 7 days (primary non function, PNF, and early allograft dysfunction, EAD) and at 6 months (presence of clinical indications for liver biopsy within 6 months from OLT).

Results: Four (3.0%) PNF and 38 (29.7%) EAD cases were recorded; 30 (27.0%) recipients needed liver biopsy within 6 months from OLT.

Notably, at multivariate analysis, the donor arteriolar thickening was correlated with PNF (p=0.026) and with the need for post-OLT needle biopsy (p=0.004). Moreover, donor dyslipidemia and fibrosis in donor biopsy were correlated with a higher percentage of EAD: 18.5% in cases with non-dyslipidemic non-fibrotic donors, *versus* 54.5% in cases with dyslipidemic fibrotic donors (p=0.012).

Conclusions: The finding of fibrosis in the liver biopsy from a dyslipidemic donor should be taken into account as an increased risk for EAD; allocation from this kind of donor should always be reconsidered. Moreover, among the histopathological variables evaluated in the donor biopsy for graft suitability, arterial wall thickening deserves more attention.

1783 Pathologic Predictive Factors for Late Recurrence of Hepatocellular Carcinoma in Chronic Liver Disease

Ji Hae Nahm[1], Haeryoung Kim[2], Jeong Eun Yoo[1], Hye Sun Lee[1], Ha Young Woo[1], Taek Chung[1], Young Nyun Park[1]. [1]Yonsei University College of Medicine, Seoul, Korea, [2]Seoul National University, Seoul

Background: Hepatocellular carcinoma (HCC) shows poor outcome with > 70% of cumulative 5-year recurrence even after a curative resection. There are early (within 2 years) and late HCC recurrence (after 2 years) after resection and the latter is regarded as de novo HCC, which usually develops through a multistep process in chronic liver disease. Recently, the molecular profiles of background liver, rather than those of HCC were reported to be related to late HCC recurrence. In this study, the pathological features to predict late HCC recurrence were evaluated and its prediction model was developed.

Design: Non-tumoral livers in 402 HCC patients with curative resection at Severance hospital (January 2008 ~ December 2013) were included. Pathological features including lobular and portoperiportal inflammatory activity, fibrosis stage, small and large liver cell change were evaluated and immunohistochemical stains for p21, rH2AX, signal transducer and activator of transcription 3 (pSTAT3), extracellular signal-regulated kinase 1/2 (pERK1/2), plasminogen activator inhibitor-1 (PAI-1), spleen tyrosine kinase (SYK) and estrogen receptor-α (ER-α) were performed.

Results: The mean age of HCC patients was 55.2 year-old and male to female ratio was 4.58. The etiologies of underlying liver disease were HBV (83%), HCV (4%), alcohol (4%) and unknown (8%). Late HCC recurrence occurred in 57 (14%) patients with median follow-up period of 54 months. HCC patients with late recurrence showed higher inflammation activity, fibrosis stage, and small and large liver cell change, and one or more immune-expressions of pSTAT3, pERK1/2 and SYK (p < 0.05 for all). Fibrosis stage 4 (cirrhosis) (odds ratio [OR] = 1.98; 95% confidence interval [CI]: 1.07-3.67), higher lobular activity (OR = 43.05; 95% CI: 3.43-540.93) and one or more immune-expressions of pSTAT3, pERK1/2 and SYK (OR = 6.37; 95% CI: 2.06-19.75) were independently associated with late HCC recurrence by multivariate cox regression analysis (P < 0.05 for all). A prediction model derived from these variables showed an area under the receiver operating characteristic curve (AUC) of 0.716 in the prediction of late HCC recurrence (95% CI: 0.65-0.78).

Conclusions: The predictive model derived from fibrosis stage 4 (cirrhosis), higher lobular activity and one or more immune-expressions of pSTAT3, pERK1/2 and SYK in background liver is suggested to be useful for prediction of late HCC recurrence after curative resection.

1784 Persistent histologic findings after achieved SVR in hepatitis C (including DAA therapy) in the setting of liver transplantation

Fadi Niyazi[1], Carlos Romero-Marrero[1], Rondell Graham[2], Mohammad Asfari[1], Baraa M Abduljawad[1], Vedha Sanghi[1], Bijan Eghtesad[1], Koji Hashimoto[1], K.V. N Menon[1], Federico Aucejo[1], Lisa Yerian[1], Daniela Allende[1]. [1]Cleveland Clinic, Cleveland, OH, [2]Mayo Clinic, Rochester, MN

Background: Sustained virological response (SVR) after antiviral therapy in Hepatitis C virus (HCV) patients leads to improved survival and reduced morbidity. Although studies have highlighted fibrosis progression in a subset of these cases after interferon (IFN) based therapy, limited information is available of the long-term outcome in patients treated with direct acting antivirals (DAA).

Design: After IRB approval, cases were retrospectively identified from clinical databases (2010-2016). Clinical data was obtained from chart review. Only cases with paired pre and post-treatment liver biopsies (bx) were included. H&E and trichrome stains and chromogenic in situ hybridization (CISH) using commercially available multiplex probes to HCV genotypes 1a, 1b and 2 and 3a and 4a were performed. Batts and Ludwig system was used for grade and stage.

Results: 37 cases (28 male, age 57-82 years) with deceased donor

orthotopic liver transplants were included. Pretreatment bx showed chronic hepatitis grade 1-2 (34/37 cases), stage 0-2 (35/37 cases) in the majority of patients. Endotheliitis (3/37, 1 in DAA), bile duct injury (6/37, 3 in DAA) and central perivenulitis (5/37, 3 in DAA) were focal. 10 patients received IFN, 27 received DAA; all achieved SVR. Post-treatment bx (1 day to 33 months post-treatment completion, mean: 8.8 months) revealed increased inflammation in 2/37 (treated with DAA), and progression of fibrosis in 6/37 (3 with IFN, 3 with DAA). Endotheliitis (2/37 in DAA), bile duct injury (3/37, 2 in DAA) and central perivenulitis (1/37 in DAA) diminished. CISH for HCV was negative in all 34 post-treatment bx with available tissue. 10/37 cases had subsequent follow up bx (6-36 months after post-treatment bx), 8/10 with no change or reduced grade/stage, while 2/10 exhibited greater inflammation and/or fibrosis progression and in the absence of plasma cell hepatitis.

Conclusions: This is the largest series including DAA treated cases. After achieving SVR, some HCV patients continue to show features of chronic hepatitis and a subset of them exhibit progression of inflammation and/or fibrosis on follow up (including after DAA treatment). These data support continuation of surveillance in these patients following SVR to further understand their true risk as well as investigation of other causes of post-transplant hepatitis.

1785 Vascular pathology is common in liver biopsies from patients with end-stage renal disease

Burcin Pehlivanoglu, Abigail Goodman, Alyssa Krasinskas. Emory University, Atlanta, GA

Background: Liver biopsies are performed in renal transplant candidates to assess for underlying liver disease and to stage fibrosis. Patients with advanced stage disease are not eligible for kidney transplant alone and may be evaluated for combined kidney-liver transplant. Renal transplant candidates with end-stage renal disease are often on dialysis. In addition to expected hemosiderin deposition, we have often noted portal tract and vascular changes in these biopsies and sought to study them systematically.

Design: Liver core biopsies from 65 potential renal transplant patients were evaluated for vascular, portal and parenchymal changes. Portal morphology was assessed similar to a prior study in normal liver biopsies (PMID: 9695993) and the presence of vascular and/or ductal abnormalities were noted.

Results: M:F ratio was 2.2 and mean age was 51 (range 29-68). Thirty-seven (66%) cases had viral hepatitis (35 HCV, 2 HBV). The average number of portal tracts per biopsy was 9.4 (range 2-39). To exclude viral hepatitis as the cause of the findings, we first compared our group of 19 patients without hepatitis to the reported findings in 16 normal biopsies (PMID: 9695993); see Table. Our biopsies had significantly more portal vein profiles (fragmentation) and bile duct profiles (proliferation) per portal tract, compared to normal, which was also noted in the biopsies with hepatitis (not shown). We also noted the following: prominent arteries (66% of all cases; 32% hyalinised, 7% sclerotic), small caliber portal veins (93%), portal vein herniation into parenchyma (64%), fibrotic/sclerotic portal tracts (79%), portal elastosis (77%), sinusoidal dilatation (79%; 63% focal, 16% diffuse) hemosiderin deposition in hepatocytes (68%) and Kupffer cells (87%), pericellular fibrosis (20%), central venular fibrosis (45%), and significant fibrosis (52% grade 2-4). The only significant difference between the cases with hepatitis and those without was the amount of portal chronic inflammation (p=.0041).

Table 1. Number of portal structures in "normal" liver biopsies (PMID: 9695993) and the non-hepatitis group. PT: portal tract, HA: hepatic artery, BD: bile duct, PV: portal vein

	Normal	No Hepatitis	P value
Total # of portal tracts (PTs)	338	171	
#HA profiles/PT (Mean±SD)	2.6±2.3	2.4±1.3	p=0.2920
#BD profiles/PT (Mean±SD)	2.3±2.2	3.6±1.8	p=0.0001
#PV profiles/PT (Mean±SD)	0.7±0.7	1.3±0.5	p=0.0001

Conclusions: It is known that patients with chronic renal disease are prone to developing cardiovascular disease and general vascular dysfunction. In our study, we found evidence of vascular alterations in the livers of these patients, including portal vein fragmentation, herniation and atrophy, as well as prominent hepatic arteries, sinusoidal dilatation, portal elastosis and sclerosis. These vascular findings should be reported, as they could contribute to altered liver function and fibrosis in these patients.

1786 Urea Cycle Enzyme Immunohistochemistry Identifies Ornithine Transcarbamylase as a Highly Sensitive and Specific Marker of Hepatocellular Differentiation

Daniel Pelletier, Andrew Bellizzi. University of Iowa Hospitals and Clinics, Iowa City, IA

Background: The hepatocellular differentiation markers HepPar1 (which recognizes carabamoyl phosphate synthetase I) and arginase (ARG) are both urea cycle enzymes. We hypothesized that the remaining urea cycle enzymes, ornithine transcarbamylase (OTC), argininosuccinate synthetase (ASS), and argininosuccinate lyase (ASL), could also represent sensitive and specific hepatocellular markers.

Design: Immunohistochemistry (IHC) for OTC, ASS, ASL, HepPar1, and ARG was performed on tissue microarrays (triplicate 1 mm cores) of 99 non-neoplastic livers (NNL; 69 with cirrhosis), 8 dysplastic nodules (DN), 32 focal nodular hyperplasias (FNH), 45 hepatic adenomas (HA), 162 hepatocellular carcinomas (HCC), 135 cholangiocarcinomas (CC), and 93 small intestinal adenocarcinomas (SIA). Tumor grade was assessed by review of original glass slides (well [WD], moderately [MD], poorly differentiated [PD]). IHC was evaluated for intensity (0-3+) and extent (0-100%) of expression with an H-score calculated (intensity*extent).

Results: OTC performed virtually identically to HepPar1. ASS and ASL were entirely non-specific. There were 144 OTC+/HepPar1+, 5 OTC+/HepPar1-, 4 OTC-/HepPar1+, and 9 OTC-/HepPar1- HCCs. Addition of the other marker increased the sensitivity for HCC from 91% (for HepPar1) and 92% (for OTC) to 94%. Detailed expression data are presented below:

Table: Detailed Expression Data: % Positive (Mean H-score, if Positive)

	NNL	DN	FNH	HA	HCC			CC	SIA
					WD	MD	PD		
OTC	100% (291)	100% (278)	100% (290)	100% (265)	97% (248)	94% (248)	75% (197)	20% (75)	38% (125)
Hep-Par1	99% (298)	100% (291)	NC	NC	97% (270)	92% (235)	79% (204)	20% (94)	42% (127)
ARG	100% (280)	100% (239)	97% (281)	100% (253)	94% (195)	79% (149)	75% (145)	NC	NC
ASS	100% (210)	75% (138)	91% (58)	91% (175)	79% (151)	76% (125)	83% (126)	73% (121)	82% (127)
ASL	100% (296)	100% (291)	100% (299)	100% (297)	100% (292)	99% (278)	100% (263)	95% (250)	98% (260)

Note: NC=not yet completed

Conclusions: The urea cycle enzyme OTC is an exquisitely sensitive marker of hepatocellular differentiation, albeit with the same diagnostic shortcomings as HepPar1. This result validates the thoughtful selection of IHC markers through the mining of the cell, developmental, and molecular biology literature.

### 1787 The Histologic Features of Portal Cavernoma Cholangiopathy

Meredith Pittman, Rhonda Yantiss, Jose Jessurun. Weill Cornell Medical College, New York, NY

Background: Portal cavernoma cholangiopathy (formerly portal biliopathy) is a type of biliary injury that occurs in the setting of a portal vein thrombus or cavernoma. Large thrombi that distend the portal vein can directly impinge on the adjacent bile duct or cause engorgement of periductal veins that compress the bile duct. A subset of patients with this disorder develop cholestatic symptoms, and the inflammatory changes around the bile ducts may produce a radiographically evident hilar mass or stricture that mimics malignancy or sclerosing cholangitis. The radiographic features of portal cavernoma cholangiopathy are well described, but reports detailing the histologic findings are lacking. In this study, we describe the clinical and histologic features of portal cavernoma cholangiopathy as encountered in three patients.

Design: The pathology electronic database was queried for the terms "portal hypertension," "portal vein thrombus," or "cholangiocarcinoma" in the clinical history; or "cholangitis" or "cholangiopathy" in the histologic diagnosis or description. Patients with established cirrhosis, history of liver transplant, or other known bile duct disorders were excluded.

Results: Three patients, all men, presented with cholestasis and portal vein thrombosis during a 10-year period. Presumptive clinical diagnoses were cholangiocarcinoma, primary biliary cholangitis, and cirrhosis, which resulted in a left hepatectomy and two liver biopsy samples, respectively. Examination of the resection and biopsy specimens demonstrated histologic features common to all. These features included portal venous abnormalities, obstructive biliary changes, and lack of substantial parenchymal fibrosis. Portal veins were small relative to the portal tracts or absent altogether (Figure 1A,

black circle). Interlobular bile ducts were present, but often displayed reactive epithelial atypia accompanied by a mixed inflammatory infiltrate with neutrophils and a ductular reaction (Figure 1B). Obliterated portal veins were highlighted with trichrome stains.
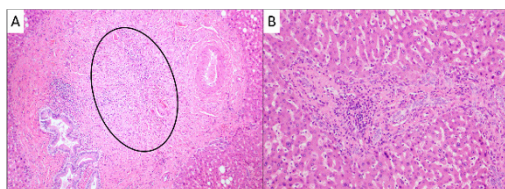
Conclusions: Portal cavernoma cholangiopathy produces histologic changes that simulate large duct obstruction and other types of chronic biliary disease. Attention to portal veins can provide helpful diagnostic clues, especially when biopsy samples are obtained from patients with a known portal vein thrombus or cavernoma.

1788 Chronic Hepatitis C and Autoimmune Hepatitis Overlap Syndrome in the Era of Direct-Acting Antiviral Agents: A Paired Liver Biopsy Assessment

Juan Putra[1], Thomas Schiano[2], Maria Isabel Fiel[3]. [1]Boston Children's Hospital, Boston, MA, [2]The Mount Sinai Medical Center, New York, NY, [3]Icahn School of Medicine at Mount Sinai, New York, NY

Background: HCV and autoimmune hepatitis (AIH) overlap syndrome (HCV-AIH) is an uncommon condition which is challenging to diagnose and manage. The diagnosis is established by a combination of clinical, immunological, and histologic features of both diseases. Interferon-based therapies have not been used to treat such patients because of the concern for worsening the AIH component of the syndrome. In this series, we report on the results of the HCV-AIH patients who were treated with direct-acting antiviral agents (DAAs) and their histological and clinical outcomes.

Design: Patients with biopsy-proven HCV-AIH from 2011 to 2016 were identified from the pathology database. Demographic, clinical, and serologic data was evaluated. Histologically, HCV was characterized by portal chronic inflammation with dense lymphocytic infiltrate. The AIH component was confirmed by the presence of interface hepatitis with a predominantly plasma cell infiltrate. The Batts-Ludwig scoring system was utilized to grade the inflammation and stage the fibrosis (both scored 0-4). CD138 immunostain (Biocare Medical, Concord, CA) was performed on available biopsy specimens to highlight plasma cells for quantitation. Plasma cell count was performed on 10 random high power fields (HPFs) in the portal tracts and the average number was compared between the initial and repeat biopsies.

Results: Five patients with HCV-AIH were included in the series (60% male; average age: 58 years at initial biopsy). The mean interval time between the initial and repeat liver biopsies was 2.4 years (range=1-4 years). All patients achieved sustained virologic response (SVR) after receiving sofosbuvir-based DAA. Table 1 is a summary of clinical and histologic data. One patient (patient 3) received immunosuppressive treatment after the diagnosis. Four of five cases (80%) showed improvement in the degree of inflammation (HCV and AIH components). However, only two cases (40%) demonstrated complete resolution of the autoimmune component.

Pa-tient	Biopsy	SVR (post-DAA)	HCV fea-tures	AIH fea-tures	Grade	Stage	AST (U/L)	ALT (U/L)	Autoim-mune markers	Plasma cell count (CD138)
1	1	-	+	+	3	1	83	132	IgG (high)	-
	2	+	+	-	1	1	46	41	-	12
2	1	-	+	-	3	4	-	-	-	-
	2	+	+	+	3	4	19	28	SM-Ab (+), IgG (high)	21
3	1	-	+	+	3	3	97	100	LKM-Ab (+)	-
	2	+	+	+	3	4	23	18	IgG (high)	21
	3	+	+	-	1	3	18	17	-	10
4	1	-	+	+	3	4	127	50	SM-Ab (+)	24
	2	+	+	+	2	4	43	16	-	10
5	1	-	+	+	3	3	137	200	SM-Ab (+), IgG (high)	17
	2	+	+	+	3	4	20	10	-	12

Conclusions: Our series underlines the potency of DAA agents in HCV-AIH patients. Histologic improvement is noted in most patients who achieved SVR after DAA treatment, despite not receiving therapy for AIH.

1789 Diagnostic Features of Drug Induced Vanishing Bile Duct Syndrome

Jia Qin[1], Thomas Schiano[2], Joseph Odin[3], Jawad Ahmad[6], Swan Thung[4], Stephen Ward[6], Maria Isabel Fiel[5]. [1]Cambridge, MA, [2]The Mount Sinai Medical Center, New York, NY, [3]Mount Sinai Hospital, [4]Mount Sinai Medical Center, New York, NY, [5]Icahn School of Medicine at Mount Sinai, New York, NY

Background: Ductopenia is defined as $\geq$ 50% bile duct (BD) loss. Vanishing bile duct syndrome (VBDS) is a group of acquired disorders resulting in progressive destruction of intrahepatic bile ducts. Drug-induced liver injury (DILI) resulting in cholestasis is commonly seen, and some of these cases progress to VBDS. In this study, we assessed the clinical and pathological features of DILI-VBDS.

Design: Seventeen DILI-VBDS cases were retrieved from the pathology database, all from 2014-2017. Chart review was performed to obtain laboratory results and medication history. Biopsy slides including H&E, trichrome, rhodanine and CK7 were reviewed concurrently by two liver pathologists and detailed histological features were scored (0=none, 1=mild, 2=moderate, 3=severe) as well as degree of fibrosis and grade of inflammation (Ishak).

Results: Study cases included 10M & 7F, mean age 54y (24-79). Fifteen of 17 (88%) had polypharmacy ($\geq$3 prescription medications); 11/17 (65%) were taking a hepatotoxic medication (4 statins, 4 ACE inhibitors, 3 antibiotics). None were on herbal dietary supplements (HDS). Mean biopsy length=2.5cm (1.3-6.2); average # of portal tracts=28 (13-56). Ductopenia was seen in 14/17 (82%) biopsies while the remaining 3 showed evolving ductopenia (40% loss). Perisinusoidal fibrosis in the absence of fatty liver was seen (59%). BD damage as characterized by cholangiocyte dropout and cytoplasmic vacuolation and eosinophilia was seen in all cases. Copper deposition was seen in 35% of cases. Inflammation was present in the majority of cases, 13/17 (77%) with the infiltrates being mixed type including lymphocytes, histiocytes, neutrophils, eosinophils and plasma cells. Induction hepatocytes were seen in 14/17 (82%). Summary of clinical and pathological details is found in the Table.

Lab values = mean (range)	Histological features
ALT= 172 (24 - 739)U/L	Ductular reaction = 17 (100%)
AST= 193 (22 - 932)U/L	Cholestasis = 17 (100%)
ALK-Phos= 287 (66 - 1418)U/L	Metaplastic hepatocytes = 17 (100%)
T Bili= 4.2 (0.4 - 11.8)mg/dL	Induction hepatocytes = 14 (82%)

Conclusions: DILI-VBDS appears to be increasing in frequency. In this series, patients who developed VBDS were on polypharmacy and majority were due to known hepatotoxins and not due to HDS. The majority of patients had elevated transaminases in addition to having raised biliary enzymes. Histological features highly suggestive of DILI-VBDS are mixed inflammation, presence of induction hepatocytes, and perisinusoidal fibrosis. These features may aid in identifying DILI-VBDS in liver biopsies and may potentially prevent the development of ductopenia.

### 1790 The Diameter of Vessels Within Hepatocellular Carcinoma

Dana Razzano, Yasmin Yusuf, Cyril Rosenfeld, Grigory Rozenblit. New York Medical College, New York, NY

Background: Transarterial particle embolization (with or without chemotherapeutic agents) is a commonly used method of local/regional therapy for hepatocellular carcinoma (HCC). Vessel lumen diameter within tumors is the decisive factor directing treatment success of particle embolization. Success of treatment relies on bead particle size as ideally it should match the diameter of the target vessels in order for the beads to appropriately lodge themselves within the tumor bed and go no further or lodge too proximal. Little to date has been documented regarding actual vessel sizes within the tumor.

Design: In this study, measurement of the diameters of vascular lumens was performed in 15 explanted livers with viable hepatocellular carcinoma. The tumors were evaluated using digital scans of H&E stained slides. The vessels were evaluated with CD34 to stain vessel endothelium and smooth muscle actin to highlight vascular walls. On each digital slide, three standardized rectangular 4.5 mm² regions of interest (ROI) were outlined in viable areas of tumor and necrotic areas were avoided. The boxes were placed as far from each other as possible in order to reduce the probability of measuring repetitive

vessels from the same vascular stem. All vessel lumens within the ROI were measured on digital high magnification to ensure precise measurements.

Results: In total, there were 1,457 intratumoral vessels measured and recorded in 15 tumors, each from one patient. The measurements demonstrated that the diameters vary between 5.0 and 220.1 μm, with over 80% measuring under 20 μm, and 96% measuring under 40 μm. Only 8 vessels measured over 80 μm in diameter.

Distribution of HCC vessels by caliber
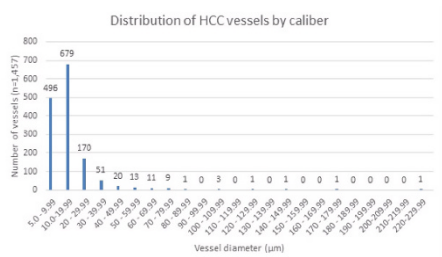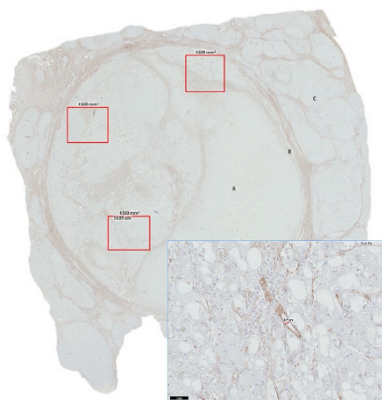
Conclusions: The obtained data may impact the selection of particle sizes used for treatment of HCC by transarterial embolization. For example, it may help direct the composition of mixtures of different sized beads with their calibers proportional to the above distribution; such mixtures may possess embolization characteristics that are closer to the optimal than the currently used commercial products. In addition, it may allow designing specific injection sequences for variable volumes of differently sized beads in order to optimize embolization results.

1791   Assessments of Pre-Transplant Steatosis by Frozen Section and Gross Examination Correlate Well with Time Zero Biopsies: Review of Current Practice in a Major Liver Transplant Center

Elizabeth Richards[1], *Konstantin Koro*[2], *Jorge D Reyes*[3], *Paul E Swanson*[1], *Maria Westerhoff*[4]. [1]University of Washington, [2]University of Washington Medical Center, Seattle, WA, [3]University of Washington Medical Center, Seattle, WA, [4]University of Michigan, Ann Arbor, MI

Background: Significant steatosis is associated with a high risk of poor liver allograft function. Pre-transplant frozen sections are an established method of estimating steatosis in potential donor livers. However, the literature is mixed with regard to their accuracy. Frozen sections are subject to freezing artifact and other technical issues which confound attempts to show their efficacy as a pre-transplant steatosis screen. Also, transplant surgeons must rely on the expertise of pathologists in the site where the organs are procured, but these pathologists may not evaluate livers on a regular basis.

Design: To determine if frozen section is a reliable basis for accepting livers for transplantation, we retrospectively compared frozen section steatosis estimates with time zero biopsies and correlated the latter with gross steatosis assessment by transplant surgeons. To achieve that goal, records from January 2015 to August 2017 were searched to identify explant livers with time zero biopsies and corresponding frozen section biopsies.

Results: 72 donor livers with time zero biopsies were identified; 43 also had frozen section biopsies. Complete agreement (<5% difference in steatosis estimate) was found in 34 cases (79%). Minimal disagreement (5-10% difference in steatosis estimate) was seen in 8 cases (19%). Only 1 case had > 10% difference (30% on frozen section vs. 10% at time zero). Among cases with any disagreement, 5 had higher steatosis estimates on frozen than time zero.

Frozen section was not done in 29 cases because the surgeon's gross assessment was negative or minimal for steatosis. Time zero biopsies supported this impression: 27 cases had < 5% macrovesicular steatosis. Only 1 liver had a discrepancy that would have affected the

surgeon's decision to use the organ.

Conclusions: In light of the growing incidence of fatty liver disease, accurate pre-transplant steatosis assessment is increasingly critical. Our study provides quality assurance for our region and shows that surgeons' gross assessments, in the setting of minimal liver steatosis, correlate well with biopsy findings. Surgeons may not have long working relationships with pathologists at the site where they are procuring organs. Our results demonstrate that, overall, regional pathologists are accurately assessing the degree of steatosis on frozen sections and assist in the critical decision making process of donor organ usage.

1792   P53 Immunohistochemistry in Hepatocellular Carcinoma Correlates with Recurrent Disease Following Liver Transplantation

Daniel Roberts, Sanjay Kakar, Ryan Gill. University of California, San Francisco, San Francisco, CA

Background: Hepatocellular carcinoma (HCC) can harbor TP53 mutations, which have been associated with poor differentiation and vascular invasion in partial resection specimens. P53 immunohistochemistry is known to correlate with TP53 mutation status. We aimed to establish the prognostic relevance of aberrant p53 staining in a well-characterized clinical cohort of liver explants containing HCC.

Design: We performed immunohistochemical stains for p53 on tissue sections from 190 explanted livers with HCC, all of which had at least two years of clinical follow-up. An aberrant result was scored as strong nuclear staining in at least 5% of tumor cells. Clinical data and tumor characteristics were extracted from the medical record and pathology reports.

Results: Within our cohort, 21 of 190 (11%) patients had tumor recurrence during the follow-up period. Overall, 28 of 190 cases (15%) showed aberrant p53 expression, which included 10 of the 21 recurrent cases (48%, p < 0.00001). In addition, explants harboring tumors with an aberrant p53 immunophenotype were more likely to demonstrate poor differentiation and show vascular invasion.

Table 1: Characteristics of p53 Immunohistochemistry in HCC-containing Liver Explants				
	Aberrant p53	Total cases	Rate	Significance
Patient outcome				<0.00001
No recurrent disease	18	169	10.7%	
Tumor recurrence	10	21	47.6%	
Tumor differentiation (WHO classification)				0.0094
Well differentiated	5	74	6.7%	
Moderately differentiated	18	102	17.6%	
Poorly differentiated	5	14	35.7%	
Vascular invasion				<0.00001
Absent	17	166	10.2%	
Present	11	24	45.8%	

Conclusions: Our data show that p53 immunohistochemistry is strongly associated with tumor recurrence following liver transplantation. In combination with histologic features, immunohistochemical evaluation of p53 may allow for improved risk stratification in the pretransplant setting, as well as further refinement of patient management in the posttransplant period.

1793   Clinical and Histopathologic Features of Hepatitis C Patients Following Sustained Viral Clearance (SVR) After Transplantation

Anthony Rubino[1], *Elizabeth Verna*[2], *Jay Lefkowitch*[3], *Michael J Lee*[4]. [1]New York Presbyterian Hospital/CUMC, New York, NY, [2]Columbia University Medical Center, [3]College/Physicians & Surgeons, New York, NY, [4]Columbia University, Long Island City, NY

Background: With the advent of new antiviral therapies (e.g., direct antiviral agents), the standard of care towards treatment of Hepatitis C virus (HCV) is evolving. Patients are deemed to be clinically cured when they have achieved sustained viral response (SVR), defined as an absence of detectable Hepatitis C RNA in the blood for at least 24 weeks after stopping treatment. The role of liver biopsy is essential in assessing grade and stage, however the clinical and histopathologic findings after SVR in the post-transplant setting need additional characterization. This study investigates the duration after transplant when recurrent hepatitis features first appear in SVR patients and whether there is an association between episodes of rejection and progression in the grade/stage.

Design: The case files were searched for liver transplants in the setting of cirrhosis due to Hepatitis C infection. We recorded the

patient's antiviral therapeutics, hepatic function tests, indication for biopsy, date of SVR, histopathologic findings and final diagnosis. 72 patients achieved SVR after transplantation and 144 biopsies were identified. We evaluated each case for duration before features of recurrent hepatitis appeared, changes in grade/stage and episodes of rejection.

Results: 144 liver biopsies from 72 HCV patients achieved SVR after transplantation. 55 patients (76%) showed evidence of recurrent hepatitis (portal and lobular inflammation and necroinflammatiory activity) within 12 months, 1 patient (1%) within 12-24 months, and 1 patient (1%) within 25-36 months (Table 1). Episodes of rejection were seen in 40 patients (55%) who achieved SVR post-transplant. 28 patients (39%) had one episode of rejection, 9 patients (13%) had 2 episodes of rejection, 2 patients (3%) had 3 episodes of rejection and 1 patient (1%) had greater than 3 episodes of rejection, with an increase in grade seen in 19% and an increase in stage seen in 13% of these patients (Table 2). 17 patients had no post-transplant liver biopsies after achieving SVR.

Table 1. 1st Biopsy to show features of HCV in patients with SVR post-Transplant

Time After Transplant	Number of Patients
0-12 months	55
12-24 months	1
25-36 months	1

Table 2. Episodes of Rejection and histopathologic changes in post-transplant SVR patients

Episodes of Rejection	Number of Patients	Increase in Grade	Increase in Stage
0	15	8	8
1	28	10	7
2	9	3	2
3	2	1	0
More than 3	1	0	0

Conclusions: Histologic features of recurrent hepatitis C persist even after eradication of hepatitis C virus and achievement of SVR. Most SVR patients exhibit features of recurrent hepatitis within the first year and some patients demonstrate a progressive increase in grade and stage over time. When comparing patients with and without episodes of rejection, there was not a significant difference in the progression of grade/stage.

1794   OVERdiagnosis of OVERlap syndrome

Natalia Rush, Craig Lammert, Romil Saxena. Indiana Univ/Medicine, Indianapolis, IN

Background: Overlap syndrome is a rare disorder affecting 10% of patients with primary biliary cholangitis (PBC) who have concurrent autoimmune hepatitis (AIH). Accurate diagnosis of overlap syndrome requires independent diagnosis of each entity (PBC, AIH) utilizing at least 2 of 3 definitive criteria for diagnosis of each entity. We hypothesize that overlap syndrome is often overdiagnosed.

Design: A clinical database was queried to identify adult patients labeled with overlap syndrome, and a control group of age and gender matched patients with AIH, who had a liver biopsy available for review. Blinded to the diagnosis, we reviewed available liver biopsy slides for these 2 groups. Histopathologic features evaluated included bile duct (BD) damage, degree of BD damage, presence of florid BD lesion/granuloma, periductal inflammation, BD scar, degree of bile ductular proliferation, degree of interface activity and lobular inflammation. A final diagnosis (PBC, AIH, or overlap) was rendered for each specimen before review of clinical information. Medical records were reviewed for biochemical (levels of alkaline phosphatase, alanine transferase, immunoglobulin G), serological (titers of ANA, AMA and ASMA) and clinical data.

Results: There were 32 adult patients (9 males, 23 females; age 26-79, average age 53) labeled as overlap syndrome. Liver biopsy of 13 patients was available for review. The control age and gender matched group consisted of 13 patients.   Out of 13 cases with presumed diagnosis of overlap syndrome, only 3 (21%) met diagnostic criteria. In most cases, the diagnosis of overlap was based on presence of mild BD damage in AIH without the presence of 2 of 3 definitive criteria (florid duct lesion, elevated AMA, alkaline phosphatase five times upper normal limit) for diagnosis of PBC. BD damage was present in 12 cases of presumed overlap and in 13 patients with AIH, respectively.

1.   Overlap syndrome is often overdiagnosed.

2.   Overdiagnosis results from the presence of bile duct damage in AIH which is often interpreted as representing PBC.

3.   Misdiagnosis can be prevented by adhering to the requierment that both processes (PBC, AIH) be diagnosed independently by utilizing at least 2 of 3 definitive criteria for diagnosis of each entity.

1795   Upregulation of METTL3, an N(6) - Adenosine Methyltransferase of PolyA+ RNA in Hepatocellular Carcinoma

Taha Sachak, Juan Barajas, Kalpana Ghoshal, Debbie Knight, Wei Chen, Wendy L Frankel. [1]The Ohio State University Wexner Medical Center, Columbus OH

Background: Reversible RNA modifications are emerging as a new mechanism of epitranscriptomic gene regulation. N6-methyladenosine (m6A) is the most prevalent internal modification found in eukaryotic mRNA. m6A is added to RNA post-transcriptionally by the m6A methyltransferase complex. Methyltransferase like protein 3 (METTL3) is the catalytic component of m6A methyltransferase that acts in concert with METTL14 to transfer methyl groups in vivo. m6A controls many aspects of the mRNA life cycle including stability, splicing, export and translation. Accumulation of m6A mRNA is found to be associated with self-renewal of cancer stem cells and some malignancies. Hepatocellular carcinoma (HCC) is the most common primary malignant neoplasm of the adult liver and second cause of cancer mortality worldwide with limited treatment options. We studied METTL3 in HCC, hepatic adenoma (HA) and non-neoplastic liver (NNL) to determine if it's RNA and protein levels are dysregulated in HCC.

Design: In order to determine METTL3 mRNA expression in HCCs and NNLs, we analyzed HCC mRNA RNA-sequence data (n=377) from The Cancer Genome Atlas Liver Hepatocellular Carcinoma (TCGA-LIHC) data. Subsequently, we identified 130 HCCs from our archives from 1997 to 2016 and additionally 12 HAs from 1997 to 2004. Tissue microarrays (TMAs) were constructed from HCC, adjacent NNL (91), and HA (12) using 1 or 2 mm cores in duplicate per case. TMAs were immunostained with METTL3 antibody and intensity was graded as 0 (absent), 1 (weak), or 2 (strong) and staining was correlated with HCC grade. Statistical analysis was performed using GraphPad Prism (chi-square and t-tests).

Results: The analysis of gene expression profiling data from TCGA-LIHC showed significant upregulation of both METTL3 and METTL4 mRNA levels in HCCs compared to NNL (Fig 1). In addition, disease-free survival was significantly reduced in HCC patients with alterations of METTL3 and METTL4 (Fig 2). TMA analysis revealed that METTL3 nuclear staining was present in 57% (74/130) of HCCs, 1.1% (1/91) of adjacent NNLs, and 8.3% (1/12) of HAs. Strong METTL3 nuclear staining was significantly associated with poor differentiation in HCC.

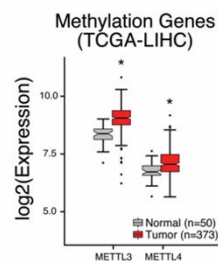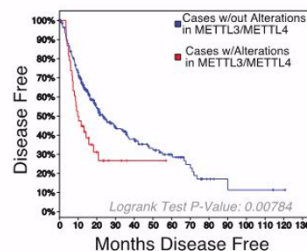Figure 1. METTL3 and METTL4 are upregulated in HCCs.

Figure 2. Disease Free Survival

Conclusions: METTL3 appears to be involved in hepatocellular carcinogensis and correlates with poor differentiation. Therefore, m6A modifications should be explored in HCC as METTL3 could serve as a therapeutic target. In addition, METTL3 immunohistochemistry may be helpful in distinguishing HCC from HA and NNL.

1796 Lacking of TERT Promoter Mutation in Fibrolamellar Hepatocellular Carcinoma (FLC)

Christian Salib[1], Hongfa Zhu[2], Katherine Sun[3], Xiang Dong[4], John T Fallon[4], Minghao Zhong[5]. [1]Westchester Medical Center at New York Medical College, Valhalla, NY, [2]Mount Sinai Hospital, [3]NYU Langone Medical Center, New York, NY, [4]Westchester Medical Center at New York Medical College, [5]Westchester Medical Center/ New York Medical College

Background: Fibrolamellar hepatocellular carcinoma (FLC) is a rare primary hepatic cancer that develops in children and young adults, with an incidence of approximately 200 new cases diagnosed worldwide each year. In contrast to typical hepatocellular carcinoma (HCC), FLC is not associated with cirrhosis and carries the *DNAJB1-PRKACA* gene fusion. *TERT* promoter mutations were identified as the most frequent genetic alterations in HCC with an overall frequency around 60%. However, *TERT* mutation status in FLC has not been investigated.

Design: We collected 15 cases of FLC samples and also included 10 consecutive HCC cases as a control cohort. The promoter region of *TERT* covering the two hotspot mutations -124C>T and -146C>T was amplified by polymerase chain reaction (PCR) as previously described. The direct sequencing was performed on the 3730XL DNA Analyzer with BigDye Terminator V 3.1 (Applied Biosystems).

Results: In the control cohort of 10 consecutive HCC, 5 (50%) of samples were detected with the presence of *TERT* promoter mutation. Interestingly, no *TERT* promoter mutation was identified in all 15 FLC samples.

Conclusions: This is the first study of *TERT* promoter mutation in FLC. Our data demonstrates that in contrast to conventional type HCC with high (~60%) association of *TERT* promoter mutation, FLC do not carry this mutation. This result provides additional evidence that carcinogenesis of FLC and HCC are different at the molecular level.

1797 Can't the Liver Be a Little More Tolerant: A Clinicopathologic Study of Immunologic Tolerant Pediatric Liver Transplant Recipients

Jason Scapa[1], Laura Wozniak[2], Bita V Naini[3]. [1]UCLA Medical Center, Los Angeles, CA, [2]UCLA Medical Center, [3]UCLA Medical Center, Santa Monica, CA

Background: Complications from immunosuppression (IS) remains one of the largest obstacles to morbidity-free long-term survival in liver transplant (LTx) recipients. Because of this, some LTx centers have started reducing and even completely withdrawing IS treatment. This immunologic tolerance is reported to occur in 20% of LTx recipients and is seen more often in pediatric patients. However, the lack of robust clinical characteristics and biomarkers along with histological correlates, makes it difficult to predict which patients achieve and maintain tolerance. Here we study the clinical characteristics and histological findings in a cohort of pediatric LTx recipients who have achieved tolerance.

Design: We identified all tolerant pediatric LTx recipients cared for at our institution. Clinical characteristics, laboratory studies, and biopsy results were followed from July 2009 to July 2017. Tolerance was defined as normal liver function off IS for ≥1 year.

Results: Eighteen patients were identified as tolerant. Those patients that had at least one liver biopsy while off IS were included in this study (n=11). Five maintained tolerance (MT) clinically and biochemically while 6 lost tolerance (LT) during the study period. The characteristics of these two groups are summarized in Table 1. Of the six LT patients, 4 lost tolerance due to acute cellular rejection confirmed on biopsy before restarting IS, 1 lost tolerance due to chronic ductopenic rejection, and 1 needed to restart IS due to a diagnosis of lupus. The biopsies from MT patients did not show any features concerning for allograft rejection. In LT patients, 3 showed fibrosis at their last recorded biopsy, all of which were grade 1 portal fibrosis. Two MT patients also exhibited fibrosis, with one showing portal fibrosis and the other having bridging fibrosis/cirrhosis in the setting of a chronic portal vein thrombosis.

Table 1: Cohort characteristics. Results presented at median (range).

	N	Males	Age at Transplant (Years)	Reason for Transplant	Time from Liver Transplant to Tolerance (Years)	Time Off Immunosuppresion (Years)	Number of Biopsies (per Patient)
Maintained Tolerance (MT)	5	5	2.5 (0.8-3.0)	Biliary Atresia (n=3) Neonatal hepatitis (n=1) Tyrosinemia (n= 1)	7.0 (4.8-21.5)	10.9 (1.9-14.7)	1 (1-8)
Lost Tolerance (LT)	6	3	1.0 (0.6-1.3)	Biliary Atresia (n=5) Non-syndromic paucity of bile ducts (n=1)	10.6 (2.9-18.0)	2.5 (1.8-18.6)	1.5 (1-10)

Conclusions: Our center follows one of the largest cohorts of tolerant pediatric LTx recipients. Interestingly all of our MT patients are males. Six of 11 patients (55%) lost tolerance during the eight-year follow-up with 5 (83%) due to biopsy-proven rejection that required restarting IS regimen. These data underscore the concept that tolerance is a dynamic, non-permanent state. As such, it is essential for patients who remain clinically stable off IS to undergo regular follow-up with laboratory monitoring and surveillance biopsies for detection of subclinical rejection and/or fibrosis.

1798 Sonic Hedgehog Immunohistochemistry Improves Inter-observer Agreement for Ballooning and the Diagnosis of Nonalcoholic Steatohepatitis (NASH) among Less Experienced Liver Pathologists

Michael Schild[1], Liyan Xu[2], Ayako Suzuki[2], Diana Cardona[3], Lani Clinton[4], Shannon McCall[5], Avani Pendse[2], Xuefeng Zhang[6], Manal F Abdelmalek[2], Anna M Diehl[2], Cynthia Guy[6]. [1]Duke University Hospital, Durham, NC, [2]Duke University, Durham, NC, [3]Durham, NC, [4]Duke University, Durham, NC, [5]Duke University Medical Center, Durham, NC, [6]Chapel Hill, NC

Background: The accurate diagnosis of nonalcoholic fatty liver (NAFL) or nonalcoholic steatohepatitis (NASH) is important for therapeutics, prognosis and research. One principal discriminating histologic lesion is hepatocellular ballooning (HB), because HB reflects severe hepatocyte injury which is linked to fibrogenesis and disease progression. Confident identification of HB can be difficult and inter-observer agreement is not ideal. Immunohistochemistry for Sonic hedgehog (Shh) marks HB. The diagnostic utility of Shh immunohistochemistry has not been fully explored.

Design: Core needle liver biopsies from 15 patients with varying degrees of histologically confirmed nonalcoholic fatty liver disease (NAFLD) were randomly selected from The Duke NAFLD Biorepository. Hematoxylin and eosin (H&E), Masson trichrome and Shh immunohistochemistry was performed. Three senior and two junior liver pathologists evaluated each case for the degree of HB and diagnosis in three rounds, with one week wash-out periods between each round. Round 1 assessed H&E only. Round 2 assessed H&E and trichrome. Round 3 assessed H&E, trichrome, and Shh. Inter-observer agreement for HB was calculated using the Kendall rank correlation coefficients. Inter-observer agreement for the diagnosis of steatohepatitis was calculated using Kappa correlation coefficients.

Results: Among junior pathologists, the agreement for HB improved from 0.42 using H&E to 0.76 with H&E and trichrome, and improved to 0.81 with the use of Shh. Experienced liver pathologists HB agreement remained stable at 0.83, 0.75, and 0.75, respectively. Less experienced pathologists had poor kappa agreement for the diagnosis of NASH on H&E (0.02) and H&E with trichrome (0.06), but good agreement (0.66) with H&E, trichrome and Shh. Senior pathologists remained stable with moderate to good agreement (0.65, 0.59, and 0.71, respectively).

H&E   Shh

A   B
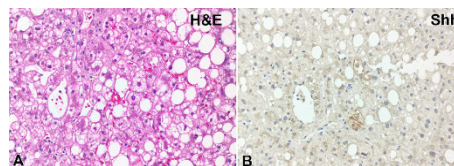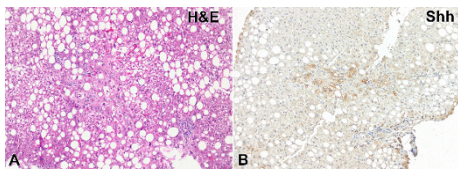
Conclusions: Shh immunohistochemistry improves inter-observer agreement moderately for HB and dramatically for the diagnostic categorization of NAFLD among less experienced liver pathologists.

1799 Mycobacterium Chimaera Hepatitis: A New Disease Entity

Nafis Shafizadeh[1], Gillian Hale[2], Najeeb S Alshak[3], Jim Nomura[4]. [1]Kaiser Permanente, Oak Park, CA, [2]Centers for Disease Control and Prevention, Atlanta, GA, [3]Kaiser Permanente, Los Angeles, CA, [4]Kaiser Permanente

Background: Mycobacterium chimaera was identified as a species within the Mycobacterium avium complex (MAC) in 2004. Until recently, it was predominantly seen in immunocompromised patients. In 2015, an outbreak of disseminated M. chimaera disease was described in European patients after undergoing open heart surgery in which contaminated heater-cooler water tanks were used. Patients present with fever, fatigue, and weight loss months to years after surgery and are found to have systemic manifestations including endocarditis, pancytopenia, renal dysfunction, chorioretinitis, and hepatitis. Preliminary reports suggest a high mortality rate despite aggressive treatment. The majority of cases have been described out of Europe, and a recent report out of the Mayo Clinic described the first three cases in the United States. The pathologic changes in the liver have not yet been described.

Design: We identified 6 cases, all of whom had liver biopsies. We report the clinical and biopsy findings of these patients.

Results: All cases were identified within the past year, and to date 4 patients have died of disease despite aggressive treatment(Table 1). All cases were culture positive by blood and/or by tissue. One case was positive by peripheral blood next-generation DNA sequencing. Only 1 liver biopsy was positive with AFB stain. Rare immunostaining was detected in 1 case at the CDC with a Mycobacterium species assay.

All 6 biopsies showed a consistent pattern of injury: small, ill-formed collections of sinusoidal histiocytes with rare multi-nucleated-giant cells, and scattered architectural changes of venous outflow obstruction, including sinusoidal dilatation, sinusoidal congestion, and hepatic plate atrophy/necrosis(Figures 1, 2). Large, necrotizing granulomas, or foamy macrophage collections were not seen.

	Age	Gender	Surgery	Latency Period (mo.)	AST	ALT	Alk Phos	T-bili	Follow-Up (FU)	Survival/ FU (mo.)
Case 1	57	M	AVR	14	85	105	223	0.7	D	1
Case 2	69	M	AVR, MVR	22	102	51	152	6.8	D	1
Case 3	77	M	AVR	14	38	35	531	1.2	D	6
Case 4	70	M	AVR	21	124	99	132	1.3	D	3
Case 5	81	F	AVR	20	110	102	523	1.2	A	2
Case 6	58	F	AVR	29	50	26	264	2.3	A	1
Mean	68.7			20.0	85	70	304	2.3		

AVR=Aortic Valve Replacement, MVR=Mitral Valve Replacement, D=dead, A=alive
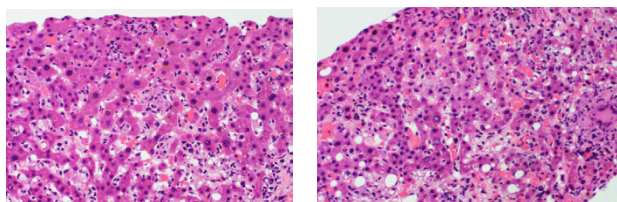
Conclusions: We report the largest series of M. chimaera disease in the United States to date, and report the liver biopsy findings of these patients. Our results corroborate the high mortality rate of this aggressive disease. Although there was no single pathognomonic finding, there was an overall consistent and characteristic pattern of injury: small, ill-formed sinusoidal granulomas with architectural changes of venous outflow obstruction. We postulate that the sinusoidal location of the granulomas contributes to the venous obstructive changes. Recognition of this pattern of injury can allow pathologists to suggest the diagnosis and prompt the appropriate

diagnostic and therapeutic interventions.

1800 Direct-Acting Antiviral Treatment in Patients with Viral Hepatitis C Results in Normalization of Serologic Markers of Autoimmune Hepatitis

Camila C Simoes[1], Omar Saldarriaga[2], Netanya Utay[3], MinKyung Yi[2], Monique Ferguson[2], Heather Stevenson[1]. [1]University of Texas Medical Branch, Galveston, TX, [2]University of Texas Medical Branch, [3]University of Texas Health Science Center at Houston

Background: Patients with viral hepatitis C (HCV) infection often have abnormal serologic markers (SM) of autoimmune hepatitis (AIH), including elevated IgG, anti-nuclear, and anti-smooth muscle/F-actin antibodies. These may be false positive results or due to superimposed AIH.

Design: Our study included 15 patients with HCV infection, with or without HIV infection, and elevated SM of AIH before starting direct-acting antiviral (DAA) therapy. Most patients (11/15: 73.3%) also had liver biopsies, either for fibrosis staging prior to treatment approval or due to their abnormal AIH-related SM. We hypothesized that their transaminases and SM of AIH would decrease or normalize following completion of their DAA treatment.

Results: Our patients included 9 females and 6 males. The median age was 58 years. Five patients have also HIV. Of the patients that had pre-treatment liver biopsies, only 27.3% (3/11), showed histopathologic features that were consistent with AIH (e.g., plasma cell-rich interface activity and/or perivenulitis) in addition to active viral hepatitis. Patients' SM of AIH started to decrease at 6 months post-treatment and 60.0 % (9/15) had complete normalization at 1 year. The majority (13/15: 86.7%) of our patients, including those with AIH features observed in their biopsies, showed normalization of their transaminase levels by 1-year post-treatment, which further supports that HCV is the driver of their abnormal laboratory studies, not AIH. Three of the 15 (20%) remaining patients had continued elevation of SM of AIH with normal transaminase levels; these patients had concomitant HIV infection with suppressed HIV RNA levels.

Conclusions: We propose that most patients with HCV and SM of AIH should first be treated with DAA prior to starting immune suppressive treatment, even if their biopsies and liver injury tests are suggestive of superimposed AIH. If SM of AIH do not begin to decrease by 6 months and/or do not normalize by one-year post-treatment, additional work-up and treatment for AIH should be considered. Additional patients will be included on our final statistical analysis when their post treatment follow up is completed.

1801 Tumor-Associated Inflammatory Cells And Immune-Checkpoints markers Correlates With Clinicopathological Characteristics In Intrahepatic Cholangiocarcinoma (ICC)

Luisa M Solis[1], Wai Chin Foo[1], Edwin R Parra[1], Barbara Mino[1], Reham Abdel-Wahab[2], Ignacio Wistuba[1], Lawrence Kwong[1], Milind Javle[1], Rachna Shroff[1]. [1]The University of Texas MD Anderson Cancer Center, Houston, TX, [2]The University of Texas MD Anderson Cancer Center, Houston, TX and Assiut University Hospital, Assiut, Egypt

Background: ICC has bad prognosis and limited therapeutic options. Recent success of immunotherapy has led to the investigation of the immune landscape in several tumors. In this study, we aim to characterize the immunoprofile of ICC.

Design: We selected 87 formalin-fixed and paraffin-embedded tumor tissues from surgically resected primary ICC with annotated clinicopathological information. We evaluated densities of tumor associated immune cells (TAICs) and immune-checkpoints markers expressed in epithelial malignant cells (MC) and in the tumor microenvironment (TM) by immunohistochemistry using digital image analysis and 13 markers (CD3, CD4, CD8, CD68, PD-L1, B7-H4, B7-H3, IDO1, ICOS, VISTA, OX40, TIM3, LAG3). We analyzed these biomarkers in the central tumor (CT) area and in the invasive margin (IM) and correlated their expression with clinicopathological information. A *p* value <0.05 was considered statistically significant.

Results: In MCs, PD-L1 was expressed in 2% of ICC; B7-H4 and B7-H3 were expressed in 74% and 62%, respectively (cut-off >5%). Using the median of expression of these biomarkers, smaller tumors have higher densities of CD3+ cells at the IM compared to larger tumors (*p*=0.0456). Poorly differentiated tumors have higher densities of LAG3+ cells (*p*= 0.0084) and CD3+ cells (*p*=0.0461) at the IM, and higher densities of PD1+ cells at the IM (*p*=0.0069) and CT areas (*p*= 0.0038). Patients with multiple tumors have higher densities of IDO-1+ cells at the IM (*p*=0.0346) and higher densities of VISTA+ cells in CT (*p*= 0.0155) compared to patients with solitary tumors. Patients with lymph-vascular invasion presented higher densities of ICOS+ cells (*p*=0.0398) in CT. Patients with metastasis to regional lymph nodes have higher densities of CD68+ cells at IM (*p*= 0.0401) and CT (*p*= 0.0462). Patients that have received neoadjuvant treatment presented

higher percentage of MCs expressing B7-H4 (p=0.0139) compared to patients with chemo-naive tumors. We observed a negative correlation between the expression of B7-H3 in MCs and densities of IDO-1+ and LAG3+ cells, and positive correlation with densities of CD4+ cells in CT. Expression of B7-H4 in malignant cells correlated negatively with density of ICOS+ cells at the IM and positively with density of CD68+ cells at IM.

Conclusions: We have characterized the immune response landscape of ICC, and identified the expression of several novel immune-checkpoints that could be used for immunotherapy approaches in this disease.

1802 Utility of Immunohistochemistry in Subclassifying Cholangiocarcinomas

M. Andrew Toussaint[1], Brian Robinson[2], Burcin Pehlivanoglu[2], David Martin[3], N. Volkan Adsay[4], Alyssa Krasinskas[2]. [1]Emory University, Decatur, GA, [2]Emory University, Atlanta, GA, [3]Univ of New Mexico, Albuquerque, NM, [4]Medical College of Wisconsin, Milwaukee, WI

Background: Cholangiocarcinomas are classified by anatomic location into intrahepatic (ICC; peripheral) and extrahepatic (ECC; perihilar or distal bile duct). The classification of ICCs into large duct type (LDT; resembling ECCs; typically S100P+ and mucin+) and small duct type (SDT; or peripheral type; typically CD56/NCAM+ and mucin-) has been shown to have clinicopathologic and molecular significance (PMID 27259014, 25181580). However, in our experience, there are cases with mixed features that are difficult to classify, and hence the goal of this study was to systematically characterize these tumors based on morphology and immunohistochemistry (IHC).

Design: 93 cases of cholangiocarcinoma (54 ICC and 39 ECC) from 2000-2015 were reviewed. Tissue microarrays and whole sections were stained with CD56, S100P, MUC1 and MUC5AC. Staining was interpreted as positive (>10% staining) or negative.

Results: 31 (57%) ICCs were SDT (cuboidal, small glands, no mucin), 7 (13%) were LDT (columnar, large glands, mucin) and 16 (30%) were mixed or indeterminate. For this study, ECC and LDT ICC were grouped together. While 98% specific, CD56 only stained 27% SDT ICC (see Table). S100P and MUC5AC had high sensitivity and specificity for large duct phenotype (ECC and LDT ICC). For cases negative for CD56 and S100P, MUC5AC positivity was 100% specific for large duct phenotype. MUC1 was positive in the majority (89%) of cases and did not separate ECC from ICC; interestingly, 7 of the 10 negative cases were ICCs.

	CD56+	S100P+	MUC5AC+	CD56-/S100P-/MUC5AC+
ICC	12 (of 53)	16 (of 54)	15 (of 54)	4 (of 27)
SDT	8	4	2	0
LDT	1	5	8	3
Mixed	3	7	5	1
ECC	0 (of 38)	26 (of 39)	29 (of 38)	8 (of 12)
p-value	0.002	<0.0001	<0.0001	0.0076
Sensitivity	27% for SDT	83% for ECC/LDT ICC	80% for ECC/LDT ICC	73% for ECC/LDT ICC
Specificity	98% for SDT	87% for ECC/LDT ICC	93% for ECC/LDT ICC	100% for ECC/LDT ICC

Conclusions: Distinguishing between SDT ICC and large duct phenotype (LDT and ECC) is becoming increasingly clinically relevant because of the association with potentially targetable molecular alterations (IDH mutations in SDT ICC and KRAS mutations in LDT ICC and ECC). CD56 and S100P help distinguish SDT from large duct phenotype, but because a significant proportion (42%) of CCs are negative for both CD56 and S100P, we found that adding MUC5AC to the panel can help subclassify these tumors.

1803 Correlation of Clinicopathological Features and Treatment Outcome of Therapeutic apheresis in Refractory Liver Allograft Rejection

Beena Umar, Mehrnoosh Tashakori, Mohammad Roufi, Ilena Lopez Plaza. Henry Ford Health System, Detroit, MI

Background: Until recently donor specific antibody (DSA) interference with graft function has not been considered a cause for liver graft loss secondary to rejection, and thus medical management has been the standard therapeutic approach, with the exception of hyperacute liver rejection when retransplantation is required. Current literature has shown that persistent elevation of donor specific antibodies (DSAs) is associated with intractable allograft liver transplant rejection and continued liver injury, and therapeutic apheresis intervention is being applied more often, as to treat other solid organ transplant rejection. We retrospectively reviewed the correlation of the laboratory findings and histopathological features in this liver allograft rejection cohort treated with plasmapheresis (TPE) and or Extracorporeal Photopheresis (ECP).

Design: Six liver transplant (LT) patients who were refractory to standard anti-rejection treatment were treated with the therapeutic apheresis (TPE/ECP) following our institutional protocol: three patients have completed treatment and 3 are still undergoing treatment. Five patients received TPE along with ECP and one patient only received ECP. The treatment regimen is: TPE 6 treatments, each followed by IVIG; ECP 4 treatment cycles (TC) weekly + 4 TC biweekly + 4 TC monthly. Each TC involves two consecutive days of ECP. The TPE, IVIG and ECP interventions have been tolerated well and without intervention related complications. Antirejection treatment response was monitored by serial liver enzymes (AST, ALT, Total Bilirubin(T.bili) & ALP), DSAs and liver biopsy.

Results: Results are summarized in table 1. Serial liver enzymes (AST, ALT, Total Bilirubin & ALP) and liver biopsy on histological examination were correlated and showed improvement and/or resolution of the rejection episode. Sequential liver biopsies showed resolving histologic parameters of rejection

Table 1: Summary of results

Patients	1	2	3	4	5	6
Diagnosis	68 y female HCV & HCC	49 y male alcoholic cirrhosis	48 y male alcoholic cirrhosis	31 y female autoimmune hepatitis	46 y female autoimmune hepatitis	61 y male alcoholic cirrhosis
Transplant year	2014	2016 x 2	2016	2012	2008	2017
Time from transplant to rejection	1 y 6 m	5 d and 12 d	7 d	4 y 4 m	8 y 11 m	2 months
DSA at rejection	Class II HLA high intensity	Class II HLA low Intensity	Class II HLA intermediate and high intensity	Class II HLA intermediate intensity	Class II HLA at high intensity	Not detected
Biopsy at rejection	Acute cellular rejection	1st Tx: Acute humoral rejection; 2nd Tx: Acute cellular rejection	Antibody mediated/humoral rejection	Acute cellular rejection	Acute cellular rejection	Acute cellular rejection
Liver enzymes at rejection	AST: 685 ALT: 598 T.bili: 13.1 ALP: 702	AST: 341 ALT: 641 T.bili: 5.3 ALP: 464	AST: 3965 ALT: 2704 T.bili: 2.8 ALP: 159	AST: 753 ALT: 123 T.bili: 5.6 ALP: 164	AST: 88 ALT: 134 T.bili: 1.5 ALP: 320	AST: 148 ALT: 318 T.bili: 9.8 ALP: 273
Liver enzymes at ECP completion	AST: 27 ALT: 23 T.bili: 0.1 ALP: 129	AST: 27 ALT: 34 T.bili: 0.7 ALP: 174	AST: 57 ALT: 42 T.bili: 0.2 ALP: 46	AST: 27 ALT: 41 T.bili: 0.3 ALP: 150	Ongoing ECP	Ongoing ECP
DSA at ECP completion	DQ8 at high Intensity	Negative	Negative	Negative	Ongoing ECP	Ongoing ECP

Conclusions: In our cohort of patients with refractory liver allograft rejection, we observed that TPE/ECP could be used as an effective additional treatment modality, which alleviates rejection as evidenced by clinic-pathologic parameters.

1804 Clinico-pathological Features of Resected Primary Liver Tumors in Adults with Special Emphasis on post Trans-arterial Chemoembolization (TACE) Resections

Gauri M Wagh, Mukta Ramadwar, Kedar Deodhar, Munita Bal, Mahesh Goel, Shraddha Patkar, Vikas Ostwal, Ashwin Polnaya. Tata Memorial Hospital, Mumbai, Maharashtra

Background: Hepatocellular carcinoma (HCC) is the commonest primary liver tumor followed by cholangiocarcinoma (CCA). Various histopathological parameters impact on prognosis. Treatment options such as Trans-arterial Chemoembolisation (TACE) and Radiofrequency Ablation (RFA) are used in patients with inoperable HCC.

Design: We reviewed histopathology of 150 primary liver tumours resected at our center from July 2011 to June 2016. Thirty-five of these patients had received neo-adjuvant TACE. We attempted to determine the prognostic significance of various histopathological parameters. In addition, we tried to correlate the degree of pathological response to TACE with survival in 35 patients. Statistical analysis included survival statistics with focus on correlation of degree of response to TACE and various histopathological parameters with survival.

Results: The male to female ratio was 6.14:1. The age range was 15-84 years (median=57 years). The 150 cases included 100 HCC (66.7%), 26 CCA (17.3%), 9 mixed HCC-CCA (6%), 8 cavernous hemangiomas (5.3%), 1 focal nodular hyperplasia (0.7%), 1 epithelioid angiomyolipoma (0.7%), 1 neuroendocrine tumor of bile duct (0.7%), 2 hepatic adenomas (1.3%) and 2 biliary cystadenomas (1.3%). Age less than 50 years turned out to be poor prognostic factor in patients with HCC. Gross and microscopic vascular invasion and cirrhotic liver (which correlated with the Hepatitis B and C reactive cases) were significant adverse prognostic factors. Histological grade and capsular

invasion were seen to affect Overall Survival (OS) and Disease Free Survival (DFS) respectively. Status of resection margin did not affect survival. In patients with HCC who had received neo-adjuvant TACE, less than 50% response was associated with reduced survival. Survival in patients with post TACE resection was better than those who were operated upfront.

Conclusions: Our study endorses vascular invasion, capsular invasion and cirrhosis as adverse histological parameters even in patients with operable HCC. TACE can be used in advanced and inoperable cases of HCC, wherein it can help downsizing the tumour and aid surgery. Moreover, our study also demonstrated that degree of pathological response to TACE also has prognostic significance.

1805 Histoarchitectural pattern does not distinguish IDH1 mutant intrahepatic cholangiocarcinomas from non-IDH mutant controls

Tao Wang[1], Efsevia Vakiani[2], Linda M Pak[3], Amber Simpson[1], William R Jarnagin[1], Jaclyn Hechtman[1], Carlie S Sigel[1]. [1]Memorial Sloan Kettering Cancer Center, New York, NY, [2]New York, NY, [3]Brigham and Women's Hospital, Boston, MA

Background: Mutations in IDH1 (mIDH1) define a distinct molecular subclass of intrahepatic cholangiocarcinoma (ICC). Diverse architectural patterns have been observed in ICC. Small molecules targeting mIDH1 are in development and in other tumor types have shown therapy-related effects on tumor differentiation. Characterizing mIDH1 ICC histomorphology is of interest for 1) efficient identification and 2) understanding the possible impact of targeted therapy on phenotype and tumor differentiation.

Design: Retrospectively, resected ICCs were selected for targeted next generation sequencing. Clinical data was obtained and tumor histology was reviewed for hilar vs peripheral type, mucin production (mucicarmine stain), and semi-quantitative analysis of architectural patterns (cholangiocellular (CLC), complex tubules (CT), simple non-anastomosing tubules (ST), and solid (SO)). A tumor was considered architecturally homogeneous if the dominant pattern represented ≥75% of the tumor. Variables were compared between mIDH1 and non-mutant ICC controls.

Results: We studied 68 ICC patients (19 mIDH1, 52 controls) and found a similar distribution of sex, age, chronic hepatitis, grade, stage, tumor size, mass forming type, and periductal infiltrating type. History of autoimmune disease was more frequent in mIDH1 (21% vs 2% P=0.02). Hilar type morphology was absent in mIDH1 and infrequent in controls (n=6 (12%) P=0.18). Extracellular mucin was seen at a similar rate (mIDH1 26% vs control 27%) while intracellular mucin was increased in mIDH1, but not significantly (mIDH1 21% vs control 8%, P=0.19). Architectural homogeneity was not significantly different between the groups with n=8 mIDH1 (42%) having homogeneous patterns of CT n=3, SO n=3, or ST n=2; compared to n=13 (25%) controls having homogeneous patterns of CT n=4, SO n=3, ST n=2, or CLC n=4 (P=0.24). CLC pattern was most often a minor histoarchitectural pattern comprising a median of 6% and 10% of mIDH1 and control tumors, respectively.

Conclusions: Peripheral type morphology was seen in all mIDH1, but histoarchitectural patterns and mucin production did not distinguish mIDH1 from controls. History of autoimmune disease was associated with mIDH1.

1806 Adenoma or Just Normal Liver -Where is the Portal Tract?

Kai Wang[1], Leona Council[1], Lei Zhao[2]. [1]University of Alabama at Birmingham, Birmingham, AL [2]Brigham and Women's Hospital, Harvard Medical School, Boston, MA

Background: Distinction between normal liver parenchyma and hepatocellular adenoma can occasionally become a problem in core biopsies of liver masses containing just liver parenchyma without any intervening portal tracts. The aim of this study is to provide a quantitative reference standard for normal distance among portal tracts in adult non-fibrotic livers.
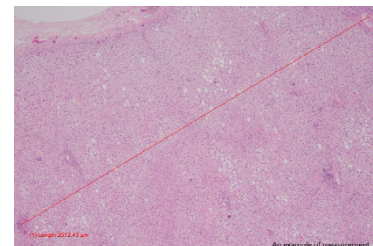
Design: Normal liver tissue sections were collected from liver resections for metastatic adenocarcinoma. Autopsy liver tissue from patients who died of conditions unrelated to liver diseases were also used. H&E slides were reviewed to ensure normal histological features and absence of fibrosis. Clinical information was examined through electronic chart review to ensure the absence of chronic liver diseases in these patients. The definition of portal tracts was defined as bile duct(s) with accompanying hepatic artery (portal dyad) or bile duct with portal vein and hepatic artery (portal triad). Isolated bile ducts without accompanying vasculature were not included. For each liver section, an index portal tract was randomly designated. The distances between the index portal tracts to all neighboring portal tracts were measured manually (Figure 1 and 2).

Results: Among the collected normal liver sections, 22 were from

surgical resections and 9 were from autopsy. There were 16 women and 12 men. The patients' ages ranged from 19 to 72 with a median of 44. A total of 438 measurements were made. The mean distance between two portal tracts was 592 μm in the female group and 582 μm in the male group (Table 1). The longest distances between two portal tracts were 2,200 μm in the female group and 1,991 μm in the male group (Figure 1).

Table 1: Summary of distance between portal tracts (average and standard deviation)

	Average Distance Between Portal Tracts (μ)	Standard Deviation (σ)	μ + 2 σ	μ + 3 σ
Female	592 μm	329 μm	1250 μm	1578 μm
Male	582 μm	328 μm	1238 μm	1566 μm
Total	587 μm	328 μm	1243 μm	1571 μm

Conclusions: Given the above reference range, the possibility of encountering a 1,571 μm (average + 3 standard deviation) or longer length of liver parenchyma without any intervening portal tracts is low and hepatocellular adenoma is a reasonable consideration in the right clinical and morphological context.

1807 Arginase-1 Is Specific for Metastatic Hepatocellular Carcinoma to Bone and Lung

Mary Wong[1], Brent K Larson[2], Maha Guindi[3]. [1]Arcadia, CA, [2]Cedars-Sinai Medical Center, West Hollywood, CA, [3]Cedars-Sinai Med Ctr, Beverly Hills, CA

Background: Hepatocellular carcinoma (HCC) most frequently metastasizes to lung and bone. Distinguishing metastatic HCC from other polygonal cell tumors can be challenging. Arginase-1 (Arg) is a sensitive and specific marker of HCC. However, no studies have specifically examined the use of Arg in metastatic HCC.

Design: Archives were searched from 1994-2017 to identify biopsies and resections of HCC metastases to bone (n=33) and lung (n=14). Polygonal cell tumors in bone and lung were retrieved as controls, including renal cell carcinoma (n=9), melanoma (n=5), well-differentiated neuroendocrine tumor (n=5), and perivascular epithelioid cell tumor (n=1). Clinical data and original glass slides, including hepatocyte paraffin antigen 1 (Hepar) and polyclonal carcinoembryonic antigen (pCEA), were reviewed to confirm diagnoses. Tumors were stained for Arg. Decalcification of bone blocks (6/33) was noted. Slides were reviewed blinded to diagnoses and other immunostain results. Two cutoffs (≥5% or ≥10%) were used to define positivity. For pCEA, only canalicular staining was considered positive. Statistical analysis was performed via Fisher's exact test.

Results: Using ≥5% as the cutoff, 21/33 (64%) metastatic HCCs and 0/20 (0%) controls were Arg-positive (P<0.0001). Arg was 70% sensitive and 100% specific for HCC. There was no significant difference in Arg positivity in blocks that had been decalcified and those that had not (P=1.00). Hepar and pCEA were positive in 27/28 (96%) and 15/15 (100%) metastatic HCCs, respectively, which is significantly higher than Arg (P=0.0064 and 0.0144, respectively). Using ≥10% as the cutoff, 31/47 (66%) HCCs were Arg-positive and 24/28 (85%) were Hepar-positive (P=0.1038). Arg's sensitivity was 66% and specificity remained 100%. Two cases were now Arg-positive, but Hepar-negative. The rate of pCEA positivity was unchanged.

Table 1: Arginase in Metastatic HCC vs. Other Polygonal Cell Tumors

	HCC	Controls
Arginase(+)	33	0
Arginase(-)	14	20
P<0.0001		

HCC – hepatocellular carcinoma

Table 2: Staining of HCC Metastases

Diagnosis	≥5% cutoff for positive staining			≥10% cutoff for positive staining		
	Arg	Hepar	pCEA	Arg	Hepar	pCEA
HCC bone metastases	21/33 (64%)	20/21 (95%)	11/11 (100%)	20/33 (61%)	18/21 (86%)	11/11 (100%)
HCC lung metastases 12/14 (86%) 7/7 (100%)			4/4 (100%)	11/14 (79%)	6/7 (86%)	4/4 (100%)
Total HCC metastases	33/47 (70%)	27/28 (96%)	15/15 (100%)	31/47 (66%)	24/28 (85%)	15/15 (100%)
P value (compared to Arg)		0.0064	0.0144		0.1038	0.0068

HCC – hepatocellular carcinoma
Arg – arginase-1
Hepar – hepatocyte paraffin antigen 1
pCEA – polyclonal carcinoembryonic antigen

Conclusions: Arg is highly specific for HCC metastases to bone and lung, and its staining rate is unchanged by decalcification. Using ≥5% to define positivity, Hepar and pCEA are more sensitive, though using ≥10% made rates of Arg and Hepar positivity similar. These findings emphasize the arbitrary nature of staining cutoffs, but suggest that Arg may be less sensitive in metastatic HCC than in primary tumors, and that use in a panel with other markers is justified.

1808 Liver regeneration after hepatic resection: Correlation with histopathological features and Fibroscan® values

Ha Young Woo[1], Jin Ho Lee[2], Taek Chung[1], Ji Hae Nahm[1], Gi Hong Choi[1] Seung Up Kim[1], Young Nyun Park[1]. [1]Yonsei University College of Medicine, Seoul, Korea [2]National Health Insurance Service Ilsan Hospital

Background: Hepatocellular carcinoma (HCC) usually occurs in chronic hepatitis, and improper liver regeneration after surgical resection of HCC might lead to postoperative liver failure. Therefore, predicting the capacity of liver regeneration after hepatic resection is important to prevent critical postoperative complications. The aim of this study is to investigate clinicopathological factors to predict the capacity of liver regeneration after resection of HCC.

Design: We evaluated 97 non-tumoral livers from HCC patients who underwent surgical resection. We performed histological review (inflammation grade, fibrosis stage, small and large liver cell change) and immunohistochemical stains for the markers of senescence (p21), DNA damage (γH2AX), proliferation (Ki67), and progenitor cell (EpCAM). The clinical data including preoperative Fibroscan® data was evaluated. Liver volume (LV) was measured at 7 days and 90 days postoperatively, using computed tomography. The liver regeneration ratio (LRE) was calculated as follows: LRE = $LV_{90\ days\ post-op}$ /$LV_{7\ days\ post-op}$.

Results: The mean age of HCC patients was 54.6±11.71 year-old, and male to female ratio was 3.41. The etiologies of liver disease were HBV (87.6%), HCV (4.1%), alcohol (2.1%) and unknown (6.2%). The majority (91/97, 93.8%) of the patients showed chronic hepatitis. There were high and low LRE group according to the median value (1.38) of LRE. The low-LRE group was associated with advanced fibrosis stage, higher expression of p21 and γ-H2AX, and lower expression of EpCAM (p<0.05 for all). Inflammation grade and small and large liver cell change showed no significant difference between two groups. EpCAM expression and fibrosis stage were independent predictors for liver regeneration by multivariate analysis (p<0.05 for all). Among the clinical data, the low-LRE group demonstrated lower serum albumin and higher Fibroscan® values (p<0.05 for all), and Fibroscan® values were well correlated with fibrosis stage (p<0.001).

Conclusions: Liver regeneration is considered to decrease with the greater degree of senescence and DNA damage of hepatocytes, higher fibrosis stage, and less progenitor cell activation. EpCAM expression and fibrosis stage are considered to be independent predictors of liver regeneration after resection. Preoperative Fibroscan® value is suggested to be useful to predict postoperative liver regeneration in noninvasive manner.

1809 Histologic Patterns of Anti-PD-1 Therapy-Induced Liver Injury

Dongwei Zhang[1], Xianzhong Ding[2], Michael Feely[1], Lindsay Yassan[3], Lindsay Alpert[3], Consuelo S Soldevila-Pico[4], John Hart[3], Xiuli Liu[1], Jinping Lai. [1]University of Florida, Gainesville, FL, [2]Loyola University Medical Center, Northbrook, IL, [3]University of Chicago, Chicago, IL, [4]University of Florida, Gainesville, FL

Background: Nivolumab and pembrolizumab, two monoclonal antibodies that block human programmed cell death-1 (PD-1), have been successfully used to treat patients with multiple advanced malignancies. The histologic patterns of anti-PD-1 treatment-induced liver injury have not been characterized.

Design: Through a multicenter search, six patients with advanced malignancies were included in this study. The mean age of the six patients was 53.7 (±3.9) years, with 5 males and 1 female. Four patients received 1 to 8 cycles of nivolumab and two patients received 4 to 6 cycles of pembrolizumab. No patients had a history of liver disease. Liver biopsies were performed to evaluate the abnormal liver function developed after anti-PD-1 treatment.

Results: Five patients had gastrointestinal symptoms or fatigue, and one was asymptomatic after anti-PD-1 agent administration. Laboratory abnormalities were detected in all six patients, including increased AST (531.3± 185.7 IU/L), ALT (628.6± 231.8 IU/L) and alkaline phosphatase (201.2±35.2 IU/L). Increased bilirubin was detected in one patient (4 mg/dl). Imaging studies in that patient showed no biliary obstruction or intrahepatic dilatation. All of the six patients underwent liver biopsy. One case demonstrated a mixed steatohepatitic and cholestatic injury pattern with severe steatosis (90%), many ballooning hepatocytes, mild lobular inflammation, ductal injury and cholestasis. Another case exhibited mild lobular inflammation and bile duct injury. Three cases showed mild steatosis (5%, 15% and 20%) and lobular spotty necrosis and dropout. The sixth case, in which the biopsy was performed 8 months after the last administration of nivolumab, demonstrated resolving acute hepatitis. The abnormal liver function recovered in all six cases after cessation of anti-PD-1 agents and corticosteroid treatment.

Conclusions: Anti-PD-1 agent can cause steatohepatitis, lobular predominant hepatitis with or without steatosis, or a mixed hepatitic and cholestatic pattern of liver injury. Withholding nivolumab/pembrolizumab and use of corticosteroids improved liver function. Our study suggests that screening patients for abnormal liver function tests prior to and monitoring periodically during anti-PD-1 treatment is necessary to prevent severe liver injury. Rather than causing autoimmune hepatitis, PD-1 inhibitors appear to produce an immune mediated acute hepatitis. This raises the possibility that simply stopping the drug is sufficient, and that steroids may not be necessary.

1810 Relationship Between Oxidative Stress (OS) and Cancer Stem Cell (CSC) Induction in Hepatocellular Carcinoma (HCC) Development

Yanmin Zhang, Dragana Kopanja, Frederick Behm, Pradip Raychaudhuri, Grace Guzman. University of Illinois at Chicago, Chicago, IL

Background: HCC, the third leading cause of cancer deaths worldwide, is often associated with chronic liver disease with various stimuli contributing to its development. OS is an imbalance between pro and anti-oxidant potential of cells leading to DNA damage. 8-hydroxy-2'-deoxyguanosine (8-OHdG) has been widely used as a biomarker for OS. CSCs are responsible for HCC growth and metastases. CD90 (Thy-1) is a 25-37 kDa glycosylphosphatidylinositol (GPI)-anchored glycoprotein involved in cell-cell and cell-matrix interactions, expressed in bone marrow-derived mesenchymal stem cells, and hepatic stem/progenitor cells (HSPCs). CD90+ but not the CD90- HCC cell lines displayed tumorigenic capacity.

Design: Explanted liver from 101 subjects with end stage liver disease and HCC were collected at the University of Illinois Health. Tissue microarrays were generated containing representative tissues with cirrhosis, dysplasia, and HCC. Standard immunohistochemistry was performed for 8-OHdG and CD90. HCC was graded from 1 to 3 based on modified Edmondson Steiner criteria. CD90 intensity and 8-OHdG stain intensity was quantified by Leico Biosystems Aperio®. Tumor characteristics and staining data were merged and statistical analysis was performed using t-test and Pearson correlation coefficient.

Results: Our study demonstrated a significant increase of 8-OHdG expression in hepatocytes from cirrhosis to HCC lesion (mean: 46.82 ± 9.02 vs 79.76 ± 8.83, P=0.02), while CD90 expression showed an increased trend. Further, in 8 patients with progressive samples of cirrhosis, dysplasia and HCC, the correlation study showed strong strength in cirrhosis (r= 0.7414), and moderate strength of relationship in dysplasia (r=-0.4687) and HCC (r= -0.4149) stage between CD90 and 8-OHdG expression.

Diagnosis	>5% cutoff for positive staining			>10% cutoff for positive staining		
	Arg	Hepar	pCEA	Arg	Hepar	pCEA
HCC bone metastases	21/33 (64%)	20/21 (95%)	11/11 (100%)	20/33 (61%)	18/21 (86%)	11/11 (100%)
HCC lung metastases	12/14 (86%)	7/7 (100%)	4/4 (100%)	11/14 (79%)	6/7 (86%)	4/4 (100%)
Total HCC metastases	33/47 (70%)	27/28 (96%)	15/15 (100%)	31/47 (66%)	24/28 (85%)	15/15 (100%)
P value (compared to Arg)		0.0064	0.0144		0.1038	0.0068

Figure 1: 8-OHdG and CD90 Expression in Representative Tissues with Cirrhosis, Dysplasia, and HCC
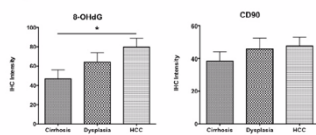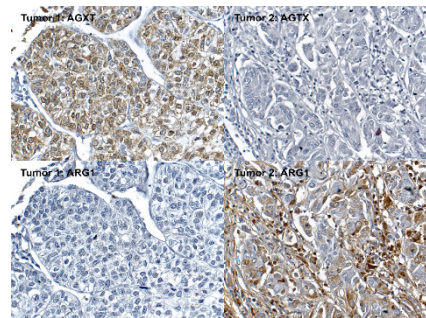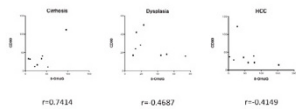
Figure 2: Pearson Correlation Coefficient Between CD90 and 8-OHdG in Eight Patients with Progressive Samples of Cirrhosis, Dysplasia and HCC

Conclusions: Our study demonstrated a significant increase of OS by 8-OHdG expressions from cirrhosis to HCC stage, which suggested an important role of OS in HCC development; while CSC CD90 expression showed only a trend of increase from cirrhosis to HCC. Interestingly, the strong strength of relationship between CD90 and 8-OHdG expressions at cirrhosis stage also suggested that CSCs induction by OS might present as an early event during HCCs development.

Conclusions: AGXT appeared as a novel hepatocellular marker with equally high specificity and slightly higher sensitivity than ARG1. AGXT, like ARG1, had lower sensitivy in less differentiated tumors. AGXT may aid in the diagnostic workup for hepatocellular carcinoma expecially in conjunction with ARG1 to increase the sensitivity.

1811 Alanine-Glyoxylate Aminotransferase (AGXT) Is a Novel Marker for Hepatocellular Carcinomas

Chaohui Zhao, Dongfang Yang, Kara A Lombardo, Li Juan Wang, Shaolei Lu. Brown University, Providence, RI

Background: Arginase 1 (ARG1) has been identified as the only marker for hepatocellular carcinoma with high sensitivity and specificity. However, its sensitivity decreases in moderately and poorly differentiated hepatocellular carcinomas. Alanine-glyoxylate aminotransferase (AGXT) is a peroxisomal enzyme that was first discovered based on a human live cDNA library. The aim of the current study is to define the efficacy of AGXT for the diagnosis of hepatocellular carcinoma.

Design: Immunohistochemistry for AGXT and ARG1 was performed in tissue microarrays of 136 hepatocellular carcinomas (HCCs) (21 well-differentiated, 92 moderately differentiated, and 23 poorly differentiated) and 318 tumors of lung, gastrointestinal tract, pancreatobiliary, gynecological and genitourinary systems. Staining was graded as absence or presence. Extent of the stain was rated in percentages. Statistic analysis was performed on JMP Pro 12.2 (SAS Institute Inc.).

Results: While ARG1 demonstrated a diffuse cytoplasmic pattern, AGXT exhibited a granular cytoplasmic pattern, consistent with its known localization in peroxisomes (Figure 1). Except 3 cases of cholangiocarcinoma, AGXT and ARG1 were negative in all non-HCC tumors in this series (99% specificity for both markers). Sensitivities of AGXT for HCC were 86% and 90% when positivity was defined as stain extent >= 5% and >=1%, respectively. Corresponding sensitivities of ARG1 were 83% and 88%. The sensitivities of both markers decreased in less differentiated tumors (Table 1). A small amount of tumors only expressed one marker (Figure 1). Six HCCs were AGXT+/ARG1-, and 2 were AGXT-/ARG1+ when 5% was used as cutoff. Using 1% as cutoff, 6 HCCs were AGXT+/ARG1-, and 3 were AGXT-/ARG1+. Sensitivity increased when presence of any marker was considered positive; they were at 87.5% and 91.9% using 5% and 1% cutoffs, respectively.

Markers		Hepatocellular carcinomas				
	Well (n=21)	Moderately (n=92)	Poorly (N=23)	Total (n=136)		
AGXT >=5%	1	11	7	19		
AGXT <5%	20	81	16	117		
Sensitivity	95%	86%	70%	86%		
AGXT >=1%	1	9	4	14		
AGXT <1%	20	83	19	122		
Sensitivity	95%	90%	83%	90%		
ARG1 >=1%	2	13	8	23		
ARG1 <1%	19	79	15	113		
Sensitivity	90%	85%	65%	83%		
ARG1 >=1%	2	8	7	17		
ARG1 <1%	19	84	16	119		
Sensitivity	90%	91%	70%	88%		
Diagnosis	>5% cutoff for positive staining			>10% cutoff for positive staining		
	Arg	Hep-ar	pCEA	Arg	Hep-ar	pCEA
HCC bone metastases	21/33 (64%)	20/21 (95%)	11/11 (100%)	20/33 (61%)	18/21 (86%)	11/11 (100%)
HCC lung metastases	12/14 (86%)	7/7 (100%)	4/4 (100%)	11/14 (79%)	6/7 (86%)	4/4 (100%)
Total HCC metastases	33/47 (70%)	27/28 (96%)	15/15 (100%)	31/47 (66%)	24/28 (85%)	15/15 (100%)
P value (compared to Arg)		0.0064	0.0144		0.1038	0.0068

FIG. 1773

Portal lymphocytic inflammation	Neutrophilic inflammation (peri-cholangitis)	Small droplet fat	Vacuolization of macrophages	Hepatocyte swelling	Regenerative changes (acinar change, disarray, multinucleated cells, rare apoptotic cells)	Cholestasis	Cholangiolar stasis	Persistent findings on 2nd biopsy after two weeks PT
9/15 (60%)	11/15 (73%)	13/15 (87%)	7/15 (47%)	13/15 (87%)	13/15 (87%)	15/15 (100.0%)	4/15 (27%)	8/8 (100%)